ROMANIAN ACADEMY

ROMANIAN ASTRONOMICAL JOURNAL

Vol. 3, No. 1
1993

EDITURA ACADEMIEI ROMÂNE

ROMANIAN ACADEMY
ROMANIAN ASTRONOMICAL JOURNAL

The ROMANIAN ASTRONOMICAL JOURNAL appears twice a year.

Orders from abroad (issues or subscriptions) should be sent to ORION SRL, Splaiul Independenţei 202 A, Bucureşti 6, PO Box 74—19, Romania, Tx 11939 CBTxR. Fax (40) 1312 24 25.

The manuscripts, the books and journals proposed in exchange and the mail should be sent to the Editorial Board.

Editorial Board's Address:
ROMANIAN ASTRONOMICAL JOURNAL
Institutul Astronomic, str. Cuţitul de Argint 5, Cod 75212, Bucureşti 28, telex: 11882 ASTRO R, tel.: 623.68.92 ROMANIA

EDITURA ACADEMIEI ROMÂNE
Calea Victoriei nr. 125, R—79717, Bucureşti, tel. 650.76.80

CORRELATED FLUCTUATING SIGNALS IN THE ANALYSIS OF THE LARGE SCALE STRUCTURE OF THE UNIVERSE

DORU MARIAN SURAN and NEDELIA ANTONIA POPESCU

Astronomical Institute of the Romanian Academy, 75212 Bucharest 28, Romania

Abstract. Recent observations of the Large Scale Structure of the Universe suggest inhomogeneities on a scale larger than previously thought. Our previous results (Suran 1991) indicated that the signals of the inhomogeneities in different 3D catalogs (galaxies, clusters, superclusters) are correlated, suggesting the presence of phase fluctuations in the long tail of the correlation function ($\xi(r)$ for $r > r_g$). The results are in good agreement with BEKS (1990, 1991 ; 1D pencil beams techniques). The comparison with different 3D simulations is made in order to derive the cosmological texture of the Universe on a scale larger than 20 Mpc. Also the comparison with the simulated power spectrum is made in order to derive the transition function $T_f(k)$ for the intermediate scale ($100h^{-1}$Mpc $< r <$ 1000 h^{-1} Mpc).

Key Words : *Large Scale Structure of the Universe* — texture ; *cosmology* — correlation function, transfer function.

1. INTRODUCTION

One important and yet unresolved problem in Cosmology is the transition scale to the homogeneity. If until 70's it was thought that the homogeneity scale is 10—20 h^{-1} Mpc (small scale), in 80's after the discovery of superclusters this scale is moved to about 150—200 h^{-1} Mpc (intermediate scale). The analysis of the density distribution for galaxies, clusters, matter show that for 1 h^{-1} Mpc $< r <$ 120 h^{-1} Mpc the spectral index lies in the range $-2 < n < -1$ (Einasto 1992 a, b ; Peacock 1991). On the other hand, the residual fluctuations have been now discovered in background radiation — COBE observations of CBR at very long scale with spectral index $n = 1$ (Smooth 1992) and with $\theta \simeq 7°$ at typical distances $z \simeq 1\,000$. This means that somewhere between 100 h^{-1} Mpc and z=10—1000 the spectrum must have a transition scale from negative to positive values (Einasto 1992 a).

In order to respond to this question, in the present paper we try to investigate the correlation function and the power spectrum at the large scale 300 h^{-1} Mpc $< r <$ 1000 h^{-1} Mpc.

For this enterprise we used deep and very deep 1D—3D catalogs (typical sizes $\simeq$ 1000 h^{-1} Mpc) and as a theoretical method we investigated the maxima of $\xi(r)$ (in real space) or $P(k)$ (in Fourier space). In the determination of the maxima and in the investigation of the periodicity of $\xi(r)$ we used two different statistical tools : FFT analysis and statistical WR tests. All results indicated the presence of large (25 h^{-1}Mpc, 60 h^{-1}Mpc), and superlarge (130 h^{-1} Mpc, 250 h^{-1} Mpc, 500 h^{-1} Mpc) features in the investigation of the long tail of the correlation function $\xi(r)$ (Suran 1991, Suran, Popescu 1992).

Using the transition function $T_f(r)$ we succeeded to tie our result both with the intermediate scale ($\leqslant 100\ h^{-1}$ Mpc) and the superlarge scale ($\geqslant 1000\ h^{-1}$ Mpc, COBE results).

A second important problem is the texture of the inhomogeneities on large scale. Recent redshift surveys show that the galaxies tend to be in long filaments and large sheets ("Great Walls") surrounding Big Voids (20—50 h^{-1} Mpc) and / or in cellular structure with even larger sizes ($\simeq 100\ h^{-1}$ Mpc). This in turn could be closely related to the mechanism of appearance of the topological defects (in models with spontaneous symmetry breaking, or CDM and HDM in gravity models). The 1D, 2D, 3D simulations for $\xi(r)$ and the comparison with the real $\xi(r)$ and pencil beam surveys could also reveal us the intimate structure of the Universe.

2. SAMPLES

We used four different kinds of samples: the pencil-beam surveys of galaxies (1D) and 3D catalogs for galaxies, clusters and superclusters.

— **Galaxies.** 'The Las Campanas Deep Redshift Survey in the two Polar Caps' (Yale, 1991, unpublished):

$$\mathrm{NP}\begin{cases}10^h \leqslant \alpha \leqslant 15^h\\ -18° \leqslant \delta \leqslant 0°\\ 0.03 \leqslant z \leqslant 0.2\end{cases} \qquad \mathrm{SP}\begin{cases}4^h \leqslant \alpha \leqslant 21^h\\ 30° \leqslant \delta \leqslant 48°\\ 0.03 \leqslant z \leqslant 0.2\end{cases} \tag{1}$$

and contains about 3500 galaxies. The correlated function was obtained at a mean separation scale $\Delta r = 10\ h^{-1}$ Mpc. The catalog was supplied by adding more than 2 000 new redshift estimations (Tucker 1992).

— **Clusters**: 'The Northern Cone of the Metagalaxy' (Kopylov et al. 1987):

$$\mathrm{NP}\begin{cases}11^h \leqslant \alpha \leqslant 15^h\\ -18° \leqslant \delta \leqslant 50°\\ 0.05 \leqslant z \leqslant 0.28\end{cases} \qquad \text{with } N_c = 58\ (R \geqslant 2) \tag{2}$$

and with a mean separation scale in $\xi(r)$ of $\Delta r = 25\ h^{-1}$ Mpc.

— **Superclusters**: 'The Northern Cone of Superclusters' (Lebedev, Lebedeva 1988):

$$\mathrm{NP}\begin{cases}8^h \leqslant \alpha \leqslant 18^h\\ -20° \leqslant \delta \leqslant 90°\\ 0.05 \leqslant z \leqslant 0.15\end{cases} \qquad \text{with } N_{sc} = 49\ (R \geqslant 0,\ D \leqslant 4) \tag{3}$$

and with a mean separation scale in $\xi(r)$ of $\Delta r = 25\ h^{-1}$ Mpc.

The common area of all these catalogs lies on :

$$\mathrm{NP}\begin{cases}11^{h} \leqslant \alpha \leqslant 15^{h} \\ 30^{\circ} \leqslant \delta \leqslant 48^{\circ} \\ 0.05 \leqslant z \leqslant 0.15,\end{cases} \tag{4}$$

some decelated features (for example the Great Wall) being in common.

The Deep Sky Surveys (BEKS 1986, 1988, 1990) consist of two deep surveys spanning 2000 h^{-1} Mpc and two previous bright surveys by others, of which common volume is well approximated by a cylinder of a constant comoving radius. This lies within the CfA slices (also the Great Wall being detected).

In order to realise a comparison between the data of all these catalogs we make a correction of the Universe curvature using the same comoving scale in the form :

$$d = cz/H_0 \quad (H_0 = 100\ h^{-1}\,\mathrm{Mpc}) \tag{5}$$

3. PROCESSING OF SIGNALS IN $\xi(r)$

Generally, the form of the correlation function is :

$$\xi(r) = \begin{cases}(r/r_i)^{-1.8} & r \leqslant r_0^i \\ f_i(r) = f(i, r) & r \geqslant r_0^i\end{cases} \quad i = g, c, sc \tag{6}$$

where r_0^i represents the typical size of the correlation function of the type i. The first term is the normal power-law function for small scales. The larger scale of $\xi(r)$ (second term — long tail of $\xi(r)$) has been poorly studied until now. If we assume $\xi(r)$ as a typical power law relation we must have :

$$\xi(r) \geqslant -1,\ \ \xi(r) \rightarrow 0 \ \text{ for } |r| \rightarrow 0, \ \Rightarrow f_i(r) = 0 \tag{7}$$

Opposite to this, the long tail of the correlation function shows some remanant fluctuations (Kopylov 1987, Suran 1991). We have many possibilities for these fluctuations : random, stationary, phase correlated and high order correlated. This can be related to the chosen model to act at the Large Scale : random gravity (fractal, multifractal), spongeous (both cellular and / or filamentary) or possible symmetry breaking mechanism (cellular).

Each $\xi(r)$ function can be split in the form :

$$\xi_i(r) = \xi_i^S(r) + \xi_i^N(r) = \xi_i^S(r) + [\,\xi_i^{cat,N}(r) + \xi_{i,i+1}{}^N(r)\,] \tag{8}$$

where $\xi^S(r)$-real signals (fluctuations) in $\xi(r)$, $\xi^N(r)$-background noise which in turn is composite by the catalog noise ($\xi^{cat,N}(r)$) and the biasing effect :

$$\xi_{i+1}(r) = [\xi_{i,i+1}(r)]^2 \, \xi_i(r), \quad i = g, c, sc \tag{9}$$

We can reduce the biasing effect considering as fundamental the matter distribution ($\langle \rho_m \rangle$) and a different *contrast parameter* :

$$F_i = \langle \rho_i \rangle \, / \, \langle \rho_m \rangle, \quad i = g, c, sc \tag{10}$$

for each matter component. We have :

$$\delta_i(x) = [\rho_i(x) - \langle \rho_i \rangle] \, / \, \langle \rho_i \rangle, \qquad \xi_i(r) \equiv \langle \delta_i(x), \delta_i(x + r) \rangle \tag{11}$$

with a direct relation $F_i(\rho) \Rightarrow \xi_i(r)$.

The $\xi_i^{cat,N}(r)$ includes the influence of observational errors, effect of periodic boundary conditions, effect of incompleteness of the data (including selection effect and galactic absorption effect) (Einasto 1992 a).

The character of the Large Scale Structure can be extracted directly from the final form of $\xi^s(r)$. Figure 1 a, b makes a comparison between the correlation function $\xi_i(r)$ for the 3D catalogs mentioned in paragraph 2. The visual inspection of these figures reveals :

(i) *correlated fluctuations* in the long tail of $\xi(r)$;

(ii) *biasing effect* :

$$\xi_{g,c} \simeq \xi_{g,sc} \simeq 5-7 \tag{12}$$

(iii) *smoothness effect* :

$$\xi_g^{old,\,10\,Mpc} \simeq \xi_g^{old,\,30\,Mpc} \simeq \xi_g^{new} \tag{13}$$

between the 'old' (Yale 1991, mediated respectively at 10 Mpc and 30 Mpc) and the 'new' (Tucker 1992) data of the YALE Catalog. The effect of *correlated fluctuations* is very important and must be accomplished by a search of periodical events in $\xi^S(r)$.

4. TESTS FOR PERIODIC FLUCTUATIONS IN $\xi^S(r)$

In order to reveal the possible periodic character of the long tail of $\xi(r)$ we have used two statistical tests : FOURIER and statistical WHITTAKER–ROBINSON method (Suran 1991).

(a) FOURRIER ANALYSIS is made by a FFT discrete transformation :

$$[\xi_i(r_j)] \Rightarrow [P_i(k_j)] \Rightarrow FT_x^i(\omega) = F_0^i \sum (A^i X_j^i \cos \omega r_j + i B^i X_j^i \sin \omega r_j) \tag{14}$$

The maxima in power spectrum indicate the possible periods (P_1) to be determined.

(b) WR STATISTICAL METHODS. We used as statistical test:

$$\lambda^2(n) = (1/N) \sum_{i=1}^{n} \xi_{si}^2(r) - (1/k) \sum_{k=1}^{n} \left\{ \sum_{i=1}^{k} [r + (i-1)n] \right\}^2, \quad k = \mathrm{Int}\,(N/n) \tag{15}$$

where the possible minima in $\lambda^2(n)$ indicate the periods (P_n) to be determined.

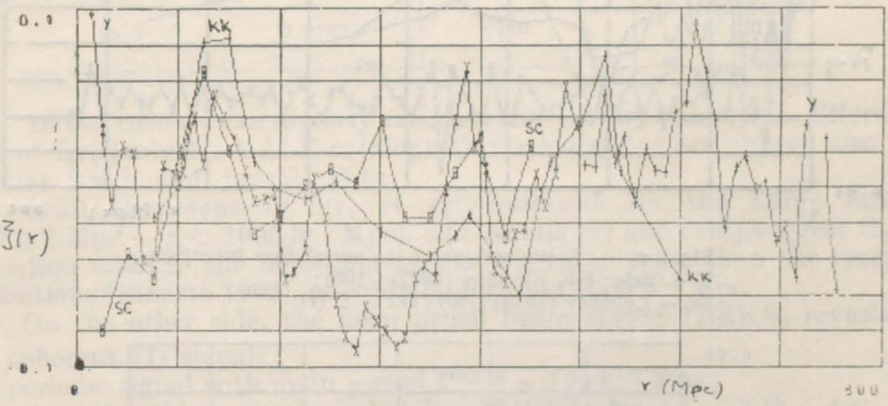

Fig. 1 a.— Comparison between the correlation functions.
Y — Yale correlation function for galaxies
KK — Kopylov et al. (1987) (/6) for clusters
SC — Lebedev, Lebedeva (1988) (/10) for superclusters.

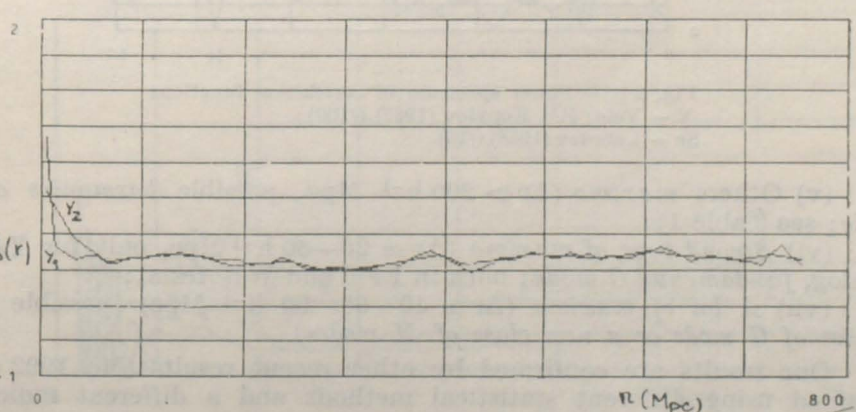

Fig. 1 b. — Yale correlation functions
Y1 — Δr = 10 Mpc
Y2 — Δr = 30 Mpc (mediate)

Figures 2a, b reveal the periodograms of the correlation functions $\xi_1(r)$ and the corresponding 1D power spectrum $P_1(k)$, calculated for the three 3D catalogs. Figure 2 c reveals the results of WR test. The periodograms reveal (Suran 1991):

(iv) *Two maxima* at $\Delta r = 130-150\ h^{-1}$ Mpc scale ($\Delta r \simeq 130$ *fundamental* L *mode* in *all catalogs*) (both in FFT and WR tests);

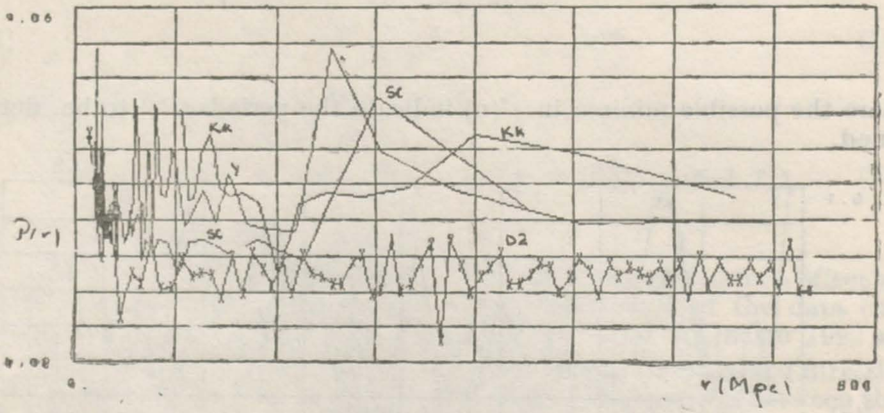

Fig. 2 a. — Periodograms of the correlation functions
Y — Yale; KK Kopylov (1987) (/100);
SC — Lebedev (1988) (/10); D2 = $\xi''(r)$.

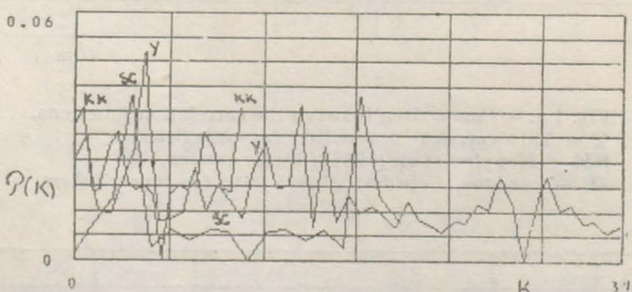

Fig. 2 b. — Power spectrum of correlation functions
Y — Yale; KK Kopylov (1987) (/100);
Sc — Lebedev (1988) (/10)

(v) Others *maxima* ($\Delta r > 200\ h^{-1}$ Mpc, possible *harmonics of* L *mode*; see Table 1);

(vi) *Second type of maxima* ($\Delta r \simeq 20-30\ h^{-1}$ Mpc, only for YALE catalog, *fundamental G mode*; both in FFT and WR tests);

(vii) *A lot of maxima* ($\Delta r \simeq 40-60-90\ h^{-1}$ Mpc) (possible *harmonics of G mode or a new class of M modes).*

Our results are confirmed by other recent results (Mo 1992 q, b) obtained using different statistical methods and a different indicator Ξ (r). But, as is shown in Einasto (1992 b) there is a direct relation between Ξ and ξ:

$$\Xi(r) = \partial^2 \xi(r) / \partial r^2 \tag{16}$$

Table 1

FFT modes (FFT Yale catalog, $\Delta r = 10\ h^{-1}$ Mpc)

P_i (Δr)	Power Spectrum $\langle\lvert\delta_k\rvert\rangle$	P_i (Δr)	Power Spectrum $\langle\lvert\delta_k\rvert\rangle$
$r \leqslant 100\ h^{-1}$ Mpc		$r \geqslant 100\ h^{-1}$ Mpc	
21.7	0.0505	126.6	0.0184
26.6	0.0382	152.0	0.0224
42.2	0.0205	253.3	0.0505
54.2	0.0142	304.0	0.0273
66.0	0.0158	380.0	0.0185
72.3	0.0278	506.6	0.0114
80.0	0.0382	$r \geqslant 550\ h^{-1}$ Mpc	(sampling frequency)
95.0	0.0282	760	0.0119

In our case we can directly estimate the $\Xi(r)$ by numerical differention of $\xi(r)$ (only for YALE catalog). Our calculations are plotted also in Figures 2 a, b and reveal that:

(viii) *the shape of* $\Xi(r)$ *is very unsmooth* on the Large Scale ($100\ h^{-1}$ Mpc $< r < 1000\ h^{-1}$ Mpc). The results (v) and (viii) suggest that transition scale to the homogeneity has a greater value than the recent estimations (Einasto 1992), possibly larger than $1000\ h^{-1}$ Mpc.

On the other side, the deep pencil beam survey (BEKS) reveals:

(A) coherent 1D signals;
(B) periodic signal with main period $P^{BEKS} \simeq 130\ h^{-1}$ Mpc;
(C) a formal null hypothesis probability of P^{BEKS} about $\simeq 2.2$ E $- 4$;
(D) splitting of maxima in N(r) function (N-number of pairs at separation r).

The comparison between our data (Figure 2 a, b) and the corresponding BEKS data (Figure 3, 4 in BEKS 1991) reveals that *our power spectra and periodograms fit very well* (*quite very precisely*) *BEKS power*

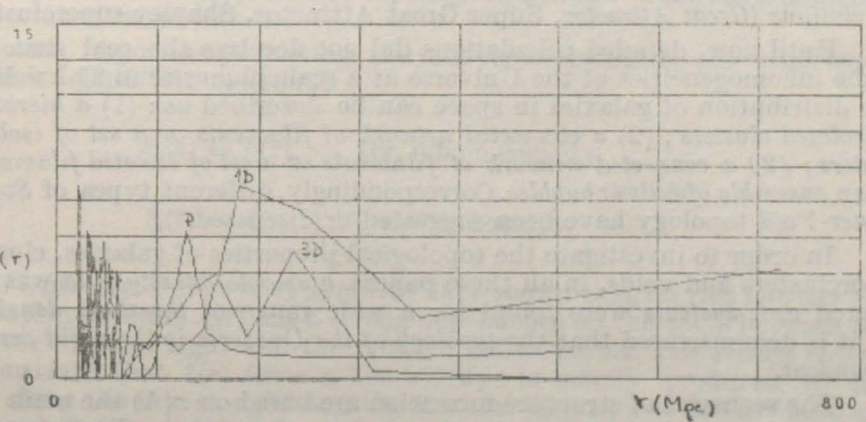

Fig. 3 a. — Periodograms for SHEETS simulations. 1D, 3D are respectively 1D, 3D, N30 periodograms (see text); P — Peebles' model.

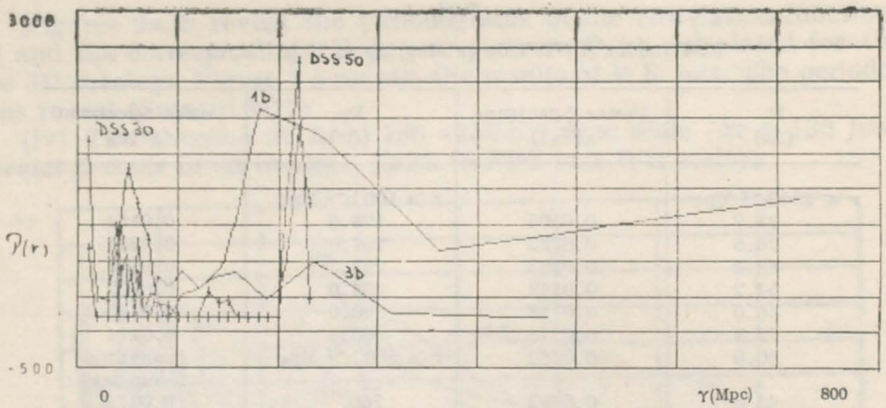

Fig. 3 b. — Comparison between deep sky surveys (DSS) and periodograms for SEEHTS simulations. DSS30 — DSS for N30; DSS50 — DSS for N50; 1D, 3D respective periodograms for N30 (see text).

spectra and periodograms. This implies that:

(ix) *The fine splitting of maxima in* N(r) *is obtained as a superposition of* G + M (?) + L *signals and is present in all four sets of data.*

(x) The *fluctuations* are: *phase correlated*, *periodic* and with the *presence of superlarge scale features up to* 800 h^{-1} Mpc.

5. TOPOLOGICAL SIMULATIONS

As we discussed in the last paragraph, the fluctuations in the long tail of $\xi(r)$ are phase correlated, periodic and with the presence of many superlarge scale features, such as: (1) *fingers of God* (1D—2D); (2) *filaments* (1D); (2) *Great Walls* (1D—2D) and possible other *very high order correlations* (*Great Attractor*, Super Great Attractor, Shapley supercluster).

Until now, detailed calculations did not decelate the real structure of the inhomogeneities of the Universe at a scale higher than 20 h^{-1} Mpc. The distribution of galaxies in space can be described as: (1) *a hierarchy of isolated clusters*; (2) *a connected network of filaments or a set of isolated clusters; (2) a connected network of filaments or a set of isolated filaments*; (3) *an ensemble of cells or bubbles.* Correspondingly, different types of *Supercluster-Void* topology have been suggested or discussed.

In order to investigate the topological properties of galaxies, clusters superclusters and voids, in all these papers, *a smooth density field* was calculated and *systems* were found for a wide range of *threshold densities.* So, it is demonstrated that the *topology of the Universe is threshold density dependent.*

The scenaries of structure formation are based on: (A) the main mechanism of instability (gravitational, symmetry breaking); (B) The initial perturbation spectrum (small Gaussian density fluctuations—$P_i(k)$); (C) The history of galactic formation (biased or not).

Consequently (a) HDM; (b) CDM; (c) String; (d) Domain Walls models could be developed. To test these models, different observational methods were imagined : (1) Two point correlation function; (2) Count in cells; (3) Genus; (4) Multifractals.

The **count in cell** is related to the correlation function of all orders. The case $P_0(V)$ (Void Probability Function—VPF) is used as discriminator of clustering models and is more related to the two point correlation function than the general scaling hierarchies. In the alternative approach, Saslaw and Hamilton (1984) obtained the Hausdorff dimension D_0 *smaller than the correlation dimension* D_2. The ratio $\beta = -W/2K$ of the gravitational correlation energy W to the kinetic energy in peculiar motion K is fixed to :

$$\beta = 0.70 \pm 0.05 \tag{17}$$

Fractal and multifractal calculation applied to the observational catalogs (CfA slices) fixes :

$$D_0 = 2.1 \pm 0.1, \quad D_2 = 1.2 \pm 0.2 \tag{18}$$

This leads to the strong conclusion that : *the Universe is not a simple fractal characterized by one dimension* :

$$D_2 \neq 3 - D_0 \tag{19}$$

The value of D_0 indicates that the characteristic structures are *sheets like* rather *filaments like* ($D_0 \simeq 1$) or *bubbles like* ($D_0 \simeq 2.9$).

The **genus** calculations found that the Universe is *sponge like* on largest scale with no evidence for a *bubbles like* structure. There are voids but they are interconnected. The topology on a smaller scale has a tendency to become *meatball-like.*

Also important in testing the Universe structure, **the correlation function** could tell us about :

$$\begin{aligned} &\xi_1(\mathbf{r}) = f_1(\mathbf{r}) \ — \text{ the inhomogeneity} \\ &\qquad\qquad\qquad\qquad\qquad\qquad \text{and/or} \\ &\xi_1(\mathbf{r}) = \xi(\mathbf{r}, \theta) \ — \text{ the anisotropy} \end{aligned} \tag{20}$$

of the Universe. Fetisova et al (1990) have shown that for rich clusters the correlation function $\xi(\mathbf{r})$ has a strong dependence on the angle between the observer's line of sight and the relative radius-vector. The results clearly demonstrate that $\xi(\mathbf{r})$ for $r \leqslant 100\ h^{-1}$ Mpc is mainly produced by the pairs along the line of sight and the features $\xi(\mathbf{r})$, at $r \sim 250\ h^{-1}$ Mpc are due to the pairs with constant sky projection. So, we have the situation :

$$\xi_{1D} \neq \xi_{2D} \tag{21}$$

Relating these results with the results of the last paragraph we obtain from obsservations the following relations :

$$1D \simeq 3D \simeq DSS;\ 1D, 3D \neq 2D;\ 1D \leqslant 3D;\ 3D_g \leqslant 3D_{cl} \simeq 3D_{sc} \quad (22)$$

These relations imply very drastic limits to the theory. For testing this we made detailed calculations for a cubic box of dimension $L = 1600\ h^{-1}$ Mpc, where we simulated different network distributions. On these network models we threw N random points. On the resulting samples we have calculated deep sky surveys (simulated 1D : DSS) and correlation functions (simulated 3D). For the correlation function we have calculated the coherent signals of $\xi(r, \theta)$ ($\theta = \langle P_i, P_j \rangle$-angular pair separation) :

$$\begin{aligned} &0 \leqslant \theta \leqslant \pi/8 \Rightarrow \text{1D radial signals (fingers of Good in z-direction; 1D)} \\ &3\pi/8 \leqslant \theta \leqslant \pi/2 \Rightarrow \text{2D transverse signals (Great Wall features; 2D)} \end{aligned} \quad (23)$$

Calculated $\xi_t(r, \theta)$ were compared with the observational data (22) in order to discriminate between the different networks.

As particular network we have chosen : (a) intersecting sheets; (b) arclets; (c) soap froth.

Intersecting sheets: Random intersecting sheets with infinitesimal thickness ($N_{sheets} = 30 - 50$; N 30, N 50) with $N = 100$ random points (g, c, sc) on these sheets. The simulated network is *the cellular model.*

Arclets: Random intersecting spheres ($N_{spheres} = 200 - 2500$) with random dimensions of spheres ($20 \leqslant d \leqslant 50$ Mpc), with infinitesimal thickness of shells on the spheres ($\Delta d \leqslant 5$ Mpc) and with $N = 100 - 400$ random points on shells. The simulated network is *the bubbles model.*

Soap Froth: Creation of a texture formed by tangent hard spheres, ergodic arranged in the volume V with random dimensions of hard spheres ($20 \leqslant d \leqslant 50$ Mpc) with infinitesimal thickness of shells on the spheres ($\Delta d \leqslant 5$ Mpc) and with random points on shells + interspaces ($N = 100 - 400$). The simulated network is that *of an ergodic theory* (symmetry breaking model).

We have obtained the following results :

Sheets: $1D \simeq 3D$ (as shape); $2D \neq 1D, 3D$; $DSS \simeq 1D, 3D$, our N30 model $\equiv$ Peebles sheets model : $\xi(r) = (1/6)\ [\lambda/r + 2\lambda/r\ \mathrm{Int}(r/\lambda) - 2]$ (for periodicity at $130\ h^{-1}$ Mpc),

$$\beta = 2.2 \text{ for N30 (de Lapparent et al. 1990) (see Figures 3 a, b)} \quad (23\text{ a})$$

Arclets: $1D \simeq 2D \simeq 3D$; $DSS \leqslant 1D, 3D$, $\beta = 2.9$ (de Lapparent et al 1990) (see Figures 4 a, b) (23 b)

Soap froth: $DSS \leqslant 1D, 3D$ (see Figure 4 a) (23 c)

From these relations we have obtained that:

(xi) *the sheets model is the most probable for the topological texture* in accordance with other estimations.

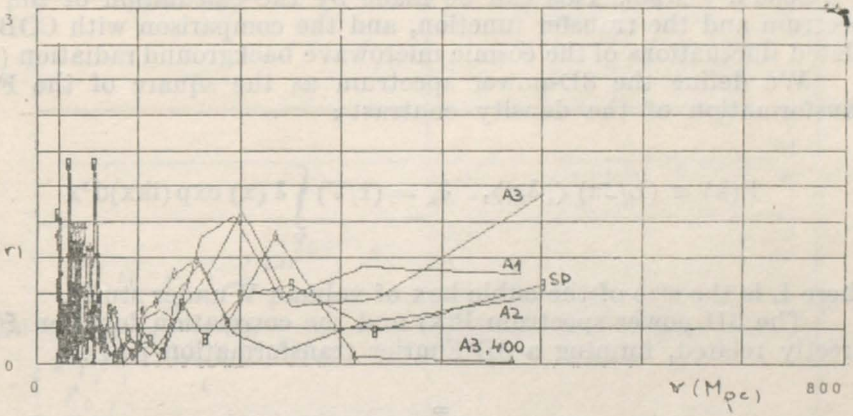

Fig. 4 a. — Periodograms for ARCLETS and SOAP FROTH simulations. A1, A2, A3 — respectively ARCLETS (N = 5000), 1D, 2D, 3D periodograms; A4, 3 — ARCLETS (N = 400) 3D periodogram; SP — SOAP FROTH 3D periodogram.

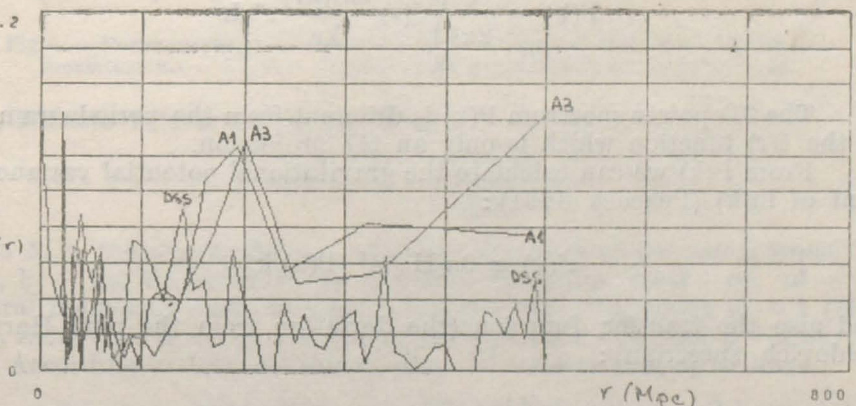

Fig. 4 b. — Comparison between deep sky surveys and periodograms for ARCLETS simulations. DSS-DSS for ARCLETS with N = 5000; other notations as in Figure 4 a.

However, there exists the possibility that at a scale larger than $r \geqslant 300\ h^{-1}$ Mpc the sheets model has not enough power to decelate super-large features ($\simeq 500\ h^{-1}$ Mpc). We have only two maxima at $130\ h^{-1}$ and $250\ h^{-1}$ Mpc (see Figures 3 a, b), and only one maximum at $130\ h^{-1}$Mpc in the Peebles model. It is possible that at scale $r \geqslant 300\ h^{-1}$ Mpc a different larger network occurs (superfilaments mainly 2D).

6. POWER SPECTRUM CALCULATIONS

One of our aims is to relate our calculations at large scale ($100\ h^{-1}$ Mpc $\leqslant r \leqslant 800\ h^{-1}$ Mpc) to a superlarge scale of the Universe ($r \geqslant 1000\ h^{-1}$ Mpc). This can be made by the calculation of the power spectrum and the transfer function, and the comparison with COBE decelated fluctuations of the cosmic microwave background radiation (CBR).

We define the 3D-power spectrum as the square of the Fourier transformation of the density contrast :

$$P(k) \equiv (L/2\pi) \langle |\delta_k| \rangle, \quad \delta_k = (1/V) \int_V \delta(x) \exp(ikx) d^3x \tag{24}$$

where L is the size of the cubic box of volume V under study.

The 3D power spectrum P(k) and the correlation function $\xi(r)$ are directly related, forming a 3D-Fourier transformation pair :

$$\xi(r) = 4\pi \int_0^\infty P(k) \frac{\sin(kr)}{kr} k^2\, dk$$

$$P(k) = \frac{1}{2\pi^2} \int_0^\infty \xi(r) \frac{\sin(kr)}{kr} r^2\, dr \tag{25}$$

The 3D power spectrum P(k) is different from the periodogram P(k) of the $\xi(r)$ function which is only an 1D projection.

From P(k) we can calculate the gravitational potential variance per unit of ln(k) (Peacock 1991) :

$$\varepsilon^2(k) \equiv 9\pi (H_0/c)^4\, [P(k)/k] \tag{26}$$

and also the transfer function (the deviation from the pure Harrison-Zeldovich spectrum) :

$$T_f(k) = \varepsilon(k)/\varepsilon_0 = (3\pi^{1/2}/\varepsilon_0)\, (H_0/c)^2\, [P(k)/k]^{1/2} \tag{27}$$

The transfer function relates initial fluctuations (i ; usual from CBR) to the final ones (f ; usual at large scale) :

$$P_f(k) = T_f(k)\, P_i \tag{28}$$

On one side we can make this calculation using the observed $\xi(r)$ from the YALE catalog of galaxies mediated at $\Delta r = 10\ h^1$ Mpc. The results are presented in Figure 5.

On the other side we can compare our results with some theoretical power spectrum determinations at both limiting intermediate scale ($10\ h^{-1}$ Mpc $\leqslant r \leqslant 100\ h^{-1}$ Mpc) and superlarge scale ($r \geqslant 1000\ h^{-1}$ Mpc). We adopt the theoretical double power spectrum in the form (Peacock

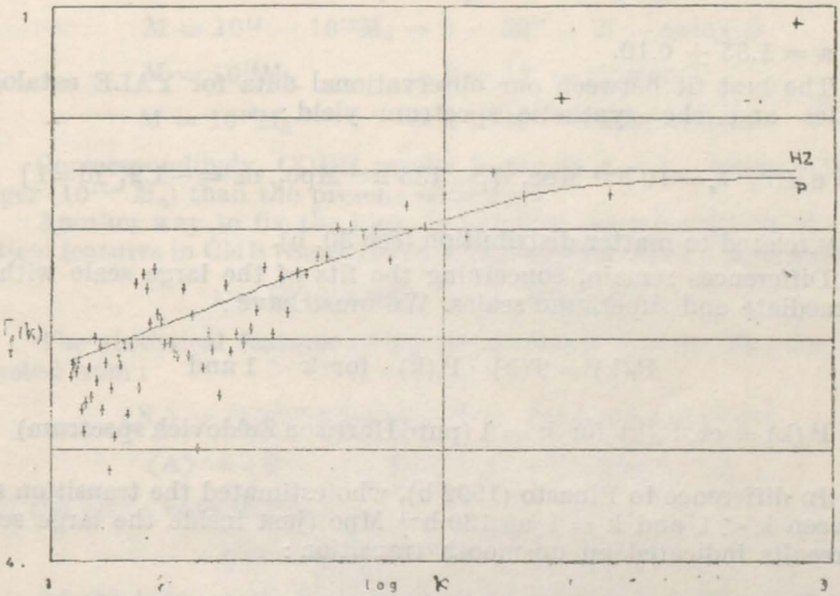

Fig. 5. — Power spectrum calculations : (+) — Yale power spectrum ; (P) Peacock simulations (ns = 1.2, nl = 1) ; HZ — Harrison Zeldovich spectrum (n = 1).

1991, Einasto 1992 a, Mo et al. 1992) :

$$P(k) = A_l \frac{(k/k_s)^{ns}}{1 + (k/k_l)^{ns-nl}} \tag{29}$$

where A_l — the amplitude, k_s — the wavenumber at the small transition scale, k_l — the wavenumber at the large transition scale ; ns, nl — the spectral indices at small and large wavelengths. We adopt nl = 1 (Harrison, Zeldovich spectrum) at the superlarge scale $r \geqslant 1000\ h^{-1}$ Mpc.

According to different estimations (Einasto 1992 a, b) we have :

$[A_c = 6.5,\ \lambda_s = 10\ h^{-1}\ \mathrm{Mpc},\ \lambda_l = 135\ h^{-1}\ \mathrm{Mpc},\ ns = -2.1,\ nl = 1]$
(clusters of galaxies Einasto 1992 a) ;

$[A_m = 0.75,\ \lambda_s = 1\ h^{-1}\ \mathrm{Mpc},\ \lambda_l = 135\ h^{-1}\ \mathrm{Mpc},\ ns = -1.2,\ nl = 1]$
(matter distribution, Einasto 1992 a) ;

$[\lambda_l = 175\ h^{-1}\ \mathrm{Mpc},\ ns = -1.6,\ nl = 1]$
(transition scale, Einasto 1992 b) ;

$[\varepsilon_0 = 2.7\ \mathrm{E} - 5,\ \lambda_l = 190\ h^{-1}\ \mathrm{Mpc},\ ns = -1.5,\ nl = 1]$
(COBE results, Peacock 1992) (30)

where $\lambda_1 = 2\pi/k_1$, $\lambda_s = 2\pi/k_s$. We have assumed to exist a relationship between the transition scale in Fourier space and real space (Einasto 1992b) :

$$\lambda_1 = a.r_1 \tag{31}$$

with $a = 1.35 \pm 0.10$.

The best fit between our observational data for YALE catalog of galaxies and the synthetic spectrum yield :

$$[A_s = 0.818,\ \lambda_s = 10\ h^{-1}\ \mathrm{Mpc},\ \lambda_1 = 135\ h^{-1}\ \mathrm{Mpc},\ ns = -1.2,\ nl = 1] \tag{32}$$

closely related to matter distribution (see 30. b).

Differences remain, concerning the fits of the large scale with the intermediate and superlarge scales. We must have :

$$P_f(k) = T(k) \cdot P_i(k) \quad \text{for } k < 1 \text{ and}$$

$$P_f(k) = ct.\ P_i(k) \ \text{ for } k = 1 \text{ (pure Harrison Zeldovich spectrum)} \tag{33}$$

In difference to Einasto (1992 b), who estimated the transition scale (between $k < 1$ and $k = 1$ at $130\ h^{-1}$ Mpc (just inside the large scale), our results indicated an unsmooth transition :

$$T_f(k) \neq ct \qquad \text{up to } 800\ h^{-1}\ \mathrm{Mpc} \tag{34}$$

(see Figure 5).

(xii) This means that the large scale ($100\ h^{-1}$ Mpc $\leqslant r \leqslant 1000\ h^{-1}$ Mpc) is *inside* and not *outside the inhomogeneity scale and the spectral index at* $r \leqslant 1000\ h^{-1}$ Mpc ($z \leqslant 0.3$) *is different yet from the spectrum* of CBR ($z \simeq z_{rec} \simeq 1000$).

Recent calculations of Mo et al. (1992) suggest that even at high redshift $1.89 < z < 3.78$ the features ($\leqslant 200\ h^{-1}$ Mpc) are the same as at low z. Campusano (1992) also reports some features 'Great Walls like' at redshift $z \simeq 1.3$, formed mainly from quasars.

(xiii). This means that *we must move* the transition scale *somewhere between* $5 < z < 1000$.

Also from Figure 5 we can estimate the local maxima in our observed $T_f(k)$ function :

$$\lambda_1 = 60\ h^{-1}\ \mathrm{Mpc},\ \lambda_2 = 90\ h^{-1}\ \mathrm{Mpc},\ \lambda_3 = 130\ h^{-1}\ \mathrm{Mpc},$$

$$\lambda_4 = 250\ h^{-1}\ \mathrm{Mpc},\ \lambda_5 = 500\ h^{-1}\ \mathrm{Mpc} \tag{35}$$

in accordance with the shape of $\xi(r)$ and $\Xi(r)$.

On the other side it is useful to compare the COBE anisotropy scale on CBR ($\simeq 7°$, Smooth 1992) with the correspondent scale of present decelated structures. We used the cosmological formulae :

$$\Delta\ \theta \simeq 17'\ \Omega^{2/3}\, h^{1/3}\, (M/10^{15}\, M_0)^{1/3} \tag{36}$$

which in the case $\Omega = h = 1$, $z = z_{rec}$ yields the typical scales :

$$\begin{aligned} M &= 10^{11} - 10^{12} M_0 \Rightarrow \theta = 50'' - 2' - \text{galaxies} \\ M &= 10^{15} M_0 \qquad \Rightarrow \theta = 18' - \text{clusters} \\ M &= 10^{16} M_0 \qquad \Rightarrow \theta = 40' - \text{superclusters} \end{aligned} \tag{37}$$

Corrterspondingly, COBE results imply at $z = z_{rec}$ features 10 times larger (10^{17-} M_0) than the present structures.

Another way to fix the ideas is to follow the calculations of the statistical features in CMB (Sanz 1990), which depend on two parameters

$$\lambda = C''(0)/C(0), \qquad \nu = T/[C(0)]^{1/2} \tag{38}$$

The statistical features of the temperature fluctuations can be extracted from :

$$\begin{aligned} \langle N_s \rangle &= (2/\pi\lambda^2)e^{-\nu}/\text{erfc}(\nu/2^{1/2}), \quad \langle N_p \rangle = \cos(\delta^2)\lambda^{\nu/2} \\ \langle A \rangle &= \langle \theta \rangle^2, \qquad \langle \theta \rangle = \pi^{-1/2}\, \lambda^2 e^{\nu/2}\, \text{erfc}(\nu/2^{1/2}) \end{aligned} \tag{39}$$

and the genus calculations :

$$\langle G \rangle = \text{erfc}(\nu/2^{1/2}) + (2/\pi)^{1/2} \lambda^4\, e^{-\nu^2/2} \tag{40}$$

At the large and superlarge scale the dominant effect is the Sachs Wolf (SW) effect with the temperature correlation function :

$$a_l^2 = (8/\pi) \int dk.k^2\, P(k) j^{\pi,2}(k),\ C(\alpha) =$$

$$= (18/\pi^2) \int dk.k^{-2} P(k) j_0(k\beta),\ \beta \equiv 2\sin(\alpha/2) \tag{41}$$

From (41) we see that the shape of C(0) and $\xi(r)$ function is similar. Also we can define :

$$\lambda_1 = \xi''(r)/\xi(r) \quad \text{and} \quad \nu_{1,l} \equiv F_l \tag{42}$$

where F_l is the threshold value.

Because in our cases ($r < 1000\ h^{-1}$ Mpc) $\xi''(r)$, $\xi(r) \neq$ ct., we have λ_1, $\nu_1 \neq$ ct ; λ, $\nu \neq$ ct. and respectively $\langle \theta \rangle$, $\langle G \rangle \neq$ ct.

7. CONCLUSIONS

Our work tries to develop a new method in the investigation of the L arge Scale Structure of the Universe : *the long tail of the correlation function.*

We made a statistical analysis of the signals in the long tail of the correlation function $\xi(r)$, for different deep 3D catalogs (galaxies, clusters, superclusters). We made a comparison of our results with tbe theoretical simulations in order to derive the present texture of the Universe. Power spectrum and transfer function calculations were also made for the correlation of our large scale ($100\ h^{-1}$ Mpc $< r < 1000\ h^{-1}$ Mpc) with the superlarge scale (COBE results for CBR spectrum).

The main results are:

● *Fluctuations* on the intermediate scale are correlated, periodically, with the presence of the superlarge scale features up to $800\ h^{-1}$ Mpc;

● The *biasing* effect is estimated at $\xi_c = 5-7$, $\xi_{sc} = 10$;

● The *periodograms* of $\xi(r)$ reveal *maxima* at intermediate scale ($25\ h^{-1}$ Mpc — G mode), medium scale (60, $90\ h^{-1}$ Mpc—M mode), large scale (130, 250, $500\ h^{-1}$ Mpc — L mode and ist harmonics).

● The shape of $\Xi(r)$ is very *unsmooth* on large scale.

The most probable *texture* of the Universe at $r < 300\ h^{-1}$ is *the cellular one*:

$$1D \simeq 3D \simeq DSS,\ 1D \simeq 3D \neq 2D,\ 1D \ll 3D,\ 3D_g \ll 3D_c = 3D_{sc},$$

$$D_0 = 2.1, \quad D_2 = 1.2 \tag{43}$$

● *Power spectrum* calculation yields: $[A_g = 0.818,\ \lambda_1 = 135\ h^{-1}\mathrm{Mpc},\ ns = -1.2,\ nl = 1]$ and confirms the existence of *local maxima* in the observed $T_f(r)$.

● The *presence of larger features* at $250\ h^{-1}$ Mpc, $500\ h^{-1}$ Mpc and the *unsmoothness* of $\Xi(r)$, show that yet we *have not decelated* the transition scale ($T_f \neq$ ct.)

● The COBE results suggest the presence of *very large fluctuations* at the CBR scale. These fluctuations are larger than our samples scale.

* Paper presented at the International Symposium *Observational Cosmology* (Milano, September 1992).

REFERENCES

Campusano, L. E. 1992, in *Symp. Observational Cosmology*, Milano (in press);
de Lapparent, V., Geller, M. J., Huchra, J. P. 1990, Ap. J., **369**,, *273*.
Einasto, J., Gramann, M., Tago, E. 1992, ESO Preprint, No. **841**.
Einasto, J., Gramann, M. 1992, ESO Preprint, No. **846**.
Fetisova, T. S., Kuznetov, D. Yu. Starobinsky, D. A. 1990, Soob. Spec. Astrophys. Obs., **64**, *97*.
Ishihara, H., Kubotani, H., Nambu, Y. 1991, *Numerical Astrophysics in Japan*, **2**, *351*;
Kopylov, A. I., Kuznetov, D. Yu, Fetisova, T. S., Schvartsman, V. I. 1987, Sobscenie SAO, **53** *59*,.
Lebedev, V. S. Lebedeva, I. D. 1988, Pisma Astr. Zh., **14**, *18*.
Mo, H. J., Xia, X. Y., Dang, Z. G., Borner, G., Fang. L. Z. 1992, Astron. Astrophys, **256**, *L23*.
Mo, H. J., Dang, Z. G., Xia, X. Y., Schiller, P., Borner, G. 1992, Astron. Astrophys, **257**, *1*.
Peacock, J. A. 1991, M.N.R.A.S., **253**, *1*.
Peebles, P. J. E. 1980, in *The Large Scale Structure of the Universe*, Princeton University Press.
Peebles, P. J. E. 1989, in *Fractals in Physics*, ed. A. Aharony, J. Feder.
Saslaw, W. C., Hamilton, A. J. S. 1984, Ap. J., **276**, *13*.
Smoot, G. 1992, in *Symp. Observational Cosmology*, Milano, (in press).
Suran, M. D. 1991, paper presented at 21 IAU General Assembly, Buenos Aires.
Suran, M. D., Popescu, N. A. 1992, in *Symp. Observational Cosmology*, Milano, (in press)
Szalay, A. S., Ellis, R. S., Koo, D. C., Broadhurst, T. J. 1990, Nature, **343**, *726* (BEKS). 1991, in *After the First Three Minutes*, ed. S. Holt.
Tucker, D. 1992, in *Symp. Observational Cosmology*, Milano (in press).

GRAVITATIONAL ENERGY FOR A CLASS OF RELATIVISTIC STELLAR MODELS

VASILE URECHE
University of Cluj-Napoca, Faculty of Mathematics, Str. M. Kogălniceanu 1, 3400 Cluj-Napoca Romania

TIBERIU OPROIU
Astronomical Institute of the Romanian Academy, Astronomical Observatory Cluj-Napoca Str. Cireşilor 19, 3400 Cluj-Napoca, Romania

Abstract. The paper deals with the determination of the gravitational energy at barotropic stellar models in a relativistic approximation. The way to calculate the gravitational packing coefficient is shown. The numerical estimates are tabulated and plotted. One can conclude that the gravitational energy represents a significant part of the total stellar energy.

Key Words: relativistic stars — barotropic models — gravitational energy

1. INTRODUCTION

As it is known, in the last phase of stellar evolution, relativistic objects are formed especially from neutronic stars and black holes (Zeldovich and Novikov, 1971; Misner et al., 1977). The relativistic stars possess a strong gravitational field, therefore an important fraction from their total energy is "packed" in form of gravitational energy. The study of energetic processes inside and outside the relativistic configurations requires the knowledge of their gravitational energy.

The measure of gravitational energy of a relativistic star is given by the coefficient of gravitational packing. The total energy of a stellar configuration is given by $E = Mc^2$ (M = total mass of the star); with the assumption of the spherical symmetry M is given by the expression

$$M = 4\pi \int_0^R \rho(r) r^2 \, \mathrm{d}r, \tag{1}$$

where $\rho(r)$ is the total mass density.

Besides the total energy E, we can define another kind of energy E_1, which includes the rest mass energy ($E_0 = M_0 c^2$), as well as the energy of the microscopic motions, but not the gravitational energy, this one being included in E.

The expression of E_1 is given by (Zeldovich and Novikov, 1971):

$$E_1 = M_1 c^2, \tag{2}$$

where

$$M_1 = \int_V \rho \, \mathrm{d}V = 4\pi \int_0^R \rho(r) r^2 \, e^{\lambda(r)/2} \, \mathrm{d}r, \tag{3}$$

$\mathrm{d}V = 4\pi r^2 \, e^{\lambda(r)/2} \mathrm{d}r$ being the elementary volume. The function $e^{\lambda(r)}$ can be obtained from Einstein's equations.

If we denote $\Delta M = M_1 - M$, then $c^2 \Delta M = -U$ represents the total gravitational energy (negative).

The ratio

$$k = |U|/E = \Delta M / M, \tag{4}$$

is called gravitational packing coefficient.

By using the non-dimensional variables (Ureche, 1980), the coefficient k can be expressed as follows :

$$k = (m_{1s} - m_s)/m_s, \tag{5}$$

where

$$m_s = \int_0^{\eta_s} \psi \eta^2 \, \mathrm{d}\eta, \tag{6}$$

$$m_{1s} = \int_0^{\eta_s} \psi \, e^{\lambda/2} \eta^2 \, \mathrm{d}\eta, \tag{7}$$

$$e^{\lambda/2} = (1 - 2\, m/\eta)^{-1/2}, \tag{8}$$

and the notations are the usual ones (Ureche, 1983).

In the next section there will be given a way to estimate the coefficient k for a class of relativistic configurations of barotropic type.

2. BASIC EQUATIONS

The theory for te relativistic approximation for a new class of barotropic stellar models was developed by Ureche (1991). The equation of state (in non-dimensional form) is :

$$p = \alpha \psi + (p_c - \alpha) \psi^2, \tag{9}$$

where the parameters p_c and α will vary in the domain

$$D = \{(p_c, \alpha) \mid 0 \leqslant p_c \leqslant 1, \, 0 \leqslant \alpha \leqslant p_c\} \tag{10}$$

The coupled equations which describe the structure of these barotropic stellar models for the relativistic approximation have the following form (Ureche, 1991):

$$\frac{\mathrm{d}m}{\mathrm{d}\eta} = \eta^2\psi, \tag{11}$$

$$\frac{\mathrm{d}\psi}{\mathrm{d}\eta} = -\frac{[(\alpha+1)\psi + (p_c-\alpha)\psi^2]\,[m + \eta^3(\alpha\psi + (p_c-\alpha)\psi^2)]}{\eta^2(1-2m/\eta)\,[\alpha + 2\,(p_c-\alpha)\psi]}, \tag{12}$$

with the boundary conditions:

$$m(0) = 0, \quad \psi(0) = 1, \quad \psi(\eta_s) = 0, \tag{13}$$

where η_s is the value of the non-dimensional coordinate η at the star surface.

In order to determine the coefficient of gravitational packing, we add to equations (11) + (12) the equation:

$$\frac{\mathrm{d}m_1}{\mathrm{d}\eta} = \psi e^{\lambda/2}\,\eta^2, \tag{14}$$

with the boundary condition:

$$m_1(0) = 0, \tag{15}$$

and $e^{\lambda/2}$ given by Eq. (8).

If, instead of the independent variable η, we shall introduce the new variable y by means of transformation:

$$\eta = \eta_s y, \tag{16}$$

where $y \in [0, 1]$ for $\eta \in [0, \eta_s]$, η_s being the non-dimensional radius of the star. Then Eqs. (11) + (12) + (14) can be written in the form:

$$\frac{\mathrm{d}m}{\mathrm{d}y} = \eta_s^3 y^2\psi, \tag{17}$$

$$\frac{\mathrm{d}\psi}{\mathrm{d}y} = -\frac{[(\alpha+1)\psi + (p_c-\alpha)\psi^2]\,\{m + \eta_s^3 y^3[\alpha\psi + (p_c-\alpha)\psi^2]\}}{y^2\,(\eta_s - 2m/y)[\alpha + 2(p_c-\alpha)\psi]}, \tag{18}$$

$$\frac{\mathrm{d}m_1}{\mathrm{d}y} = \eta_s^3\, e^{\lambda/2} y^2\psi, \tag{19}$$

with the boundary conditions :

$$m(0) = 0, \ \psi(0) = 1, \ \ m_1(0) = 0, \tag{20}$$

and the integration is performed on the interval $[0, 1]$; the nondimensional pressure is given by Eq. (9).

In this case, the packing coefficient k is given by relation :

$$k = \frac{m_1(1)}{m(1)} - 1 = \frac{\int_0^1 y^2\psi(y)\, e^{\lambda/2}\, \mathrm{d}y}{\int_0^1 y^2\psi(y)\, \mathrm{d}y} - 1, \tag{21}$$

with the assumption that the functions $m = m(y)$, $\psi = \psi(y)$, $y \in [0, 1]$ are known.

3. NUMERICAL RESULTS

The system of Eqs. (11)+(12) + (14) with the boundary conditions (13) + (15) has been integrated numerically by using the Runge-Kutta method (Gill's variant). The numerical integration has been considered to end when :

$$|\psi(\eta)| < \varepsilon \tag{22}$$

where we considered $\varepsilon = 0.01$. The value of η for which the previous inequality is fulfilled is considered to be equal to η_s. The parameters $m_s = m(\eta_s)$ and $m_{1s} = m_1(\eta_s)$, from which the coefficient k can be found, are simultaneously obtained.

The coefficient of gravitational packing, k, was computed for the following values of p_c, $p_c = ih$, $h = 0.1$, $i = \overline{0,10}$; $p_c = 1/3$ and values of α in the interval $[0, p_c]$, with the step 0.1 (except the case $\alpha = 1/3$). For each couple (p_c, α), both k and η_s were computed. The results are listed in Table 1. Some precision as to this table : the integration step was taken 0.05 ; the accuracy in computing the functions $m(\eta)$, $\psi(\eta()$, $m_1(\eta)$ was taken 0.0001 ; the value η_s for which $|\psi(\eta_s)| < 0.01$ can be considered as having the accuracy of 0.05.

Let us introduce the function

$$K(y, p_c, \alpha) = \frac{m_1(y) - m(y)}{m(y)}, \tag{23}$$

Obviously, $k = K(1, p_c, \alpha)$. Table 2 lists the values of the function $K(y, p_c, \alpha)$ vs. y for $\alpha \in \{0.05, 0.2\}$ and $p_c \in \{0.2, 1/3, 1\}$ for each α. There are also given the values of η_s. The data from Table 2 were obtained by numerical integration of Eqs. (17) — (20); the integration step was taken 0.01 and accuracy in computing was taken 0.0001.

Table 1

k		1.0	0.9	0.8	0.7	0.6	0.5	0.4	1/3	0.3	0.2	0.1	0.0	α / p_c
0.0	—	15.70	15.65	15.65	15.60	15.45	15.20	14.70	14.05	13.55	10.40	4.50	2.10	1.0
0.1	0.124	0.158	15.65	15.65	15.60	15.45	15.20	14.75	14.15	13.70	10.65	4.55	2.05	0.9
0.2	0.210	0.189	0.249	15.65	15.55	15.45	15.20	14.80	14.20	13.80	10.95	4.65	2.00	0.8
0.3	0.274	0.248	0.255	0.306	15.55	15.45	15.20	14.80	14.30	13.90	11.30	4.80	1.90	0.7
1/3	0.292	0.268	0.259	0.307	0.321	15.40	15.20	14.80	14.35	14.00	11.65	5.05	1.85	0.6
0.4	0.322	0.303	0.267	0.309	0.322	0.344	15.15	14.80	14.40	14.05	12.05	5.45	1.80	0.5
0.5	0.360	0.346	0.282	0.313	0.325	0.346	0.370	14.75	14.40	14.10	12.45	6.15	1.70	0.4
0.6	0.391	0.378	0.298	0.318	0.329	0.349	0.372	0.387	14.35	14.10	12.65	6.90	1.60	1/3
0.7	0.415	0.404	0.315	0.324	0.333	0.352	0.374	0.389	0.398	14.10	12.75	7.40	1.55	0.3
0.8	0.436	0.424	0.332	0.330	0.339	0.355	0.376	0.390	0.400	0.405	12.90	9.15	1.40	0.2
0.9	0.453	0.441	0.348	0.336	0.343	0.358	0.378	0.392	0.401	0.406	0.408	10.50	1.15	0.1
1.0	0.467	0.455	0.362	0.343	0.348	0.362	0.380	0.394	0.402	0.407	0.410	0.409	—	0.0
p_c / α	0.0	0.1	0.2	0.3	1/3	0.4	0.5	0.6	0.7	0.8	0.9	1.0	η_s	

Table 2

y	$\alpha = 0.05$			$\alpha = 0.2$		
	$p_c = 0.2$	$p_c = 1/3$	$p_c = 1.0$	$p_c = 0.2$	$p_c = 1/3$	$p_c = 1.0$
	$\eta_s = 3.80$	$\eta_s = 3.04$	$\eta_s = 2.92$	$\eta_s = 12.88$	$\eta_s = 12.63$	$\eta_s = 10.40$
0.0	0.000	0.000	0.000	0.000	0.000	0.000
0.1	0.028	0.018	0.017	0.164	0.211	0.193
0.2	0.102	0.072	0.068	0.240	0.302	0.433
0.3	0.177	0.152	0.150	0.257	0.309	0.456
0.4	0.210	0.232	0.254	0.261	0.303	0.448
0.5	0.217	0.280	0.360	0.260	0.294	0.435
0.6	0.218	0.294	0.429	0.258	0.286	0.421
0.7	0.217	0.296	0.459	0.255	0.277	0.406
0.8	0.216	0.296	0.466	0.253	0.270	0.391
0.9	0.215	0.296	0.466	0.251	0.264	0.376
1.0	0.214	0.295	0.466	0.249	0.259	0.362

Figure 1 plots $k = k(p_c, \alpha)$ for $p_c \in \{0,5, 1\}$ Observe an obvious minimum on both curves for $\alpha < 0.3$, and a tendency of maximum for $\alpha < 0.1$. For $\alpha > 0.3$ the coefficient k presents a quasi-linear increase, tending to an asymptotic stabilization.

Figure 2 plots $k = k(p_c, \alpha)$ for $\alpha \in \{0, 0.1, 0.3, 0.5\}$. Observe that for α near zero the values $k = k(p_c)$ increase faster than in other cases (e.g. for $\alpha > 0.3$). For $\alpha > 0.5$ the dependence of k on p_c is weaker.

Figure 3 plots $K = K(y, p_c, \alpha)$ for $\alpha = 0.05$ and $p_c \in \{0.2, 1/3, 1\}$. Observe that for small values of y (near configuration centre) K increases rapidly (great slope), then seems to be stabilized.

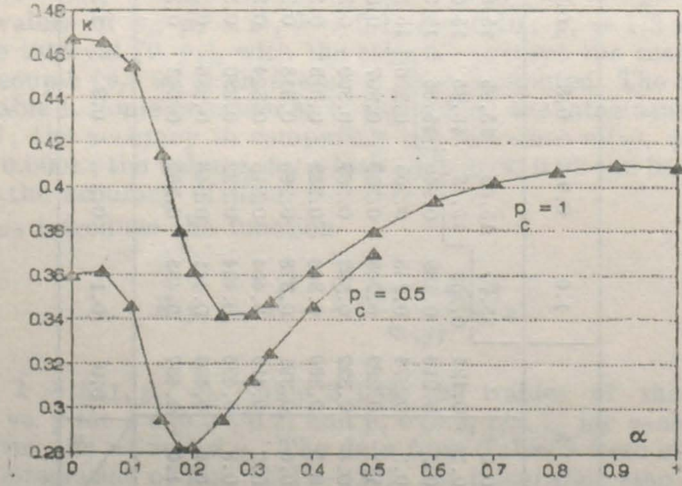

Fig. 1

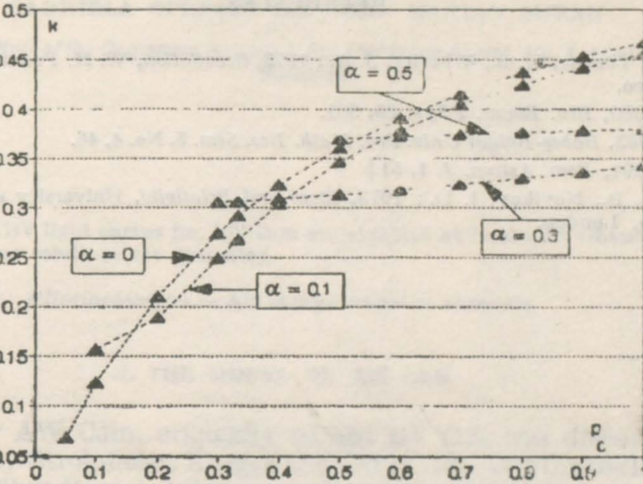

Fig. 2

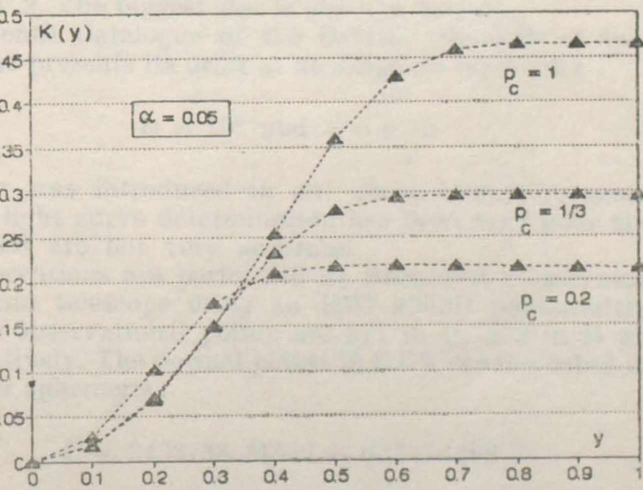

Fig. 3

Both tables and figures lead to the following conclusions :

(1) The relativistic configurations belonging to the considered class pack a significant fraction of the total energy under the form of gravitational energy.

(2) For fixed α the gravitational energy increases with p_c, as expected.

(3) For fixed p_c the gravitational energy considered as a function of α has a minimum for a certain value of α, value to which corresponds the configuration with the weakest gravitational field (for the considered p_c).

REFERENCES

Misner, C. W., Thorne, K. S., Wheeler, J. A. : 1973, *Gravitation*, W. H. Freeman and Co., San Francisco.

Ureche, V. : 1980, *Rev. Roum. Phys.* 25, 301.

Ureche, V. : 1983, *Babeş-Bolyai Univ. Fac. Math. Res. Sem.* 5, No. 4, 46.

Ureche, V. : 1991, *Rom. Astron. J.* 1, 51.

Zeldovich, Ya. B., Novikov, I. D. : 1973, *Stars and Relativity*, University of Chicago Press, Chicago, London.

THE STELLAR SYSTEM AW Cam

GABRIELA OPRESCU and DORU MARIAN SURAN

Astronomical Institute of the Romanian Academy, Str. Cuţitul de Argint, No. 5, 75212 Bucharest 28, Romania

Abstract. UBV light curves for AW Cam are obtained at Bucharest Observatory. Light curves solutions are presented.

Key Words: *eclipsing binaires* — AW Cam photometry, elements

1. THE MODEL OF AW CAM

The star AW Cam, originally named BV 412, was discovered as a variable star by Strohmeier, Knigge and Ott (1963). The Cracovian Annual for 1992 describes it as a 8.0 magnitude star, with minima of amplitude $0.^m35$ and $0.^m06$ respectively.

Photometrically and spectroscopically it is considered that the principal minimum is a transit. The spectral classes of the two components are AΦV and F 2. The biggest star is also the hottest.

The Seventh Catalogue of the Orbital Elements of Spectroscopic Binary Systems presents its orbit as an elliptical one with:

$$\omega = 10^\circ \text{ and } e = 0.12.$$

This star was introduced in our observational program because until now the light curve determination has been very poor and the elements computed are not very accurate.

Our observations are performed at Bucharest Observatory with a 50 cm Cassegrain telescope using an EMI 9502B photomultiplier. The number of the observational points are 371 in U, 372 in B and 403 in V filters respectively. The normal points in UBV are indicated in Table 1.

Using the ephemeris:

$$P = 2438738.^d4522 + 0.^d7713468.E$$

two minima were calculated. The (O−C) values obtained are respectively:

Julian Date	O−C	Min	Filter
2447972.2460	+0.0013	I	V
2445408.2819	−0.0061	I	V

Table 1

UBV light curves (normal points):

V curve		B curve		U curve	
Phase	ΔV	Phase	ΔB	Phase	ΔU
1	2	3	4	5	6
.0059000	.4070000	.0061000	.4540000	.0049000	.3200000
.0161000	.3590000	.0142000	.3530000	.0131000	.2070000
.0261000	.3070000	.0247000	.3190000	.0239000	.0365000
.0356000	.2580000	.0356000	.3150000	.0356000	.0685000
.0443000	.1530000	.0420000	.1650000	.0448000	.0463000
.0531000	.0796000	.0522000	.1040000	.0536000	.0599000
.0659000	.0543000	.0658000	.0666000	.0648000	—.0798000
.0758000	.0827000	.0756000	.0291000	.0737000	—.0813000
.0873000	.0370000	.0827000	—.0096000	.0823000	—.1160000
.1050000	.0218000	.0918000	.0238000	.0922000	—.0968000
.1140000	.0480000	.1050000	.0220000	.1050000	—.1210000
.1250000	.0295000	.1143000	.0234000	.1150000	—.0989000
.1350000	.0016000	.1250000	.0142000	.1250000	—.1340000
.1460000	—.0046000	.1360000	.0099000	.1370000	—.1800000
.1540000	.0003000	.1436000	—.0190000	.1430000	—.1850000
.1660000	.0050000	.1540000	—.0125000	.1520000	—.2060000
.1750000	—.0033000	.1660000	—.0060000	.1650000	—.1690000
.1850000	—.0315000	.1750000	—.0421000	.1740000	—.1710000
.1950000	—.0315000	.1840000	—.0545000	.1840000	—.1760000
.2050000	—.0786000	.1940000	—.0711000	.1940000	—.2120000
.2160000	—.0290000	.2050000	—.0415000	.2050000	—.2220000
.2260000	—.0259000	.2160000	—.0394000	.2160000	—.1880000
.2360000	—.0536000	.2250000	—.0373000	.2240000	—.2120000
.2440000	—.0412000	.2360000	—.0354000	.2400000	—.1620000
.2550000	—.0579000	.2430000	—.0488000	.2550000	—.1830000
.2600000	—.0184000	.2540000	—.0639000	.2650000	—.1740000
.2750000	—.0538000	.2650000	—.0610000	.2740000	—.1600000
.2840000	—.0393000	.2750000	—.0511000	.2840000	—.1910000
.2950000	—.0155000	.2860000	—.0509000	.2950000	—.1230000
.3060000	—.0220000	.2950000	—.0156000	.3030000	—.1620000
.3150000	—.0125000	.3040000	—.0312000	.3150000	—.1620000
.3250000	—.0272000	.3150000	—.0991000	.3230000	—.1340000
.3380000	—.0210000	.3250000	—.0583000	.3360000	—.1150000
.3560000	—.0170000	.3350000	—.0415000	.3450000	—.1950000
.3650000	—.0142000	.3450000	—.0531000	.3550000	—.1650000
.3750000	—.0014000	.3530000	—.0663000	.3640000	—.1570000
.3850000	—.0176000	.3650000	—.0381000	.3740000	—.1480000
.4010000	—.0031000	.3730000	—.0536000	.3850000	—.1530000
.4100000	.0018000	.3850000	—.0453000	.3960000	—.1330000
.4470000	—.0200000	.3950000	—.0290000	.4070000	—.1830000
.5140000	.0743000	.4110000	—.0543000	.4260000	—.1590000
.5270000	.0352000	.4490000	—.0600000	.4390000	—.1590000
.5350000	.0897000	.4810000	.0713000	.4510000	—.1510000
.5450000	.1050000	.4930000	.0425000	.4840000	—.0372000
.5550000	.1010000	.5060000	.0322000	.4930000	—.0633000
.5650000	.0107000	.5150000	.0604000	.5050000	—.0351000
.5760000	—.0111000	.5250000	.0018000	.5140000	—.0385000
.5840000	.0498000	.5350000	.0612000	.5250000	—.0285000
.5940000	—.0216000	.5450000	.0684000	.5340000	—.0268000
.6050000	—.0002000	.5550000	.0391000	.5500000	—.0162000
.6150000	.0028000	.5640000	.0293000	.5650000	—.0690000
.6250000	—.0003000	.5760000	—.0149000	.5760000	—.0577000

Table 1 (continued)

1	2	3	4	5	6
.6350000	—.0156000	.5850000	.0028000	.5840000	—.0428000
.6460000	—.0120000	.5940000	—.0052000	.5930000	—.1030000
.6560000	—.0489000	.6050000	—.0091000	.6050000	—.1790000
.6660000	—.0191000	.6220000	.0595000	.6180000	—.1690000
.6760000	—.0117000	.6350000	—.0244000	.6250000	—.1520000
.6850000	—.0386000	.6460000	—.0222000	.6360000	—.1570000
.6950000	.0029000	.6570000	—.0534000	.6460000	—.1650000
.7040000	.0262000	.6660000	—.0431000	.6560000	—.1510000
.7140000	—.0884000	.6810000	—.0504000	.6660000	—.1570000
.7270000	—.0227000	.6950000	—.0471000	.6790000	—.1630000
.7360000	—.0547000	.7060000	—.0777000	.7270000	—.1550000
.7440000	—.0534000	.7120000	—.0771000	.7370000	—.1740000
.7530000	—.0146000	.7270000	—.0620000	.7480000	—.1870000
.7630000	.0243000	.7410000	—.0701000	.7620000	—.1630000
.7750000	.0157000	.7590000	—.0363000	.7750000	—.1590000
.7850000	.0077000	.7750000	—.0312000	.7900000	—.1690000
.7940000	—.0079000	.7900000	—.0838000	.8110000	—.2100000
.8060000	—.0059000	.8050000	—.0206000	.8290000	—.1080000
.8140000	—.0068000	.8180000	—.0086000	.8440000	—.1520000
.8220000	—.0296000	.8360000	—.0611000	.8590000	—.1200000
.8360000	—.0448000	.8480000	—.0293000	.8680000	—.1220000
.8470000	—.0279000	.8630000	—.0321000	.8800000	—.1520000
.8580000	—.0326000	.8800000	.0069000	.8960000	—.0895000
.8670000	—.0158000	.8950000	.0593000	.9060000	.0072000
.8750000	.0009000	.9350000	.1140000	.9230000	.0023000
.8830000	.0048000	.9450000	.1510000	.9450000	.0434000
.8950000	.0285000	.9560000	.2560000	.9550000	.0662000
.9350000	.1970000	.9650000	.3020000	.9650000	.3000000
.9450000	.2030000	.9750000	.3600000	.9750000	.3820000
.9560000	.2620000	.9860000	.4170000	.9860000	.3240000
.9660000	.3110000	.9950000	.3610000	.9950000	.2700000
.9750000	.3770000				
.9870000	.4200000				
.9960000	.3660000				

We used a Wood model for the determination of the elements of the system. Because the observational scatter is large, we have used an "alternate directions" method for light curve solution with six steps in computation. In the first step, we try to obtain solutions using two different routes to perform the differential corrections on the mathematical hypersurface ($i, \omega, e, a_1, k, u_2, T_2$) of the solution :

$$[(i, a_1, k, T_2), (\omega, e)] \text{ and } [(\omega, e), (i, a_1, k, T_2)], \quad \text{respectively.}$$

The next steps were taken by an alternation of

$$[(u_2, T_2), (i, a_1, k, T_2)] \text{ calculations.}$$

During this process two "relative minima" were found, with practically the same $\sum(O-C)^2 = 0.05$ values. The larger scatter of the observed light curve does not permit us to discriminate better between these two solutions. The results for the two minima in B filter are:

ELEMENT	SOLUTION 1 B	SOLUTION 2 B
i	78.3	78.2
esinω	0.071	0.095
ecosω	0.040	0.046
u_1	0.6	0.6
u_2	0.3	0.28
a_1	0.36	0.376
k	0.55	0.537
β_1	0.25	0.25
β_2	0.25	0.25
T_1	9520	9520
T_2	5030	4687
q	0.5	0.5
$\Sigma(O-C)^2$	0.053	0.052

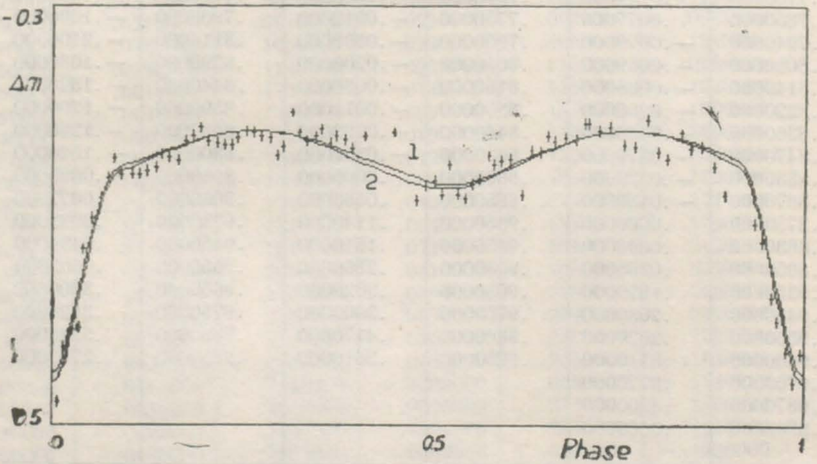

Fig. 1. — AW Cam B filter, Lines — models 1, 2 ; (+) observational points.

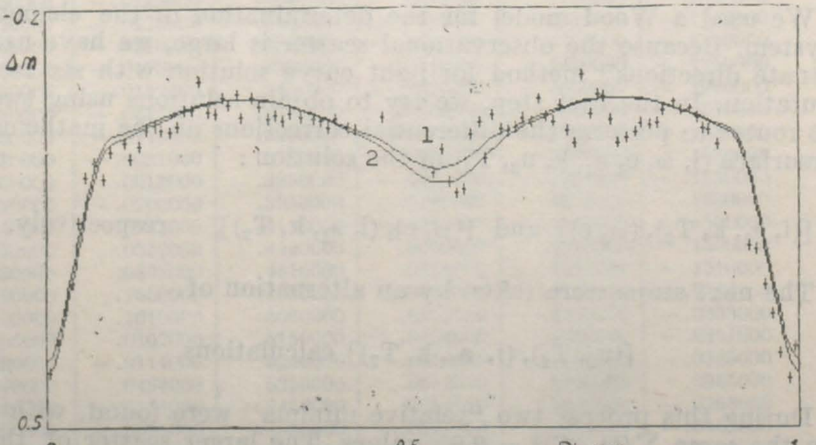

Fig. 2. — AW Cam V filter Lines — model 1, 2 ; (+) observational points.

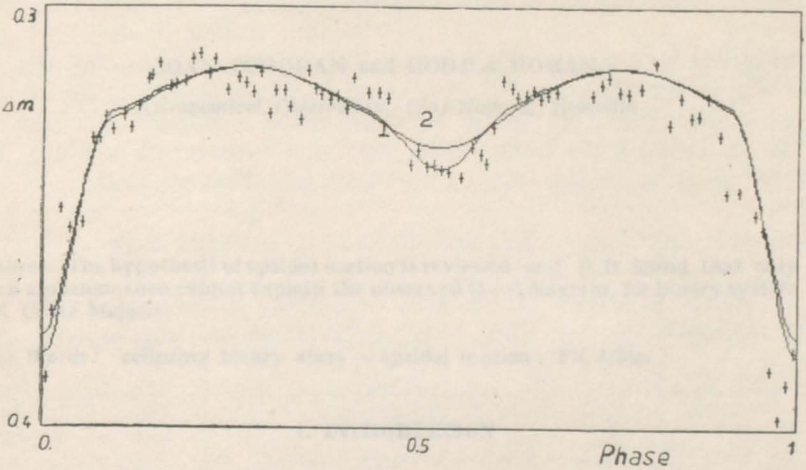

Fig. 3. — AW Cam U filter. Lines — models 1, 2 ; (+) observational points.

REFERENCES

Strohmeier, W., Knigge, R., Ott, H. 1963, Veröff. Remeis-Sternwarte Bamberg, V, No. 16.
Batten, A. H. *et al.* 1978, Seventh Catalogue of the Orbital Elements of Spectroscopic Binary Systems, Publ. Dom. Astrophys. Obs., 15, No. 5.

REMARKS ON THE APSIDAL MOTION OF *TX URSAE MAJORIS*

IOAN TODORAN and RODICA ROMAN
Astronomical Observatory, Cluj-Napoca, Romania

Abstract. The hypothesis of apsidal motion is reviewed and it is found that only such a phenomenon cannot explain the observed O—C diagram, for binary system TX Ursae Majoris.

Key Words: eclipsing binary stars — apsidal motion : TX UMa.

1. INTRODUCTION

At the time when Batten (1973) prepared his book *Binary and Multiple System of Stars* only three Algol-type systems were suspected to have remarkable apsidal motion : *W Delphini*, β *Persei* and *TX Ursae Majoris*. Nevertheless, Batten (1973, p. 244) has written :

"The low values of k_{22} found for the three secondary components of Algol-type systems... indicate that these are not contracting stars still to reach the main sequence".

Now, such a nice evolutive conclusion has been a very good stimulent for a new review of apsidal motion in the above mentioned semi-detached close binary systems. Moreover, the observed O—C diagram of W Delphini was discussed by Agerer and Todoran (1992) who make evident the fact that, if the corresponding O—C curve is periodic one, its period must be U > 90 years ; while Plavec (1960) has determined U ≃ 50 years for the assumed apsidal period.

On the other hand, β Persei is a triple system, that is why the observed O—C diagram could be interpreted by the superposition of the three effects : sudden erratic changes, apsidal motion and light-time effect.

The last semi-detached binary system where apsidal motion could be still postulated is TX Ursae Majoris. Moreover, such an important remark was also underlined by Semeniuk (1968) who has written :

"It is the only semi-detached system for which we can expect the apsidal motion as derived from the periodic term in the epochs of the primary minima to be real... for other systems with subgiant secondary component ... there is no sufficient evidence as yet, that the periodic changes of the primary minima may be treated as a result of apsidal motion".

Consequently, the aim of this note will be the problem of apsidal motion in the semi-detached system TX Ursae Majoris.

2. OBSERVATIONAL DATA

In order to resume the problem of apsidal motion of the binary system TX Ursae Majoris, we have used Plavec's (1960) table of primary minima, which was completed with observed minima obtained subsequently. In Table 1 we have listed the "new" observed minima. The residuals O−C refer to the linear ephemeris (see Plavec, 1960)

$$\text{Min.hel.} = \text{J.D.}2416426.783 + 3\overset{d}{.}0633175\,E$$

As shown in Figure 1, the run of normal differences O−C clearly puts in evidence the fact that these differences are not caused only by

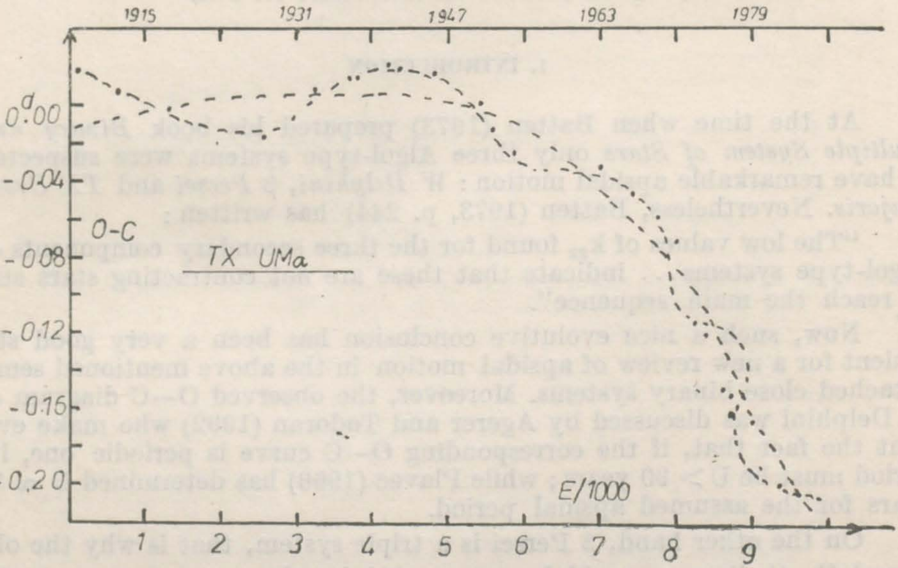

Fig. 1

apsidal motion. It was impossible for Plavec to reach this conclusion in 1960 because the time interval covered by observed minima was too short.

As we can see, in Table 1 we have collected 71 new observed primary minima and formed 12 normals which are listed in the second part of the Table 2, after Plavec's normals.

3. CONCLUDING REMARKS

As it is easy to see in Figure 1, the run of the differences O−C is determined by the supposition of at least two effects among which one could be considered as a periodic function, while the other one may also be considered as being a periodic one, but with a very long period. Moreover, this last effect could also be considered as being determined by a continuous decrease of the orbital period.

Therefore, TX Ursae Majoris could have an apsidal motion superposed over the light-time effect or over a strong variation of the corresponding stellar masses.

Table 1

TX URSAE MAJORIS (Observed primary minima 1962—1987)

J.D.hel. 24 ...,	O—C	E	Observer	Reference
	d			
37701.494	—0.029	6945	Jungbluth, H.	AN 288
37701.496	— .027	6945	Reichert, J.	,,
37747.458	— .015	6960	Fernandes, M.	,,
38470.365	— .051	7196	Schubert, H.	AN 290
38856.354	— .040	7322	Pohl, E. Kizilirmak, A.	IBVS 185 ,,
39193.308	— .051	7432	,,	,,
39245.394	— .041	7449	Robinson, J.	IBVS 15
39245.378	— .057	7449	Eckert, W.	AN 292
39245.391	— .044	7449	Braune, W.	,,
39245.391	— .044	7449	Schubert, H.	,,
39245.400	— .035	7449	Hübscher, J.	,,
39248.454	— .044	7450	,,	,,
39348.457	— .041	7450	Braune, W.	,,
39536.405	— .045	7544	Schubert, H.	,,
39536.394	— .056	7544	Pohl ,E. Kizilirmak, A.	IBVS 185
39968.343	— .035	7685	Hermann Peter	Orion 107
40066.375	— .029	7717	,,	Orion 108
40314.474	— .059	7798	Kurt Locher	Orion 112
40357.343	— .076	7812	Pohl, E. Kizilirmak, A.	IBVS 647
40363.477	— .069	7814	Kurt Locher	Orion 113
40599.351	— .070	7891	,,	,, 117
40985.3034	— .0960	8017	,,	,, 123
40988.381	— .082	8018	,,	,, 123
40988.381	— .082	8018	Hermann Peter	Orion 124
41000.619	— .097	8022	Ernst, M.	,,
41089.477	— .075	8051	Andres, M.	Orion 126
41181.340	— .112	8081	,,	,,
41717.4200	— .1123	8256	Pohl, E. Kizilirmak, A.	IBVS 937
41763.359	— .123	8271	Robert Germann	BBSAG 8
41763.371	— .111	8271	Hermann Peter	,,
41766.427	— .118	8272	,,	,,
41815.433	— .125	8288	Robert Germann	BBSAG 9
41815.436	— .122	8288	Hermann Peter	,,
41815.4459	— .1125	8288	Pohl, E. Kizilirmak, A.	IBVS 937
42008.416	— .131	8351	Herman Peter	BBSAG 12
42152.402	— .121	8398	Kurt Locher	BBSAG 15
42201.396	— .140	8414	Robert Germann	BBSAG 16
42201.413	— .123	8414	Hermann Peter	,,
42201.4143	— .1221	8414	Pohl, E. Kizilirmak, A.	IBVS 1053
42826 309	— .144	8618	György Zajàcz	BBSAG 26
42826.311	— .142	8618	András Fenyvesi	,,
42826.377	— .076	8618	Hermann Peter	,,

Table 1 (Continued)

J.D.hel. 24...,	O−C	E	Observer	Reference
	d			
42884.510	— .156	8637	Kurt Locher	BBSAG 27
42887.564	— .156	8638	Weigele, M.	AN 300
43123.442	— .153	8715	Ennio Poreti	BBSAG 31
43216.522	— .136	8716	,,	BBSAG 32
43212.283	— .148	8744	Robert Germann	BBSAG 33
43215.352	— .143	8745	Ennio Poreti	,,
43218.400	— .158	8746	,,	,,
43466.530	— .157	8827	,,	BBSAG 35
43466.534	— .161	8827	Maurizio Franchini	BBSAG 36
43509.412	— .161	8841	Herman Peter	,,
43512.477	— .159	8842	Ennio Poreti	,,
43552.295	— .164	8855	Robert Germann	,,
43555.362	— .161	8856	Hermann Peter	,,
43941.337	— .164	8982	Hermann Peter	BBSAG 42
43941.339	— .162	8982	Ennio Poreti	,,
44039.366	— .161	9014	Robert Germann	BBSAG 44
44278.289	— .177	9092	,,	,,
44330.371	— .171	9109	Luciano Ficola	BBSAG 53
44336.483	— .186	9111	Herman Peter	BBSAG 47
44382.420	— .198	9126	,,	BBSAG 48
44388.536	— .209	9128	Kurt Locher	,,
44716.324	— .196	9235	Robert Germann	BBSAG 54
45007.338	— .197	9330	George Mavrofridis	BBSAG 59
45056.336	— .212	9346	,,	,, 60
45105.367	— .194	9362	Robert Germann	,,
45105.368	— .193	9362	Hermann Peter	,,
45111.485	— .203	9364	Michael Kohl	,,
46872.887	— .209	9939	Vystavěl, R.	CNCOPB 30
46903.505	−0.224	9949	Czipes, J.	,,

AN = Astronomische Nachrichten.
BBSAG = Bedeckungsveränderlichen Beobachter der Schweizerischen Astronomischen Geselschaft,
CNCOPB = Contribution of the Nicholas Copernicus Observatory and Planetarium in Brno,
IBVS = Information Bulletin on Variable Stars.

Table 2

No. of observed minima	O−C (average)	E (average)	No. of observed minima	O−C (average)	E (average)
Plavec			Todoran and Roman		
	d			d	
5	+0.021	109	5	−0.032	7074
3	+ .009	658	10	— .046	7467
1	.000	1371	6	— .056	7786
9	— .019	1978	6	— .091	8035
6	— .014	2623	7	— .118	8276
8	+ .010	3298	5	— .127	8398
13	+ .017	3749	5	— .148	8626
1	+ .016	3869	5	— .147	8733
3	+ .023	4226	6	— .162	8844
1	+ .021	4356	4	— .166	9018
1	+ .019	4831	5	— .192	9142
1	+ .002	5396	5	— .200	9353
7	— .011	5579	2	−0.217	9944
3	−0.024	5854			

Having in view the difficulties raised by the interpretation of the corresponding O—C diagram, we are of the opinion that TX Ursae Majoris need to be observed for new minima, especially there is very important to observe secondary minima in order to *remove* the contribution of the effect of the apsidal motion.

Now, we are considering that it is nowadays premature to speak about the evolutive character of the apsidal motion constants k_{22} in semidetached systems.

REFERENCES

Agerer, F. and Todoran, I. : 1992, IBVS 3731.

Batten, A. H. : 1973, *Binary and Multiple Systems of Stars*, Pergamon Press, Oxford—New York—Toronto—Sydney—Braunschweig.

Plavec, M. : 1960, Bull. Astr. Inst. Czechosl. **11**, 148.

Semeniuk, I. : 1968, Acta Astronomica, **18**, 1.

CONVECTION IN THE PRESENCE OF SUNSPOTS

VARUJAN V. PAMBUCCIAN

University of Bucharest, Department of Mathematics

Abstract. The present paper deals with three dimensional stationary convection in the presence of a general weak magnetic field and of a strong magnetic field generated by a sunspot or a group of sunspots. This strong magnetic field will drive the entire phenomenon.

1. INTRODUCTION

The problem of modelling the magnetic convection is relatively old so there are a lot of models having in view the observational aspects. The great majority of these models are directed as to obtain a morphology having resemblance with the experimental facts. This is what I'll do in this paper using a different approach for the magnetic field of the sunspots and making these spots to drive the entire phenomena.

The most important fact that I use in this paper is that the sunspot has a strong magnetic field by comparison with the general solar magnetic field. To model this strong field I shall start from the Nicholson's empirical formulae that describe the magnetic field of the sunspot's nucleus. Let R be the radius of the spot (considered to be circular), r the distance of a given point to the spot's centre and θ the angle between the normal to the surface and the magnetic field vector c. According to [1] we have :

$$\theta = \frac{\pi}{2}\,\frac{r}{R}$$

$$\chi(r) = \chi_0\left(1 - \frac{r^2}{R^2}\right) \tag{1}$$

χ_0 being the magnitude of the magnetic field in the centre of the spot.

We shall adopt this empiric formulation of the magnetic field to the problem that we shall study. Let us consider an $Oxyz$ coordinate system, O being placed on the solar convective bottom surface within the group of spots, Oxy plane being tangent to the solar spherical surface and Oz axis following the normal to this sphere. If the group is not too large (its diameter is much smaller than the Sun's) we can assume that the whole group lies in the Oxy plane. Since the size of the spot is not significant as compared to the scale of the phenomenon, one may assume the spot s being punctually localized. Taking into account that the nuclei of the spots are mainly unipolar [1], the magnetic field of a $(a, b, 0)$ centred spot is given by :

$$\chi = \chi_0 \delta(x + a, y + b, 0)\,\mathbf{k} \tag{2}$$

δ being Dirac's distribution. In the case of a group of sunspots centred at $(a_i, b_i, 0)$ each having the intensity χ_i, the field will be :

$$\chi = \sum_{i=1}^{n} \chi_i \delta(x + a_i, y + b_i, z)\,\mathbf{k} \tag{3}$$

Hence the Lorentz force developed by this field is :

$$\mathbf{L} = -\frac{\mu}{2}\sum_{i=1}^{n} \chi_1^2[\delta'(x + a_i)\,\delta(y + b_i, z)\,\mathbf{i} + \\ + \delta'(y + b_i)\,\delta(x + a_i, z)\,\mathbf{j}] \tag{4}$$

In the proposed model the spots behave like punctually localized sources of field and force. Since we shall study a stationary convection problem in which the sunspot's field will be assumed stationary, the sports will act only as force field sources.

2. THE CONVECTION PROBLEM

We shall consider a stationary convection problem in the presence of a general magnetic field having the intensity H_0 and a punctually localized magnetic field of intensity χ produced by a sunspot. The fluid model we shall adopts is the Boussinesq approach [2]. Since we are interested to describe the motion around the sunspot (or in the vicinity of a sunspot group), we can consider that the motion takes place between two parallel planes one of them being tangent to the solar sphere in the centre of the sunspot. So, we shall choose a rectangular system centred in the middle of the sunspot and having the axis in such a way as to have Oxy tangent to the solar sphere and Oz normal to it (see Fig. 1). Let d be the distance between the planes where the motion takes place. Since the first plane we shall consider to be Oxy the se-

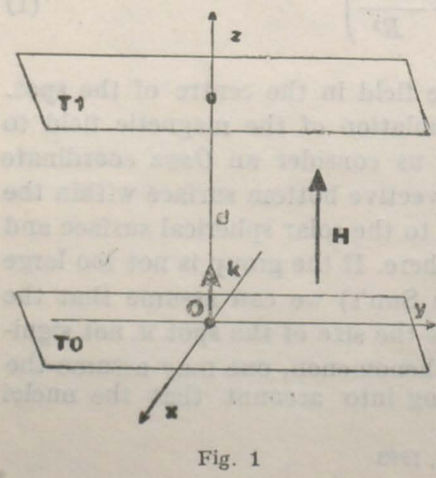

Fig. 1

cond plane will be $z = d$. In this layer of fluid a steady adverse temperature gradient is maintained :

$$\beta = \frac{(T_0 - T_1)}{d} \tag{5}$$

where T_0 is the temperature at the bottom of the fluid layer and T_1 the temperature at the top of it. The general magnetic field will be considered to be :

$$\mathbf{H} = H_0\mathbf{k} \tag{6}$$

with H_0 constant. We denote by i, j, k the versors of $Ox\, Oy$ and Oz axes.

Let us consider a linear steady flow of this inviscid Boussinesq fluid. We shall denote the total pressure in this fluid by :

$$\omega = \frac{p}{\rho} + \frac{\mu H_0}{\rho}\mathbf{h}\cdot\mathbf{k} \tag{7}$$

where p is the pressure, ρ is the specific mass of the fluid, μ is the magnetic permeability and $h = (h_1, h_2, h_3)$ the magnetic field intensity in the linear approximation.

The equations that describe this flow in the presence of a steady strong magnetic field generated by a spot placed in O are :

$$-\nabla\omega + g\,\alpha\theta\mathrm{k} + \frac{\mu H_0}{\rho}\frac{\partial\mathbf{h}}{\partial z} = -\frac{1}{2}\frac{\mu\chi^2}{\rho}\left[\delta'(x)\,\delta(y, z)\,\mathbf{i} + \delta'(y)\,\delta(x, z)\mathbf{j}\right]$$

$$\beta u_3 + \varkappa\nabla^2\theta = 0$$

$$H_0\frac{\partial\mathbf{u}}{\partial z} + \eta\nabla^2\mathbf{h} = 0 \tag{8}$$

$$\nabla\cdot\mathbf{u} = 0$$

$$\nabla\cdot\mathbf{h} = 0$$

where $u = (u_1, u_2, u_3)$ is the velocity, g is the acceleration due to gravity, α is the coefficient of volume expansion, $\varkappa$ is the coefficient of thermometric conductivity and η is the resistivity.

Let us consider the characteristic length be d, the characteristic velocity be v_A (the Alfvén velocity), H_0 the characteristic magnetic field intensity and T the characteristic temperature. We shall introduce by asterisks the dimensionless variables :

$$\mathbf{x} = d\mathbf{x}^* \qquad \mathbf{u} = v_A\mathbf{u}^*$$

$$\mathbf{h} = H_0\mathbf{h}^* \qquad \chi = H_0\chi^* \tag{9}$$

$$\theta = T\theta^* \qquad \boldsymbol{\omega} = v_A\boldsymbol{\omega}^*$$

So the system (8) becomes (denoting the * objects with their old symbols) :

$$-\nabla\omega + Rg\theta\mathbf{k} + \frac{\partial\mathbf{h}}{\partial z} = -\frac{1}{2}\chi^2[\delta'(x)\,\delta(y,z)\,\mathbf{i} + \delta'(y)\,\delta(x,z)\mathbf{j}]$$

$$R_t u_3 + \nabla^2\theta = 0$$

$$R_m \frac{\partial\mathbf{u}}{\partial z} + \nabla^2\mathbf{h} = 0 \tag{10}$$

$$\nabla\cdot\mathbf{h} = 0$$

$$\nabla\cdot\mathbf{u} = 0$$

where :

$$R_g = \frac{g\alpha d}{v_A^2} \quad R_t = \frac{\beta v_A}{\varkappa d^2} \quad R_m = \frac{v_A d}{\eta} \tag{11}$$

The mathematical problem will be (10) with the conditions :

$$\lim_{(X,\,Y)\to\infty} (\mathbf{u}, \mathbf{h}, \theta, \omega) = (\mathbf{0}, \mathbf{0}, 0, 0)$$

$$u_1|_{d=0,1} = u_2|_{d=0,1} = 0 \quad \left.\frac{\partial u_3}{\partial z}\right|_{d=0,1} = 0$$

$$\omega|_{d=0,1} = 0$$

To solve the system (9) we shall apply the Fourier transformation :

$$\bar{\varphi}(\xi) = \mathrm{F}[\varphi](\xi) = \int_{-\infty}^{+\infty}\int_{-\infty}^{+\infty}\int_{-\infty}^{+\infty} \varphi(\mathbf{x})\, e^{-i\mathbf{x}\cdot\xi}\,d\mathbf{x}$$

Here $\xi = (\xi, \eta, \zeta)$, and $\mathbf{x} = (x, y, z)$.

We'll obtain the algebraic linear system (having the unknowns $\bar{u}, \bar{h}, \bar{\theta}, \bar{\omega}$) :

$$i\xi\bar{\omega} + R_g\bar{\theta}\mathrm{k} - i\zeta\bar{\mathrm{h}} = \frac{i}{2}\chi^2(\xi\mathbf{i} + \eta\mathbf{j})$$

$$\mathrm{R}_t\bar{u}_3 - |\xi|^2\theta = 0$$

$$iR_m\zeta\bar{u} + |\xi|^2\bar{\mathrm{h}} = 0 \tag{12}$$

$$\xi\cdot\bar{\mathrm{h}} = 0$$

$$\xi\cdot\bar{\mathbf{u}} = 0$$

One can see that the last two equations of (12) are not independent, so the system (12) gives the solution of (10) in the form :

$$u_1 = -\frac{\chi^2}{2R_m}\frac{\partial^3}{\partial x \partial z^2}\nabla^2\Phi \quad u_2 = -\frac{\chi^2}{2R_m}\frac{\partial^3}{\partial y \partial z^2}\nabla^2\Phi$$

$$u_3 = \frac{\chi^2}{2R_m}\frac{\partial}{\partial z}\nabla^2\Delta_{xy}\Phi$$

$$h_1 = \frac{\chi^2}{2}\frac{\partial^4\Phi}{\partial x \partial^3 z} \quad h_2 = \frac{\chi^2}{2}\frac{\partial^4\Phi}{\partial y \partial^3 z} \quad h_3 = -\frac{\chi^2}{2}\frac{\partial}{\partial z}\Delta_{xy}\Phi \tag{13}$$

$$\omega = -\frac{\chi^2}{2}\left(Q + \frac{\partial^2}{\partial z^2}\right)\Delta_{xy}\Phi$$

$$\theta = -\frac{\chi^2}{2}\frac{R_t}{R_m}\frac{\partial}{\partial z}\Delta_{xy}\Phi$$

where :

$$\Phi(x, y, z) = \mathrm{F}^{-1}\left(\frac{1}{\zeta^2|\xi|^2 - Q(\xi^2 + \eta^2)}\right) \tag{14}$$

$Q = \dfrac{R}{R_m}$ and $R = R_g R_t$ is the Rayleigh number. So Q represents the ratio or the Rayleigh number and the magnetic Reynolds number.

This means that we have to compute the inverse Fourier transformation :

$$\Phi(x, y, z) = \int_{-\infty}^{+\infty}\int_{-\infty}^{+\infty}\int_{-\infty}^{+\infty}\frac{e^{i\mathbf{x}\cdot\xi}d\xi\,d\eta\,d\zeta}{\zeta^2|\xi|^2 - Q(\xi^2 + \eta^2)} \tag{15}$$

To compute this integral we shall use cylindrical coordinates. We shall have :

$$\Phi(r, \theta, z) = \int_{-\infty}^{+\infty}\int_{0}^{+\infty}\int_{0}^{2\pi}\frac{\rho e^{ir\rho\cos(\varphi-\theta)}e^{iz\zeta}d\zeta\,d\rho\,d\varphi}{\zeta^4 + \zeta^2\rho^2 - Q\rho^2} =$$

$$= 2\pi\int_0^{+\infty}\left(\rho J_0(r\rho)\int_{-\infty}^{+\infty}\frac{e^{iz\zeta}\,d\zeta}{\zeta^4 + \rho^2\zeta^2 - Q\rho^2}\right)d\rho$$

To compute the interior integral it is equivalent to solve the differential problem:

$$z^{\mathrm{IV}} - r^2 z^{\mathrm{II}} - Qr^2 z = \delta(z) \tag{16}$$

which has the solution of the form $Z(z) = \theta(z)\,\Xi(z)$, where $\theta(z)$ is the Heaviside function and $\Xi(z)$ is the solution of the problem:

$$\begin{gathered} \Xi^{\mathrm{IV}} - r^2 \Xi^2 - Qr^2 \Xi = 0 \\ \Xi(0) = \Xi^{\mathrm{I}}(0) = \Xi^{\mathrm{II}}(0) = 0 \\ \Xi^{\mathrm{III}}(0) = 0 \end{gathered} \tag{17}$$

This problem has the solution:

$$\Xi(z) = \frac{1}{a^2 + b^2}\left(\frac{\sin\mathrm{h}(az)}{a} - \frac{\sin(bz)}{b}\right) \tag{18}$$

where:

$$\begin{gathered} a^2 = \frac{\sqrt{r^4 + 4Qr^2} + r^2}{2} \\ b^2 = \frac{\sqrt{r^4 + 4Qr^2} - r^2}{2} \end{gathered} \tag{19}$$

Using (18) and (19) we can put (15) in the form:

$$\Phi(r, \psi, z) = 4\sqrt{2\pi}\,\theta(z) \int_0^{+\infty} \frac{J_0(r\rho)}{\sqrt{r^2 + 4Q}} \left(\frac{\sin\mathrm{h}\left(\dfrac{(\sqrt{r^4 + 4Qr^2} + r^2)}{2} z\right)^{1/2}}{(\sqrt{r^4 + 4Qr^2} + r^2)^{1/2}} - \frac{\sin\left(\dfrac{(\sqrt{r^4 + 4Qr^2} - r^2)}{2} z\right)^{1/2}}{(\sqrt{r^4 + 4Qr^2} - r^2)^{1/2}} \right) \mathrm{d}\rho$$

where J_0 is the Bessel function.

This integral may be solved using some approximations, but in the following paragraph we shall study an exact solution for a particular form of the spot's magnetic field.

3. THE CASE OF $\chi\sqrt{(\sin(\pi z))}\delta(x,y)\mathbf{k}$ MAGNETIC FIELD OF THE SPOT

Let us consider the magnetic field of the sunspot being:

$$\chi = \chi\sqrt{\sin(\pi z)}\,\delta(x, y)\mathbf{k} \tag{20}$$

In this case the Lorentz force developed by this field is:

$$\mathbf{L} = -\frac{\chi^2}{2}\sin(\pi z)\,(\delta'(x)\,\delta(y)\,\mathbf{i} + \delta(x)\,\delta'(y)\,\mathbf{j}) \tag{21}$$

The form (20) of the field assumes that the sunspot's magnetic field vanishes at the top and at the bottom of the fluid layer. This particular form leads to a simple solution for (15), $\Phi(r, z)$ being of the form:

$$\Phi(r, z) = R(r)\sin(\pi z) \tag{22}$$

where $R(r)$ is the solution of:

$$(Q - \pi^2)\,\frac{1}{r}\,(rR')' + \pi^4 R = \frac{\chi^2}{2}\,\delta(r) \tag{23}$$

One can easily see that this solution is:

$$R(r) = \frac{\chi^2}{2(Q-\pi^2)}\,J_0\left(\frac{\pi^2}{\sqrt{Q-\pi^2}}\,r\right)$$

if $\sqrt{Q} > \pi$ and:

$$R(r) = \frac{\chi^2}{2(Q-\pi^2)}\,K_0\left(\frac{\pi^2}{\sqrt{Q-\pi^2}}\,r\right)$$

if $\sqrt{Q} < \pi$. Here J_0 and K_0 are the usual cylindrical functions. We shall denote them in the following considerations by R_0. In this particular case, the solution of the problem (10) becomes:

$$u_1(x, y, z) = \frac{\chi^2}{2R_m}\,\frac{a^3(\pi^2 + a^2)}{\pi^2}\,\frac{x}{\sqrt{x^2 + y^2}}\;R_0(a\sqrt{x^2 + y^2})\sin(\pi z)$$

$$u_2(x, y, z) = \frac{\chi^2}{2R_m}\,\frac{a^3(\pi^2 + a^2)}{\pi^2}\,\frac{y}{\sqrt{x^2 + y^2}}\;R_0(a\sqrt{x^2 + y^2})\sin(\pi z)$$

$$u_3(x, y, z) = \frac{\chi^2}{2R_m}\,\pi a^2(\pi^2 + a^2)\,R_0(a\sqrt{x^2 + y^2})\cos(\pi z)$$

$$\theta(x, y, z) = \frac{R_t\chi^2}{R_m}\pi a^2 R_0(a\sqrt{x^2+y^2})\cos(\pi z)$$

$$h_1(x, y, z) = -\frac{\chi^2}{2}a\pi^3\frac{x}{\sqrt{x^2+y^2}}R_1(a\sqrt{x^2+y^2})\cos(\pi z)$$

$$h_2(x, y, z) = -\frac{\chi^2}{2}a\pi^3\frac{y}{\sqrt{x^2+y^2}}R_1(a\sqrt{x^2+y^2})\cos(\pi z)$$

$$h_3(x, y, z) = -\frac{\chi^2}{2}a^2\pi^2 R_0(a\sqrt{x^2+y^2})\sin(\pi z)$$

$$\omega(x, y, z) = -\frac{\chi^2\pi^4}{2}R_0(a\sqrt{x^2+y^2})\sin(\pi z)$$

where $a = \dfrac{\pi^2}{\sqrt{Q-\pi^2}}$.

Let us see the behaviour of the fluid in this particular case. First of all we see that rectangular convection cells appear between the planes $d = 0$ and $d = 1$. The diameters of these cells decrease when we move off the spot. Right in the place where the spot is centred a strong descending movement appears. This movement takes down the fluid from the upper plane. At the same time one can see (Fig. 2) that in the cells near the spot the strong circulation of the fluid takes place in the regions far off the spot. One can also see that the cells depend on Q. As Q increases the cells tend to become narrow and elongated.

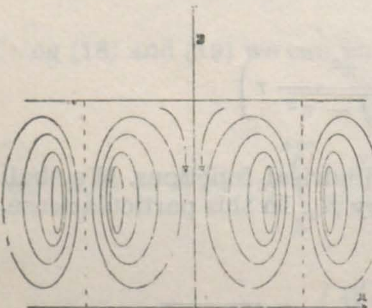

Fig. 2

The flow presented in Fig. 1 was determined in the hypothesis that $Q > \pi$. For a given number a, the relation between the Rayleigh number R and the magnetic Reynolds number R_m will be :

$$R = \frac{\pi^2 + a^2}{a^2}\pi^2 R_m$$

Since a represents the wave number we can obtain, for a given $R_m = \left(\frac{\mu}{\rho}\right)^{\frac{1}{2}}\frac{Hd}{\eta}$, the Rayleigh number at which the convection takes place with that wave number.

REFERENCES

1. Aller, L. H., *Astrophysics, The Atmosphere of Sun and Stars*. Ronald Press Company, 1953.
2. Chandrasekhar S., *Hydrodynamic and Hydromagnetic Stability*, Oxford, 1961.

THE GLOBAL ANALYSIS OF TIME DETERMINATIONS MADE IN BUCHAREST DURING 1962–1989 (II)

MAGDA STAVINSCHI, DANA DINESCU, GHEORGHE VASS, ALINA DONEA

Astronomical Institute of the Romanian Academy, Cuțitul de Argint 5, 75212 Bucharest 28, Romania

Abstract. The first part of this work was presented during the 7th International Symposium of Geodesy and Geophysics of the Earth – the IAG No 122 Symposium – in Potsdam and it was published in the Proceedings of the Symposium (Springer Verlag, in print). Because at the moment of the Symposium we only had preliminary results of the analysis, in the present paper a complete image of the data processing and of the results has been included.

Key words: Earth's Rotation, Time Determination

During 1957–1990, the Astronomical Observatory of Bucharest has participated in the astronomical time determination and, implicitly, in the determination of Earth rotation irregularities by observations made at the passage instrument Zeiss 100/1000 mm. The time determination has been in regular operation by the Astronomical Observatory of Bucharest since the International Geophysical Year. During this time, the Observatory has been a full contributor of optical astrometrical data to the Earth Rotation Parameters.

The time determinations (generally two series per night, each containing about ten stars) were obtained by Hansen's method and referred to the atomic time through the quartz-clocks (Belin till 1967, then Rohde & Schwarz).

The coordinates of the stars were those of the "Apparent Places of the Fundamental Stars" (Astronomisches Rechen-Institut Heidelberg). All coordinates were reduced to the 1979 BIH System, by using the corrections given in the Annual Report of the BIH for 1980.

The resulting differences UTO–UTC were periodically sent to the main data centers: BIH (Bureau International de l'Heure), IPMS (International Polar Motion Service), Etalonnoe and Vsemirnoe Vremja, and, in the last period, to the International Center of Optical Astronomy o Shanghai.

Because we did not succeed in modernizing the instrument and because the new International Earth Rotation Service uses only the new techniques, we were obliged to stop the time determinations in 1990, trying to obtain a GPS.

However, the great amount of data accumulated during the mentioned period, as well as the fact that it was included in the UTdef, made us analyse the data to detect some significant periodicities.

So, the spectral analysis for UTO—AT data during 1962—1989 was done (the data from 1957 to 1962 were rejected because of their unhomogeneousness).

The determinations from 2178 nights were analysed with Scargle's programs (Scargle, 1989), applicable to unequally spaced time series data.

Before this treatment of UTO—AT data, the secular variation term was removed using a least squares determination of it (Figs. 1—2).

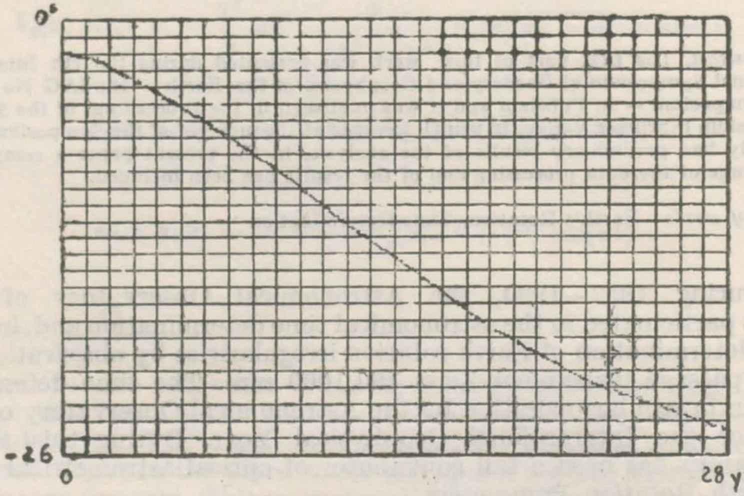

Fig. 1. — Distribution of the initial UTO—AT data determined in Bucharest, during 1962—1989 (28 years).

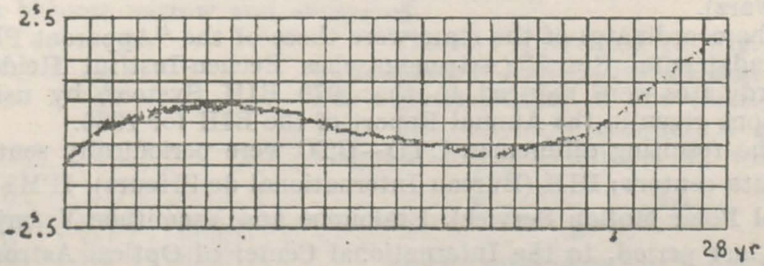

Fig. 2. — Distribution of the same data, after the removing of the first degree secular term.

Since the total lapse of time covered by the data is sufficiently long as against the period of different periodic terms, we were able to establish the spectrum of these periodic terms. So we observed some obvious peaks and other central peaks accompanied by a series of nearby peaks with smaller amplitudes (Figs. 3—6 and Table 1).

We first recognized the period of 18.55 yr, with an amplitude of 0.52 s, very close to the period of the main nutation term (about 18.62 yr); it is surprising that other authors did not find this periodicity.

We also found the half of it, a component of 9.28 yr (Fig. 3).

A second significant period is one of 6.96 yr, found by other authors, too (Poma and Proverbio, 1980).

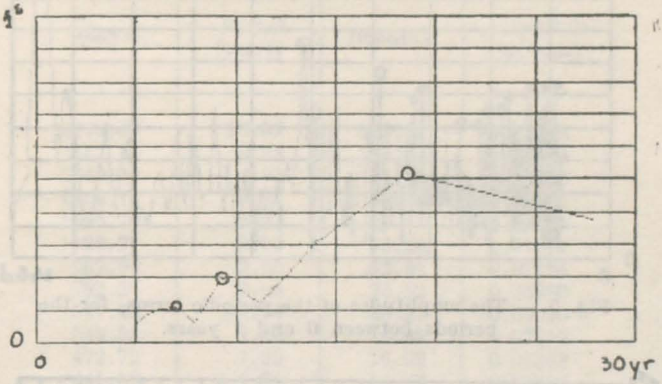

Fig. 3. — The amplitudes of the periodic terms, for the periods between 5 and 30 years.

All the following terms, with periods smaller than 5 years, have amplitudes smaller than 0.1 s (see Table 1 and Figs. 4—6).

We proved (Fig. 4) the existence of 3.71 yr period, obtained by Emetz and Korsun (1979), as well as 3.27, 3.09 (see also Iijima and Okazaki, 1972) and 2.65 years.

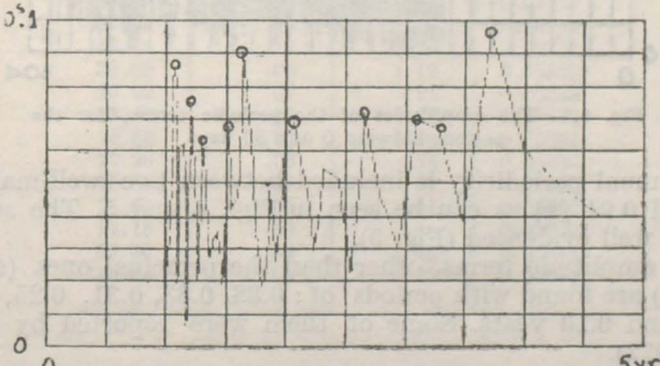

Fig. 4. — The amplitudes of the periodic terms, for the periods between 1 and 5 years.

The biennial period (2.06 yr) confirms the existence of a 26 months period term which was reported firstly by Iijima and Okazaki (1966, 1972, 1972 a).

Two interesting components have periods of 1.64 yr and 1.50 yr.

We also found a period of 1.29 yr and one of 1.21 yr, discovered by Iijima and Okazaki (1956).

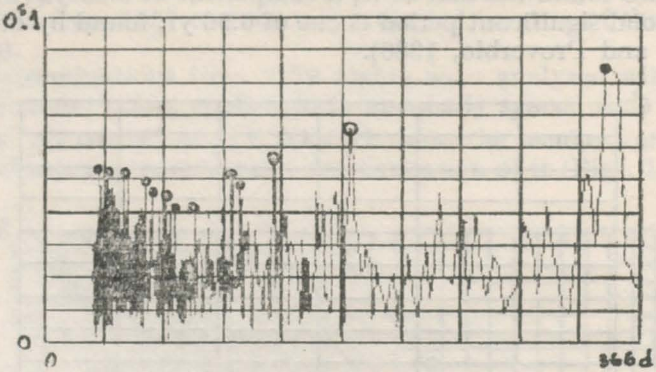

Fig. 5. — The amplitudes of the periodic terms, for the periods between 0 and 1 years.

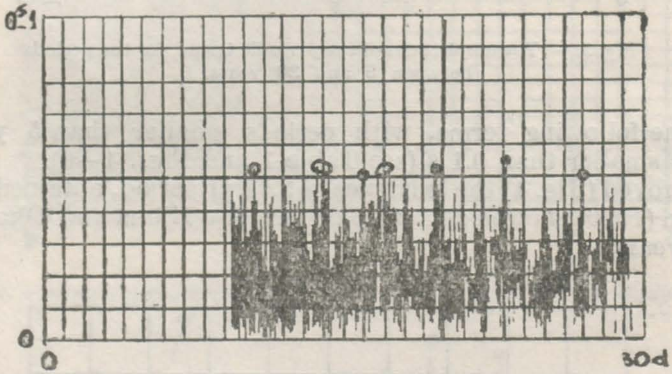

Fig. 6. — The amplitudes of the periodic terms, for the periods between 0 and 30 days.

The annual periodicity is included between two well-marked terms (1.07 yr and 0.94 yr) as can be seen in Figs. 4 and 5. The semi-annual term is also well evidenced (Fig. 5).

Minor amplitude terms, other than the principal ones (annual and semi-annual) are found with periods of : 0.38, 0.33, 0.31, 0.25, 0.22, 0.20, 0.18, 0.14 and 0.10 years. Some of them were reported by Iijima and Okazaki (1972).

Short period terms were also found for 36, 33, 26, 23, 20, 17, 16, 14 and 10 days.

CONCLUSIONS

It can be seen that, even though the visual passage instrument was not a powerful one, the obtained results seem to be real, being confirmed by other authors.

The 18.55 yr term is something interesting to study in the future.

The study of the data analysis behaviour after the consecutive extraction of the most important terms must also be interesting ; we intend to do it as soon as possible.

Table 1

Periods and amplitudes

(days)	Period (years)	(months)	Amplitude (seconds)
6775.63	18.55	229.68	0.52042
3387.81	9.28	114.84	0.20214
2540.86	6.96	86.13	0.10816
1355.13	3.71	45.94	0.09632
1195.70	3.27	40.53	0.06734
1129.27	3.09	38.28	0.07001
967.95	2.65	32.81	0.07194
752.85	2.06	25.52	0.06860
597.85	1.64	20.27	0.09090
549.38	1.50	18.62	0.07015
472.72	1.29	16.02	0.06368
441.89	1.21	14.98	0.07494
390.90	1.07	13.25	0.08592
344.52	.94	11.68	0.08514
186.49	.51	6.32	0.06608
140.19	.38	4.75	0.05646
120.28	.33	4.08	0.04837
114.84	.31	3.89	0.05219
92.39	.25	3.13	0.04181
79.71	.22	2.70	0.04185
73.65	.20	2.50	0.04515
65.78	.18	2.23	0.04601
61.41	.17	2.08	0.04839
50.82	.14	1.72	0.04970
37.85	.10	1.28	0.05422
36.63	.10	1.24	0.05124
33.05	.09	1.12	0.05325
26.92	.07	.91	0.05046
23.07	.06	.78	0.05502
19.58	.05	.66	0.05202
17.26	.05	.58	0.05254
16.65	.05	.56	0.05096
16.01	.04	.54	0.05952
14.16	.04	.48	0.05240
13.60	.04	.46	0.05333
10.44	.03	.35	0.05075

REFERENCES

Emetz, A., Korsun, A. : 1979, IAU Symp., **82**, 59.
Iijima, S., Okazaki, S. : 1956, Publ. Astron. Soc. Japan, **8**, 2.
Iijima, S., Okazaki, S. : 1966, J. Geod. Soc. Japan., **12**, 2.
Iijima, S., Okazaki, S. : 1972, Publ. Astron. Soc. Japan, **24**, 1.
Iijima, S., Okazaki, S. : 1972 a, IAU Symp., **48**, 68 .
Poma, A., Proverbio, E. : 1981, Proc. of 4th Int. Sym. Geogesy and Physics of the Earth, part I.
Scargle, J. : 1982, Ap. J., **263**, 835.
Scargle, J. : 1989, Ap. J., **343**, 874.
Stavinschi, M., Dinescu, D., Vass, G. : 1992, Proc. of. 7th Int. Sym. Geodesy and Physics of the Earth, in print.

COLLISION AND NEAR-COLLISION ORBITS IN POST-NEWTONIAN GRAVITATIONAL SYSTEMS

GEORGE BALLINGER *, FLORIN N. DIACU **

Department of Mathematics and Statistics, University of Victoria
P. O. Box 3045, Victoria, B. C., Canada, V8W 3P4

Abstract. We study the central force problem involving a particle of unit mass orbiting a centre while subjected to a post-Newtonian gravitational force proportional to $r^{-2}(1 + \alpha \ln r)$, where r is the distance to the centre and $|\alpha| < 1$. We examine the behaviour of the particle at and near collision with the centre. By using McGehee-type transformations we blow up the singularity at $r = 0$ and obtain regularized equations of motion. After proving the collision manifold to be a torus, a qualitative study of the flow is performed. Collision-ejection solutions are shown to be block-regularizable. Finally we draw the conclusion that post-Newtonian laws of this type, with $-1 < \alpha < 0$, are similar to the Newtonian one in the neighbourhood of singularities.

Key Words: celestial mechanics – post-Newtonian gravitational law-collisions

1. INTRODUCTION

A century ago post-Newtonian laws of gravity were proposed, primarily in an attempt to explain the discrepancy between Mercury's observed variation of the perihelion and the theoretical value based on Newton's law of gravitation. Most such laws were slightly modified versions of Newton's inverse square law. In 1873 G. Bertrand proposed that the force of gravity be inversely proportional to r^n, where r denotes the distance between two particles and $n > 2$. In order to fit the observed secular variations of Mercury and of the other inner planets, in 1895 A. Hall and S. Newcomb computed $n = 2.00000016$ and $n = 2.0000001574$, respectively. However, a few years later E. W. Brown showed that n differed from 2, if at all, by less than 0.00000004 following observations of the motion of the Moon's perigee (Hagihara, 1972). From this perspective, the theory was deemed a failure. Such *ad hoc* modifications of the gravitational law have proven inadequate in explaining Mercury's advance of the perihelion. Laws of this type state that the gravitational forces vary directly with $r^{-2+\alpha}$ where $|\alpha| \ll 1$. This led to the idea of considering approximations of such laws that fit better with observational data. By keeping only the first two terms in the expansion $r^\alpha = 1 + \alpha \ln r + (\alpha \ln r)^2/2! + (\alpha \ln r)^3/3! + \ldots$, one finds that the force of gravitation is proportional to $r^{-2}(1 + \alpha \ln r)$, where $|\alpha| \ll 1$. Mücket and Treder (1977) introduced a gravitational potential whose corresponding post-Newtonian

* Research supported in part by an NSERC University Undergraduate Student Research Award.

** Research supported in part by NSERC Grant 3–48376.

gravitational force was of this type. They determined the perihelion advance of a planet. Mioc and Blaga (1991) later adopted this force and studied orbital motion using a perturbative treatment.

In order to check whether such a force is acceptable, it is natural to test the behaviour of orbits in the neighbourhood of singularities. We will therefore consider Mücket-Treder's gravitational potential and study the collision and near-collision orbits of a particle orbiting a fixed centre. To do this we begin with the equations of motion of a unit mass subjected to a central force which is proportional to $r^{-2}(1 + \alpha \ln r)$, where we assume $|\alpha| < 1$. Note that in our analysis we do not require $|\alpha| \ll 1$; in fact our study could be generalized further by considering values of α outside the interval $(-1, 1)$. Next we carry out a sequence of McGehee-type transformations on the system in order to eliminate the singularity at the origin. We "blow up" the singularity, replace it with an invariant boundary called a *collision manifold*, and then perform a qualitative study of the flow on and near the collision manifold. We conclude that the qualitative behaviour of the flow (near collision) associated with this vector field is the same as that in the classical Kepler central force problem (Devaney, 1981). Since the near-collision orbits are characteristic of eccentric orbits, Mücket-Treder's law may be suitable to the study of the motion of comets in the neighbourhood of the Sun.

2. EQUATIONS OF MOTION

Consider a particle of unit mass orbiting a central point mass M (which is fixed at the origin of a plane $\mathbf{R}^2$) and having gravitational *potential energy*

$$V(\mathbf{q}) = -\mu(1 + \alpha + \alpha \ln|\mathbf{q}|)/|\mathbf{q}|. \tag{1}$$

Here, $\mathbf{q} = (q_1, q_2) \in \mathbf{R}^2$ is the position or *configuration* of the orbiting point mass, $|\cdot|$ denotes the Euclidean norm, $\mu = G_0 M > 0$ is the gravitational parameter of the two-body system where G_0 denotes the Newtonian gravitational constant, and α is a small numerical parameter such that $|\alpha| < 1$. Expression (1) is our version of the gravitational potential introduced by Mücket and Treder (1977). The potential energy function V is real-valued, analytic, and has an isolated singularity at the origin. The point $\mathbf{q} = (0, 0)$ corresponds to collision of the particle with the central mass. The potential energy function (1) gives a family of post-Newtonian gravitational forces

$$\mathbf{F}_\alpha(\mathbf{q}) = -\nabla V(\mathbf{q}) = -\mu(1 + \alpha \ln|\mathbf{q}|)\,\mathbf{q}/|\mathbf{q}|^3, \tag{2}$$

where ∇ is the gradient operator.

Newton's equations of motion are given by the second order system

$$\ddot{\mathbf{q}} = -\nabla V(\mathbf{q}). \tag{3}$$

By introducing the momentum vector $\mathbf{p} = \dot{\mathbf{q}}$, (3) may be written as a system of four scalar first order differential equations

$$\dot{\mathbf{q}} = \mathbf{p}, \qquad \dot{\mathbf{p}} = -\nabla V(\mathbf{q}). \tag{4}$$

Let $\mathbf{Q} = \mathbf{R}^2 - \{(0, 0)\}$ and $\mathbf{P} = \mathbf{R}^2$. We call $\mathbf{Q}$ the *configuration space* and $\mathbf{P}$ the *momentum space* of the system. Then (4) is a vector field on the *phase space* $\mathbf{Q} \times \mathbf{P}$.

Let $T(\mathbf{p}) = |\mathbf{p}|^2/2$ denote the *kinetic energy* of the particle. The integral of energy of (4) is given by

$$H(\mathbf{q}, \mathbf{p}) = T(\mathbf{p}) + V(\mathbf{q}) = h, \tag{5}$$

where h is a constant of integration. H is the Hamiltonian or total energy function. The integral of angular momentum is given by

$$L(\mathbf{q}, \mathbf{p}) = c, \tag{6}$$

where c is a constant of integration and $L(\mathbf{q}, \mathbf{p}) = q_1p_2 - q_2p_1$ is the *angular momentum* function. We can reduce the dimension of our system by considering (4) as a vector field on the surface of constant energy. Thus we have

$$\dot{\mathbf{q}} = \mathbf{p}, \qquad \dot{\mathbf{p}} = -\mu(1 + \alpha \ln |\mathbf{q}|)\mathbf{q}/|\mathbf{q}|^3, \tag{7}$$

with the energy relation

$$|\mathbf{p}|^2/2 - \mu(1 + \alpha + \alpha \ln |\mathbf{q}|)/|\mathbf{q}| = h.$$

Using McGehee-type transformations (McGehee, 1974) we will regularize the system (7) and eliminate the singularity at $\mathbf{q} = (0, 0)$. Our first step is to introduce polar coordinates by making the following transformation of variables. Let

$$\left.\begin{aligned} r &= |\mathbf{q}| \\ \theta &= \operatorname{arc\,tan}(q_2/q_1) \end{aligned}\right\} \quad \text{standard polar coordinates,} \tag{8}$$

$$y = \dot{r} = (q_1p_1 + q_2p_2)/|\mathbf{q}| \qquad \text{radial velocity,}$$

$$x = r\dot{\theta} = (q_1p_2 - q_2p_1)/|\mathbf{q}| \qquad \text{tangential velocity.}$$

The inverse relations are given by

$$q_1 = r \cos \theta,$$

$$q_2 = r \sin \theta, \tag{9}$$

$$p_1 = - x \sin \theta + y \cos \theta,$$

$$p_2 = x \cos \theta + y \sin \theta.$$

We have defined a real analytic diffeomorphism

$$\mathbf{Q} \times \mathbf{P} \to (0, \infty) \times \mathbf{R} \times [0, 2\pi) \times \mathbf{R}$$

$$((q_1, q_2), (p_1, p_2)) \mapsto (r, y, \theta, x). \tag{10}$$

In these new coordinates the equation of motion (7) becomes

$$\begin{aligned} \dot{r} &= y && \text{radial velocity,} \\ \dot{y} &= x^2/r - \mu(1 + \alpha \ln r)/r^2 && \text{radial acceleration,} \\ \dot{\theta} &= x/r && \text{angular velocity,} \\ \dot{x} &= - xy/r && \text{tangential acceleration,} \end{aligned} \tag{11}$$

with the energy relation

$$- \mu(1 + \alpha + \alpha \ln r)/r + (x^2 + y^2)/2 = h.$$

Furthermore, the equation of conservation of angular momentum (6) becomes

$$rx = c. \tag{12}$$

Note that the singularity set for (11) now corresponds to $r = 0$. From the energy relation it is clear that if $\alpha > 0$ then collision is not possible since in the limit, as $r \to 0$, the left-hand side of the energy relation tends to infinity while h is constant. If $\alpha = 0$ then the problem reduces to the classical Kepler central force problem. We will consider the case when $-1 < \alpha < 0$. From (12) we find that $x = c/r$. If $c = 0$ then all motion takes place along a fixed straight line through the origin (Pollard, 1966). If $c \neq 0$ then by substituting c/r for x in the energy relation and taking the limit as $r \to 0$ we find again that the left-hand side of the energy equation tends to infinity while h remains constant. Thus collision with the origin is not possible unless motion is rectilinear. As $r \to 0$, we have $x^2 + y^2 \to \infty$ and so the next step is to scale down these components of velocity. Since we are studying the local behaviour of the solutions near the singularity, we need only consider small values of r. As such, the following transformation is valid for $0 < r < 1$. Define the real analytic diffeomorphism

$$(0, 1) \times \mathbf{R} \times [0, 2\pi) \times \mathbf{R} \to (0, 1) \times \mathbf{R} \times [0, 2\pi) \times \mathbf{R}$$
$$(r, y, \theta, x) \mapsto (r, v, \theta, u) \tag{13}$$

where

$$v = r^{1/2} (-\ln r)^{-1/2} y,$$

$$u = r^{1/2} (-\ln r)^{-1/2} x.$$

The new equations of motion become

$$\dot{r} = r^{-1/2}(-\ln r)^{1/2} v,$$

$$\dot{v} = r^{-3/2}(-\ln r)^{1/2} [v^2(1 - 1/\ln r)/2 + u^2 + \mu\alpha + \mu/\ln r],$$

$$\dot{\theta} = r^{-3/2}(-\ln r)^{1/2} u, \tag{14}$$

$$\dot{u} = r^{-3/2}(-\ln r)^{1/2}(-uv/2)(1 + 1/\ln r),$$

with the energy relation

$$u^2 + v^2 = [2rh + 2\mu(1 + \alpha)]/(-\ln r) - 2\mu\alpha.$$

This system still has a singularity at $r = 0$, but it can be removed by performing two additional transformations. We first make a change of time scale by introducing a fictitious time variable τ via

$$\mathrm{d}t = r^{3/2}(-\ln r)^{-1/2}\, \mathrm{d}\tau. \tag{15}$$

Then, maintaining (by abuse) the same notations for the new functions of τ, the equations (14) become

$$r' = rv,$$

$$v' = v^2(1 - 1/\ln r)/2 + u^2 + \mu\alpha + \mu/\ln r,$$

$$\theta' = u, \tag{16}$$

$$u' = -uv(1 + 1/\ln r)/2,$$

with the same energy relation

$$u^2 + v^2 = [2rh + 2\mu(1 + \alpha)]/(-\ln r) - 2\mu\alpha,$$

where the prime indicates differentiation with respect to τ. These are given by a vector field on $(0,1)\times\mathbf{R}\times[0,2\pi)\times\mathbf{R}$. To eliminate the singularity at $r=0$ we make a final transformation by scaling the distance r. Define the real analytic diffeomorphism

$$\begin{aligned}&(0,1)\times\mathbf{R}\times[0,2\pi)\times\mathbf{R}\to(0,\infty)\times\mathbf{R}\times[0,2\pi)\times\mathbf{R}\\&(r,v,\theta,u)\mapsto(z,v,\theta,u)\end{aligned}\tag{17}$$

where

$$z=-1/\ln r.$$

Then system (16) becomes

$$\begin{aligned}z'&=z^2v,\\v'&=v^2(1+z)/2+u^2+\mu\alpha-\mu z,\\\theta'&=u,\\u'&=uv(z-1)/2,\end{aligned}\tag{18}$$

with the energy relation

$$u^2+v^2=2hz\exp(-1/z)+2\mu(1+\alpha)z-2\mu\alpha.$$

This is a vector field on $[0,1)\times\mathbf{R}\times[0,2\pi)\times\mathbf{R}$ where collision corresponds to $z=0$. Note that the vector field has been extended analytically to the boundary $z=0$, and this boundary is invariant under the flow since $z'=0$ when $z=0$. The energy relation also extends to the boundary. We can write the energy relation as follows:

$$u^2+v^2=2hg(z)+2\mu(1+\alpha)z-2\mu\alpha,\tag{19}$$

where

$$g(z)=\begin{cases}z\exp(-1/z), & z>0,\\0, & z=0.\end{cases}$$

Since g is of class C^∞ in $[0,\infty)$ then the energy relation extends smoothly to the boundary $z=0$ and on the boundary the energy relation reduces to $u^2+v^2=-2\mu\alpha$. We denote the boundary of the phase space by

$$\Lambda=\{(z,v,\theta,u)\mid z=0\quad\text{and}\quad u^2+v^2=-2\mu\alpha\},\tag{20}$$

and call it the *collision manifold*. Note that Λ is independent of the energy level h and so all of the energy levels share this boundary.

3. THE FLOW ON AND NEAR THE COLLISION MANIFOLD

Clearly the collision manifold Λ is a two-dimensional torus defined by

$$u^2 + v^2 = -2\mu\alpha, \qquad \theta \text{ arbitrary.} \tag{21}$$

The vector field on Λ is then given by

$$v' = u^2/2, \qquad \theta' = u, \qquad u' = -uv/2, \tag{22}$$

where the energy relation has been used to simplify v'. The rest points of system (22) are $(v, \theta, u) = (\pm(-2\mu\alpha)^{1/2}, \theta_0, 0)$, where $\theta_0 \in [0, 2\pi)$ is arbitrary. In other words there are two circles of equilibria on the boundary Λ. Since $v' > 0$ when $u \neq 0$, then all other solutions move from the lower circle $v = -(-2\mu\alpha)^{1/2}$ to the upper circle $v = +(-2\mu\alpha)^{1/2}$. We introduce the angular variable ψ via

$$u = (-2\mu\alpha)^{1/2} \cos\psi, \qquad v = (-2\mu\alpha)^{1/2} \sin\psi. \tag{23}$$

The system on Λ then becomes

$$\psi' = ((-2\mu\alpha)^{1/2}/2) \cos\psi, \qquad \theta' = (-2\mu\alpha)^{1/2} \cos\psi, \tag{24}$$

and so we have

$$d\psi/d\theta = 1/2. \tag{25}$$

Figure 1 illustrates the solutions of this vector field.

We next look at the set of orbits which begin and end in collision. By fixing $\theta = \theta_0$ and $u = 0$ we have $\theta' = u' = 0$ and so the corresponding (z, v)-plane is invariant under the flow. Restricted to this plane, system (18) becomes

$$z' = z^2 v, \qquad v' = v^2(1+z)/2 + \mu\alpha - \mu z = h(1+z)\, g(z) + \mu(1+\alpha) z^2. \tag{26}$$

Although this system is difficult to solve, its phase portrait is sketched in Figure 2.

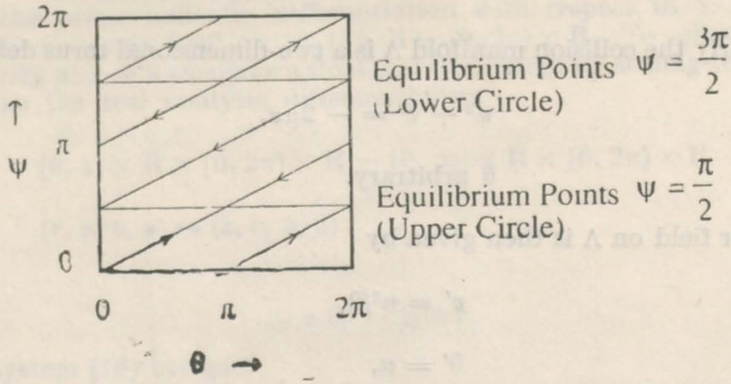

Fig. 1 — The flow on Λ.

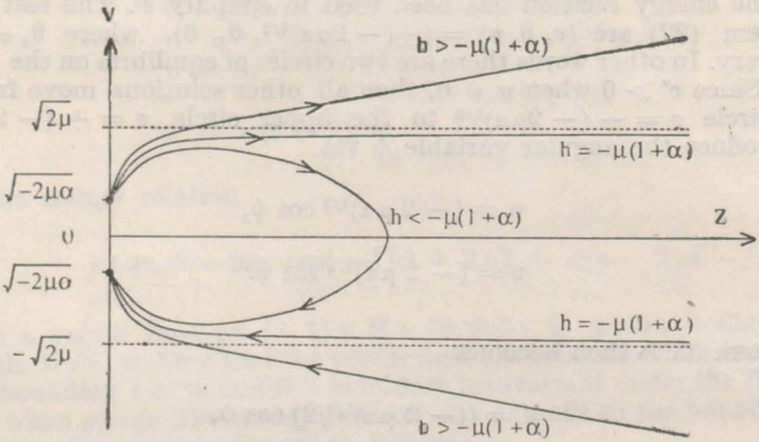

Fig. 2. — The flow on the invariant (z, v)-plane.

For each fixed energy level $h < -\mu(1 + \alpha)$, a unique solution exists which begins and ends in collision with $z = 0$, satisfying $\theta = \theta_0$ and $u = 0$ for all time. In configuration space, these orbits are rectilinear; they begin with ejection, reach the zero velocity curve at some point $r < 1$, and then fall back to collision. As discussed in the previous section, because angular momentum is conserved, such rectilinear orbits are the only collision-ejection orbits for the system. Thus the flow on and near the boundary is as shown in Figure 3. A collision orbit will come to reach the lower circle, then travel once around the torus in either a clockwise or counterclockwise direction, and finally eject from the upper circle.

Orbits passing near the origin follow a collision orbit until coming close to Λ, whereupon they follow either a clockwise or a counterclockwise path about Λ. In either case θ is forced to change by 2π, a decrease corresponding to a clockwise direction and an increase corresponding to a coun-

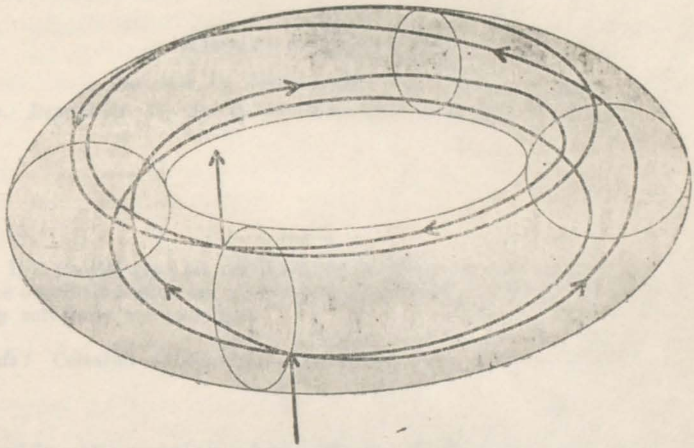

Fig. 3. — The flow on and near Λ.

terclockwise direction. Orbits then escape from a neighbourhood of collision near an ejection orbit. Hence, the behaviour of the flow near collision is the same as that in the classical Kepler central force problem (Devaney, 1981). Notice that in our case the equilibrium points on the circles are not hyperbolic. However, due to the continuity of the solutions of (18) with respect to data; as well as the fact that the only collision-ejection orbits lie in the invariant set of rectilinear solutions, the above conclusions about near-collision orbits can be drawn. This further implies that collision orbits are *block-regularizable* (Easton, 1971). In other words a near-collision orbit will be very eccentric. All these results show that the qualitative behaviour of the Mücket-Treder laws with $-1 < \alpha < 0$ is similar to the classical Newtonian law in the neighbourhood of singularities.

REFERENCES

Devaney, R. L., : 1981, in *Ergodic Theory and Dynamical Systems*, Boston, 211.
Diacu, F. N., Pál, Á. : 1987 a, *Babeş—Bolyai Univ. Fac. Math. Phys. Res. Sem.* **9**, No.2,3
Diacu, F. N., Pál, Á. : 1987b, *Babeş—Bolyai Univ. Fac. Math. Phys. Res. Sem.* **9**, No. 10, 19
Easton, R. : 1971, *J. Diff. Eq.*, **10**, 92.
Hagihara, Y. : 1972, *Celestial Mechanics*, Vol. 2, Part I : *Perturbation Theory*, MIT Press, Cambridge.
McGehee, R. : 1974, *Inventiones Math.*, **27**, 191.
Mioc. V., Blaga, P. : 1991, *Romanian Astron. J.*, **1**, 103.
Mücket, J. P., Treder, H.-J. : 1977, *Astron. Nachr.*, **298**, 65.
Pollard, H. : 1966, *Mathematical Introduction to Celestial Mechanics*, Prentice-Hall, Inc., Englewood Cliffs, New Jersey.

ON THE CURVATURE OF THE TRAJECTORIES IN THE RESTRICTED PROBLEM OF THREE BODIES

MIRA-CRISTIANA ANISIU

Institute of Mathematics, Cluj-Napoca

Str. Republicii 37, P. O. Box 68, 3400 Cluj-Napoca, Romania

Abstract. It is proved that for the restricted problem of three bodies there are at most three osculating solutions at one point. Points where there are three or two osculating solutions are specified.

Key Words: Celestial Mechanics — Restricted Three-Body Problem

We consider the motion of a body of negligible mass in the gravitational field due to two bodies, named primaries, of masses $1 - \mu$ and μ revolving in circular orbits around their common center of mass. The body whose motion is studied does not influence the motion of the primaries and it moves in the plane determined by their orbits.

In the synodic coordinate system, the dimensionless form of the equations governing the motion of the body of negligible mass in the restricted problem of three bodies is:

$$\begin{cases} \ddot{x} = 2\dot{y} + F_x \\ \ddot{y} = -2\dot{x} + F_y \end{cases} \tag{1}$$

where

$$F(x, y) = (x^2 + y^2)/2 + (1 - \mu)/r_1 + \mu/r_2, \tag{2}$$

$$r_1 = [(x + \mu)^2 + y^2]^{1/2}, \quad r_2 = [(x + \mu - 1)^2 + y^2]^{1/2}. \tag{3}$$

By F_x, F_y we denote the partial derivatives of F and in fact we have

$$F_x = x - (1 - \mu)(x + \mu)/r_1^3 - \mu(x + \mu - 1)/r_2^3$$

$$F_y = y(1 - (1 - \mu)/r_1^3 - \mu/r_2^3)$$

Many results on the system (1) are to be found in the book of V. Szebehely (1967). In a paper of A. Breazna (1989), some considerations on the number of osculating trajectories at one point are made and it is said that this number is at most two. In this note we show that there are points through which three such trajectories are passing.

Let the point $(X, Y) \in \mathbb{R}^2 \setminus \{(-\mu, 0), (1-\mu, 0)\}$ be given such that at this point $v \neq 0$ (where $v = (\dot{x}^2 + \dot{y}^2)^{1/2}$ is the modulus of the velocity at (X, Y)). Two or more solutions passing through (X, Y) are called *osculating solutions* if their velocities at (X, Y) are collinear and their curvature at the point (X, Y) is the same.

The curvature k at (X, Y) is given by

$$k = (\dot{x}\ddot{y} - \dot{y}\ddot{x})/v^3. \tag{4}$$

Let $\mathbf{v} = (\dot{X}, \dot{Y})$ such that $v \neq 0$. We obtain from (4)

$$k = -2/v + (\dot{X}F_y(X, Y) - \dot{Y}F_x(X, Y))/v^3, \text{ where } v = (\dot{X}^2 + \dot{Y}^2)^{1/2}.$$

We now look for $\lambda = \mathbb{R} \setminus \{0\}$ such that $k = k(\lambda)$, where $k(\lambda)$ is the value given by (4) for the initial conditions (X, Y) and $\lambda(\dot{X}, \dot{Y})$.
The relation $k = k(\lambda)$ gives the following equation:

$$\begin{aligned} &-2/v + (\dot{X}F_y - \dot{Y}F_x)/v^3 = \\ &= [-2/v + (\dot{X}F_y - \dot{Y}F_x)/(\lambda v^3)]/|\lambda| \end{aligned} \tag{5}$$

Let us denote

$$(\dot{X}F_y - \dot{Y}F_x)/v^3 = a; \quad -2/v = b < 0. \tag{6}$$

The equation (5) has then the form:

$$(a + b)|\lambda| \cdot \lambda - b\lambda - a = 0. \tag{7}$$

If $a + b = 0$, the equation (7) gives $\lambda = 1$. In the following we suppose $a + b \neq 0$.

Case 1°. Let us consider $\lambda > 0$. The equation (7) has two positive distinct solutions:

$$\lambda_1 = 1, \ \lambda_2 = -a/(a+b) \tag{8}$$

if $a \in (0, -b/2) \cup (-b/2, -b)$, and only one positive solution, namely $\lambda = 1$, if $a \in (-\infty, 0] \cup \{-b/2\} \cup (-b, \infty)$.

Case 2°. Let $\lambda < 0$, The equation (7) becomes

$$(a + b)\lambda^2 + b\lambda + a = 0.$$

and has $\Delta \geqslant 0$ if and only if $|b - 2a| \geqslant 2\sqrt{2}\ |a|$.

Denote $b_1 = b(\sqrt{2} - 1)/2 < 0$.

The equation has two negative distinct solutions if $a \in (b_1, 0)$, and only one negative solution if $a \in [0, -b)$ or $a = b_1$.

The conclusion is that the equation (7) has:
— three distinct solutions if $a \in (b_1, -b) \setminus \{0, -b/2\}$;
— two distinct solutions if $a \in \{b_1, 0, -b/2\}$;
— only the solution $\lambda = 1$ if $a \in (-\infty, b_1) \cup [-b, +\infty)$.
We obtain the following

THEOREM. Let the initial conditions $x(0) = X$, $y(0) = Y$, $\dot{x}(0) = \dot{X}$ and $\dot{y}(0) = \dot{Y}$ be given for the system (1) ($(X, Y) \in \mathbb{R}^2 \setminus \{(-\mu, 0), (1-\mu, 0)\}$, $\dot{X}^2 + \dot{Y}^2 \neq 0$) and denote

$$a = (\dot{X}F_y(X, Y) - \dot{Y}F_x(X, Y))/(\dot{X}^2 + \dot{Y}^2)^{3/2}$$

$$b = -2/(\dot{X}^2 + \dot{Y}^2)^{1/2}.$$

If $a \in (b(\sqrt{2} - 1)/2, -b) \setminus \{0, -b/2\}$, then there are three distinct osculating solutions through (X, Y).

If $a \in \{b(\sqrt{2} - 1)/2, 0, -b/2\}$, then there are two distinct osculating solutions through (X, Y).

If $a \in (-\infty, b_1) \cup [-b, +\infty)$, then for the solution given by the above initial conditions there are no osculating solutions through (X, Y). ■

We show now that the three mentioned possibilities occur indeed.

Let $X = 1/2 - \mu$, $\dot{X} = 1$, $\dot{Y} = 0$. The value $Y = y \in \mathbb{R}$ is not fixed at this moment.

We have $a = y\,[1 - (1/4 + y^2)^{-3/2}]$ and $b = -2$.

The continuous function

$$f: \quad \to \mathbb{R},\ f(y) = y[1 - (1/4 + y^2)^{-3/2}]$$

satisfies the conditions $f(-\infty) = -\infty$, $f(+\infty) = \infty$, hence it is surjective. Then for each value $a \in \mathbb{R}$, there is $y \in \mathbb{R}$ such that $f(y) = a$.

Applying the theorem we obtain:

1°. Let $y \in \mathbb{R}$ be given such that $a \in (1 - \sqrt{2}, 0)$. Then the solutions of (1) given by the initial conditions

$$(1/2 - \mu, 1, 0),\ (1/2 - \mu, y, \lambda_1, 0),\ (1/2 - \mu, y, \lambda_2, 0),$$

with λ_1, λ_2 the solutions of $(a - 2)\lambda^2 - 2\lambda + a = 0$, are osculating at $(1/2 - \mu, y)$.

2°. Let $y \in \mathbb{R}$ be given such that $a \in (0, 2) \setminus \{1\}$. Then the solutions of (1) given by the initial conditions

$$(1/2 - \mu,\ y,\ 1,\ 0),\quad (1/2 - \mu, y,\ a/(2 - a),\ 0),$$

$$\left(1/2 - \mu, y,\ \frac{-1 - \sqrt{1 + 2a - a^2}}{2 - a},\ 0\right)$$

are osculating at $(1/2 - \mu, y)$.

3°. Let $y \in \mathbb{R}$ be given such that $a = 1 - \sqrt{2}$, repectively $a = 0$ or $a = 1$. Then the solutions of (1) given by the initial conditions

$$(1/2 - \mu, y, 1, 0), \ (1/2 - \mu, y, 1 - \sqrt{2}, 0)$$

respectively

$$(1/2 - \mu, y, 1, 0), \ (1/2 - \mu, y, -1, 0)$$

or

$$(1/2 - \mu, y, 1, 0), \ (1/2 - \mu, y, -1 - \sqrt{2}, 0)$$

are osculating at $(1/2 - \mu, y)$.

For $y \in \mathbb{R}$ such that $a \in (-\infty, 1 - \sqrt{2}) \cup [2, +\infty)$ there is no osculating solution to that corresponding to the initial conditions $(1/2 - \mu, y, 1, 0)$.

REFERENCES

1. Breazna, A. : 1989, *Bull. Math. Soc. Sci. Math. RSR*, **33**, 217.
2. Szebehely, V. : 1967. *Theory of Orbits. The Restricted Problem of Three Bodies*, Academic Press, New York, San Francisco, London.

TWO-BODY PROBLEM WITH ANISOTROPIC GRAVITATIONAL CONSTANT

VASILE MIOC, CRISTINA BLAGA

Astronomical Institute of the Romanian Academy
Astronomical Observatory Cluj-Napoca
Str. Cireşilor 19, 3400 Cluj-Napoca, Romania

Abstract. The two-body problem corresponding to a gravitational force with anisotropic G is treated by means of perturbation theory. The integration of Newton-Euler equations shows that the perturbed orbit is of elliptic type, lies in a fixed plane, and its semimajor axis, eccentricity, and argument of pericentre, obtained as functions of the argument of latitude, undergo 2π-periodic variations. The nodal period, determined with an accuracy of first order in a small parameter σ and third order in eccentricity, results to be shorter than the corresponding Keplerian period. The problem approached here constitutes a particular case of the very general two-body problem with changing equivalent gravitational parameter.

Key Words: celestial mechanics — equivalent gravitational parameter — anisotropy of gravitation — orbital motion — perturbation theory.

1. INTRODUCTION

Consider a point mass m orbiting a point mass M at distance r under the only action of the gravitational force

$$\mathbf{F} = -(GMm/r^3)\mathbf{r}. \tag{1}$$

An eventual anisotropy in the gravitational constant G:

$$G = G_\infty(1 + \varepsilon(\mathbf{V}\cdot\mathbf{r}/r)^2/c^2) \tag{2}$$

and the possibility to detect it by laboratory experiments have been discussed by Will (1971). In (2) G_∞ = Newtonian attraction constant, c = speed of light, $\varepsilon < 0.015$ (see Vinti, 1972), while $\mathbf{V}$ stands for the velocity of the laboratory system with respect to a so-called parametrized post-Newtonian (PPN) system. The quoted papers identify practically $\mathbf{V}$ with Sun's velocity relative to the Galaxy's centre.

The two-body problem which results with the force (1) in which G has the expression (2) was solved by Vinti (1972) on the basis of a Binet-type equation. He constructed a fixed ellipse (which is not an osculating one, and represents the solution of the homogeneous equation) to define orbital elements, and compared the motion corresponding to the general solution of the unhomogeneous Binet-type equation with the Keplerian motion obtained for $\varepsilon = 0$, especially as regards dynamic orbital parameters (true longitude, anomalies).

Rom. Astr. J., Vol. 3, No. 1, p. 65–72, Bucharest, 1993

Here we shall approach this problem in a perturbative manner. A comparison with Vinti's (1972) method and results will be made in the last section of this paper.

We have to emphasize the fact that this problem constitutes a particular case of a much more general one: the two-body problem with changing equivalent gravitational parameter (see Mioc et al., 1988 a).

2. EQUIVALENT GRAVITATIONAL PARAMETER

The force (1) being central, it is clear that the motion of m relative to M will be planar. Denote: β = angle between $\mathbf{V}$ and orbit plane, $\mathbf{V}_2$ = vector resulting by projecting $\mathbf{V}$ onto orbit plane, θ = angle between $\mathbf{V}_2$ and $\mathbf{r}$, w = angle from $\mathbf{V}_2$ to the ascending node of the orbit (defined with respect to a fundamental plane). It results immediately

$$\theta = w + u, \tag{3}$$

where u = argument of latitude. Notice that $\mathbf{V}_2$ is fixed in an inertial space (Vinti, 1972), and the orbit plane is fixed, too; hence both $\mathbf{V}_2$ and the line of nodes keep their positions constant in the orbit plane; thus w is constant.

Vinti's (1972) geometric considerations lead to

$$G = G_\infty(1 + \sigma \cos^2 \theta), \tag{4}$$

with $\sigma = \varepsilon (V/c)^2 \cos^2\beta$. Taking into account (1) — (4), the relative orbit of m will be described by the equation

$$\mathrm{d}^2r/\mathrm{d}t^2 - h^2/r^3 = -\mu/r^2, \tag{5}$$

in which h = constant angular momentum, and μ has the expression

$$\mu = H + JA^2 + KB^2 - LAB, \tag{6}$$

where we denoted:

$$H = G_\infty(M + m); \tag{7}$$

$$J = \sigma H \cos^2 w, \quad K = \sigma H \sin^2 w, \quad L = \sigma H \sin(2w); \tag{8}$$

$$A = \cos u, \quad B = \sin u. \tag{9}$$

One sees by (5) and (6) that this is a two-body problem in which the equivalent gravitational parameter μ (see Mioc et al., 1988 a) is variable. We shall treat this problem perturbatively; in other words, taking into account (5) and (6), we shall consider that in the right-hand side of (5) the term $-H/r^2$ features the effective Newtonian attraction, while the term $(LAB - JA^2 - KB^2)/r^2$ features a perturbing force due to the anisotropy of G. That is why we use hereafter a perturbation theory terminology.

3. EVOLUTION OF THE ORBITAL ELEMENTS

Since the perturbing force depends explicitly on u, we study the motion on the basis of Newton-Euler equations written with respect to the argument of latitude (e.g. Mioc and Radu, 1991; Mioc et al., 1992):

$$
\begin{aligned}
&\mathrm{d}p/\mathrm{d}u = 2(Z/H)r^3T,\\
&\mathrm{d}\Omega/\mathrm{d}u = (Z/H)r^3W/(pD),\\
&\mathrm{d}i/\mathrm{d}u = (Z/H)r^3AW/p,\\
&\mathrm{d}q/\mathrm{d}u = (Z/H)\,(r^3kBCW/(pD) + r^2T(r(q+A)/p + A) + r^2BS),\\
&\mathrm{d}k/\mathrm{d}u = (Z/H)\,(-\,r^3qBCW/(pD) + r^2T(r(k+B)/p + B) - r^2AS),\\
&\mathrm{d}t/\mathrm{d}u = Zr^2(Hp)^{-1/2},
\end{aligned}
\tag{10}
$$

in which $Z = (1 - r^2C\dot{\Omega}/(Hp)^{1/2})^{-1}$, p = semilatus rectum, ω = argument of pericentre, e = eccentricity ($q = e\cos\omega$, $k = e\sin\omega$), Ω = longitude of ascending node, i = inclination ($C = \cos i$, $D = \sin i$), while S, T, W = radial, transverse, and binormal components of the perturbing acceleration, respectively.

But the perturbing force is radial; so

$$S = (IAB - JA^2 - KB^2)/r^2, \quad T = 0, \quad W = 0, \tag{11}$$

and the first three equations (10) yield immediately

$$p = p_0, \quad \Omega = \Omega_0, \quad i = i_0, \tag{12}$$

where subscripts refer to the initial position $u = u_0$. Hence the orbit plane is fixed (this is natural since the force acting on m is central), and the semilatus rectum keeps a constant value.

By (12), $Z = 1$; with (11) the fourth and fifth equations (10) acquire the form

$$\mathrm{d}q/\mathrm{d}u = (IAB^2 - JA^2B - KB^3)/H, \tag{13}$$

$$\mathrm{d}k/\mathrm{d}u = (JA^3 + KAB^2 - IA^2B)/H. \tag{14}$$

Observe that equations (13) and (14) are no more coupled. Integrating them, the behaviour of q and k in the interval $[u_0, u]$ is given respectively by

$$q = q_0 + (Q - Q_0)/(3H), \tag{15}$$

$$k = k_0 + (P - P_0)/(3H), \tag{16}$$

where we used the abbreviations

$$Q = Q(u) = LB^3 + (J - K)A^3 + 3KA, \tag{17}$$

$$P = P(u) = LA^3 - (J - K)B^3 + 3JB, \tag{18}$$

and $Q_0 = Q(u_0)$, $P_0 = P(u_0)$. It is easy to see that the expressions (15) and (16) are 2π-periodic functions of u.

Let us now pass to more intuitive orbital elements. Using the definitions of q and k, and expressions (15) — (18), then substituting (8) and (9) into the results, we get (to first order in σ) the behaviour of the eccentricity :

$$e = e_0 - \sigma((1/2)\sin((u + u_0)/2 - 2w + \omega_0)\sin((u - u_0)/2) +$$
$$+ (1/6)\sin(3(u + u_0)/2 + 2w - \omega_0)\sin(3(u - u_0)/2) -$$
$$- \cos(2w)\sin((u + u_0)/2 + \omega_0)\sin((u - u_0)/2) +$$
$$+ \sin((u + u_0)/2 - \omega_0)\sin((u - u_0)/2)), \tag{19}$$

and that of the argument of pericentre :

$$\omega = \omega_0 - (\sigma/e_0)((1/2)\cos((u + u_0)/2 - 2w + \omega_0)\sin((u - u_0)/2) -$$
$$- (1/6)\cos(3(u + u_0)/2 + 2w - \omega_0)\sin(3(u - u_0)/2) -$$
$$- \cos(2w)\cos((u + u_0)/2 + \omega_0)\sin((u - u_0)/2) -$$
$$- \cos((u + u_0)/2 - \omega_0)\sin((u - u_0)/2)). \tag{20}$$

With $p = a(1 - e^2)$, (12), and (19), we easily obtain the evolution of the semimajor axis a :

$$a = a_0 - 2a_0e_0\sigma((1/2)\sin((u + u_0)/2 -$$
$$- 2w + \omega_0)\sin((u - u_0)/2) +$$
$$+ (1/6)\sin(3(u + u_0)/2 + 2w - \omega_0)\sin(3(u - u_0)/2) -$$
$$- \cos(2w)\sin((u + u_0)/2 + \omega_0)\sin((u - u_0)/2) +$$
$$+ \sin((u + u_0)/2 - \omega_0)\sin((u - u_0)/2))/(1 - e_0^2). \tag{21}$$

It is clear that expressions (19), (20), and (21) are 2π-periodic functions of u, too.

By the last two expressions (12) and (19)—(21) we can say that along the interval $[u_0, u_0+2\pi]$ the osculating orbit lies in a fixed plane, but undergoes changes, in shape, dimensions, and orientation. As to the evolution of these changes, putting $\Delta y = y(u) - y_0$, with $y \in \{a, e, \omega\}$, and knowing that $y(u_0) = y(u_0 + 2\pi) = y_0$, there are the following possible situations:

(i) Δy does not admit zeros in the interval $(u_0, u_0 + 2\pi)$, that is, during a revolution (except, of course, the starting and ending points) the respective element is systematically greater or smaller than its initial value;

ii) Δy admits zeros in the interval $(u_0, u_0 + 2\pi)$, that is, during a revolution the respective element oscillates around its initial value.

The kind of change undergone by the element y depends on the values assigned to the initial parameters u_0 and ω_0, and to the constant w.

For the trajectory of the point mass m, using the orbit equation in polar coordinates $r = p / (1 + e \cos v)$, where v = true anomaly, under the form

$$r = p/(1 + qA + kB), \tag{22}$$

and taking into account (12), (15), and (16), we get

$$p_0/r = 1 + (q_0 + (Q - Q_0)/(3H))A + (k_0 + (P - P_0)/(3H))B, \tag{23}$$

with Q, P (and Q_0, P_0) provided by (17), (18), respectively. We can hence say that equation (23) describes an ellipse whose eccentricity undergoes continuous and 2π-periodic changes, according to one of the above mentioned situations.

4. THE NODAL PERIOD

The nodal period, defined by

$$T_\Omega = \int_0^{2\pi} (\mathrm{d}t/\mathrm{d}u)\,\mathrm{d}u, \tag{24}$$

will be estimated by means of the method proposed by Zhongolovich (1960) and extended by Mioc (1992). According to this method, whose principles were also sketched in the papers of Mioc (1980), Mioc and Blaga (1991), Mioc and Radu (1991 b), Mioc et al. (1992) and will not be repeated here, the nodal period (perturbed by an arbitrary force depending on a small parameter σ) is given to first order in σ by

$$T_\Omega = T_0 + \Delta^{(1)} T_\Omega, \tag{25}$$

where

$$T_0 = p_0^{3/2} H^{-1/2} \int_0^{2\pi} g^{-2}\,\mathrm{d}u, \tag{26}$$

and

$$\Delta^{(1)} T_\Omega = p_0^{3/2} H^{-1/2} (-2I_q - 2I_k + (3/2) p_0^{-1} I_p + p_0^2 H^{-1} I_\sigma), \tag{27}$$

with

$$I_p = \int_0^{2\pi} g^{-2}\, \Delta p\, \mathrm{d}u,\ I_q = \int_0^{2\pi} g^{-3} A \Delta q\, \mathrm{d}u,$$

$$I_k = \int_0^{2\pi} g^{-3} B\, \Delta k\, \mathrm{d}u,\ I_\sigma = \int_0^{2\pi} g^{-5} B(\partial (CW/D)/\partial\sigma)_0 \sigma\, \mathrm{d}u. \tag{28}$$

In these formulae H is given by (7), $\Delta y = y(u) - y_0$, $y \in \{p, q, k\}$, while $g = g(u) = 1 + q_0 A + k_0 B$.

In our problem, where the small parameter is just σ which appears in (4), we observe that $I_p = 0$, $I_\sigma = 0$, expand g^{-2} and g^{-3} to third order in q_0, k_0 (or equivalently in e_0), replace the results and Δq, Δk given by (15) — (16) into (26) and (28), perform the integrations, and calculate the expression (27). The results are:

$$T_0 = 2\pi p_0^{3/2} H^{-1/2} (1 + 3(q_0^2 + k_0^2)/2), \tag{29}$$

$$\begin{aligned}\Delta^{(1)} T_\Omega = &- \pi p_0^{3/2} H^{-3/2} (2(J + K) + 2(q_0 Q_0 + k_0 P_0) + \\ &+ 2q_0 k_0 L + 5(q_0^2 J + k_0^2 K) + 7(q_0^2 K + k_0^2 J) + \\ &+ 5(q_0^2 + k_0^2)(q_0 Q_0 + k_0 P_0)).\end{aligned} \tag{30}$$

Now, in order to compare the perturbed nodal period with the corresponding Keplerian period, we replace in (29) — (30): the definitions of q and k, the relation $p = a(1 - e^2)$, the expressions (17) — (18), then (8) and (9); performing the sum (25), we get the perturbed nodal period with an accuracy of first order in σ and third order in eccentricity:

$$T_\Omega = 2\pi a_0^{3/2}\, H^{-1/2} (1 - \sigma f(e_0, \omega_0, u_0, w)), \tag{31}$$

where

$$\begin{aligned} f = 1 + [&\cos\omega_0 (2 \sin w \sin^2 u_0 \sin(w + u_0) + \cos u_0 (\sin^2 w + \cos^2 u_0)) + \\ &+ \sin\omega_0 (2\cos w \cos^2 u_0 \sin(w + u_0) + \sin u_0 (\cos^2 w + \sin^2 u_0))] \times \\ &\times (e_0 + e_0^3) + (1 + \sin^2 (w + \omega_0)) e_0^2. \end{aligned} \tag{32}$$

As long as f has positive values (and this is generally the case, as we shall see), the nodal period T_Ω will be shorter than the corresponding Keplerian period $T_K = 2\pi a_0^{3/2}\, H^{-1/2}$, the difference being of order at most

σT_K. So, the anisotropy in G has the tendency to accelerate the motion. This speeding is maximum when the initial position is in pericentre σ ($u_0 = \omega_0$), and in addition the initial line of nodes is perpendicular to $\mathbf{V}_2(w + u_0 = \pi/2$ or $3\pi/2)$, that is, (32) reduces to

$$f = 1 + 2e_0 + 2e_0^2 + 2e_0^3, \tag{33}$$

and minimum when the initial position is in apocentre ($u_0 = \omega_0 + \pi$), and the above second condition is fulfilled, too; in this case (32) reduces to

$$f = 1 - 2e_0 + 2e_0^2 - 2e_0^3. \tag{34}$$

Two remarks are to be made. Firstly, observe from (31) and (34) that to have $T_\Omega > T_K$ (decelerated motion) the initial eccentricity must exceed 0.65 roughly. But for such high eccentric initial orbits an accuracy of third order in e_0 is absolutely insufficient; therefore, with the accuracy of (31) — (32), we can say that the nodal period is always shorter than the corresponding Keplerian period. Secondly, observe from (3) and (4) that the second condition imposed to u_0 in order to get an extremum for f leads to an initial value of G equal to G_∞ (initially Keplerian motion governed by the purely Newtonian attraction; this is a natural and usual condition).

5. CONCLUSIONS AND COMMENTS

The possible anisotropy in G presumed by Will (1971) to be of the form (2) leads to a two-body problem in which the gravitational force is anisotropic. Vinti (1972), whose paper constituted the departure point for our investigation, solved this problem by integrating a Binet-type equation, while our treatment is a perturbative one based on the integration of Newton-Euler equations. More concretely, Vinti compared the motion described by his equation (through orbital elements defined on a non-osculating fixed ellipse) with the unperturbed motion obtained by making $\varepsilon = 0$ in (2); we consider the anisotropy of G to be a perturbing factor and compare the real perturbed orbit with the initial Keplerian orbit.

The major purpose of Vinti's (1972) paper is to estimate quantitatively the effects of the anisotropy of G on orbits in the solar system (by identifying practically $\mathbf{V}$ with Sun's velocity with respect to Galaxy's centre), The present paper studies the evolution of an arbitrary elliptic-type orbit in the case of an anisotropic gravitational constant.

Our results indicate an elliptic-type motion in a fixed plane. The semimajor axis, eccentricity, and argument of pericentre, obtained as functions of u, present 2π-periodic variations. The nodal period, determined with a first order accuracy in σ and third order accuracy in e_0, is shorter than the corresponding Keplerian period, the difference being of order at most σT_K. A speeding of the motion having this order of magnitude results from Vinti's investigation, too.

The use of the argument of latitude as independent variable (and the consecutive determination of the nodal period as basic time interval) allows the study of very low eccentric orbits, even circular.

By (5) and (6) this is a problem which belongs — we repeat — to the general two-body problem with changing equivalent gravitational parameter in the meaning of Mioc et al. (1988 a). The variation of μ can be of very different natures (see e.g. Duboshin, 1963 ; Savedoff and Vila, 1964 ; Glikman, 1976, 1978 ; Saslaw, 1978 ; Giurgiu, 1988) and of various types. Among such changes, those with cyclic character, especially the periodic ones, were approached by Saslaw (1978), Mioc et al. (1988 b, c), Mioc (1989), Şelaru et al. (1992). The anisotropy of μ constitutes an apart case of periodic variation (see Saslaw, 1978), and this class of problems includes the situation we studied in this paper, too.

REFERENCES

Duboshin, G. N. : 1963, *Celestial Mechanics. Basic Problems and Methods*, Nauka, Moscow (Russ.).

Giurgiu, I. : 1988, Thesis, University of Cluj-Napoca.

Glikman, L. G. : 1976, *Astron. Zh.*, **53**, 185.

Glikman, L. G. : 1978, *Astron. Zh.*, **55**, 873.

Mioc, V. : 1980, *Astron. Nachr.*, **301**, 311.

Mioc, V. : 1989, *Studia Univ. Babeş-Bolyai*, ser. *Physica*, **34**, No. 2, 64.

Mioc, V. : 1992, *Romanian Astron. J.*, **2**, 53.

Mioc, V., Blaga, P. : 1991, *Romanian Astron. J.*, **1**, 103.

Mioc, V., Radu, E. : 1991 a, *Astron. Nachr.*, **312**, 327.

Mioc, V., Radu, E. : 1991 b, *Bull. Astron. Inst. Czechosl.*, **42**,, 395.

Mioc, V., Pál. Á., Giurgiu, I. : 1988 a, *Babeş-Bolyai Univ. Fac. Math. Phys. Res. Sem.*, **10**, No. 1, 79.

Mioc, V., Pál, Á. Giurgiu, I. : 1988 b, *Studia Univ. Babeş-Bolyai*, ser. *Mathematica*, **33**, No. 4, 67

Mioc. V., Pál, Á., Giurgiu, I. : 1988 c, *Studia Univ. Babeş-Bolyai*, ser. *Physica*, **33**, No. 2, 85.

Mioc, V., Radu, E., Blaga, C. : 1992, *Rev. Mexicana Astron. Astrofis.*, **24**, 15.

Saslaw, W. C. : 1978, *Astrophys, J.*, **226**, 240.

Savedoff, M. P., Vila, S. : 1964, *Astron. J.*, **69**, 242.

Şelaru, D., Cucu-Dumitrescu, C., Mioc, V. : 1992, *Astron. Nachr.*, **313**, 257.

Vinti, J. P. : 1972, *Celest. Mech.*, **6**, 198.

Will, C. M. : 1971, *Astrophys. J.*, **149**, 141.

Zhongolovich, I. D. : 1960, *Byull. Inst. Teor. Astron.*, **7**, 521.

NODAL PERIOD IN MOTION PERTURBED BY A FORCE ACTING IN ORBIT PLANE

VASILE MIOC

Astronomical Institute of the Romanian Academy
Astronomical Observatory Cluj-Napoca
Str. Cireşilor 19, 3400 Cluj-Napoca, Romania

Abstract. An analytic estimate (much improved as against the actual ones) of the nodal period corresponding to an orbit which experiences perturbations due to a force depending on a small parameter and acting in the orbit plane is obtained. The case of radial perturbing force is treated separately. An accuracy of any order in the small parameter and of a desired order in eccentricity can be reached. The main formulae are applicable to various concrete astronomical situations modellable by this theory.

Key Words : celestial mechanics — perturbation theory — orbital motion — nodal period

1. INTRODUCTION

Consider a point mass orbiting an attractive centre at distance r under the influence of two forces : the Newtonian attraction and a perturbing force depending on a small parameter σ. Let us describe the motion in terms of classic Keplerian orbital elements by means of Newton-Euler equations written in the form (e.g. Mioc and Radu, 1991 ; Mioc et al., 1992) :

$$\begin{aligned}
&\mathrm{d}p/\mathrm{d}u = 2(Z/\mu)r^3T,\\
&\mathrm{d}\Omega/\mathrm{d}u = (Z/\mu)r^3BW/(pD),\\
&\mathrm{d}i/\mathrm{d}u = (Z/\mu)r^3AW/p, \qquad (1)\\
&\mathrm{d}q/\mathrm{d}u = (Z/\mu)(r^3kBCW/(pD) + r^2T(r(q+A)/p + A) + r^2BS),\\
&\mathrm{d}k/\mathrm{d}u = (Z/\mu)\,(-\,r^3qBCW/(pD) + r^2T(r(k+B)/p + B) - r^2AS),\\
&\mathrm{d}t/\mathrm{d}u = Zr^2(\mu p)^{-1/2},
\end{aligned}$$

where $Z = (1 - r^2C\dot{\Omega}/(\mu p)^{1/2})^{-1}$, μ = gravitational parameter of the dynamic system, p semilatus rectum, Ω=longitude of ascending node, i = inclination ($C = \cos i$, $D = \sin i$), $q = e\cos\omega$, $k = e\sin\omega$ (e=eccentricity, ω = argument of pericentre), u = argument of latitude ($A = \cos u$, $B = \sin u$), S, T, W = radial, transverse, and binormal components of the perturbing accceleration, respectively.

The nodal period defined as

$$T_{\Omega} = \int_{0}^{2\pi} (\mathrm{d}t/\mathrm{d}u)\,\mathrm{d}u \tag{2}$$

was analytically estimated by Zhongolovich (1960), to first order in σ, for the case of a point mass motion in the attraction field of a rotation level ellipsoid. The method was extended to various perturbing factors (for a brief survey see Mioc, 1992). A second order (in σ) approximation of T_{Ω}, which can be used to orbits of arbitrary subunitary eccentricity, was given by Mioc (1992).

In this paper we propose a much improved analytic estimate of the nodal period, to any order in σ, for the situation when the perturbing force acts in the orbit plane. The simpler case of radial perturbing force and the more general case of nonradial perturbing force (acting however in the orbit plane) will be separately treated.

2. AUXILIARY RESULTS

Let us firstly establish some preliminary results which will be helpful for expressing the integrand of (2) in terms of u only.

PROPOSITION 1. *Let x be a real variable, let M, N be real valued functions which do not depend on x, such that $M + Nx \neq 0$, and let w, s be natural numbers. The following relation holds :*

$$\frac{\partial^{w}(M+Nx)^{-s}}{\partial x^{w}} = (-1)^{w}\frac{(s+w-1)!}{(s-1)!}(M+Nx)^{-s-w}N^{w}. \tag{3}$$

Proof. The proof is immediate by introduction. For $w = 1$ we have

$$\frac{\partial(M+Nx)^{-s}}{\partial x} = -\,s(M+Nx)^{-s-1}N.$$

Suppose that (3) holds for $w = m$, and calculate the derivative for $w = m + 1$; we have

$$\frac{\partial^{m+1}(M+Nx)^{-s}}{\partial x^{m+1}} = \frac{\partial}{\partial x}\left[\frac{\partial^{m}(M+Nx)^{-s}}{\partial x^{m}}\right] =$$

$$= \frac{\partial}{\partial x}\left[(-1)^{m}\frac{(s+m-1)!}{(s-1)!}(M+Nx)^{-s-m}N^{m}\right] =$$

$$= (-1)^{m+1}\frac{(s+m)!}{(s-1)!}(M+Nx)^{-s-m-1}N^{m+1},$$

hence (3) is true, and Proposition 1 is proved.

PROPOSITION 2. *Let q, k be real independent variables, let A, B be real valued functions which do not depend on q, k, such that $1 + Aq + Bk \neq 0$, and let n, j be natural numbers, $j \leqslant n$. The following relation holds :*

$$\frac{\partial^n (1 + Aq + Bk)^{-2}}{\partial q^{n-j}\, \partial k^j} = (-1)^n (n+1)!\, (1 + Aq + Bk)^{-n-2} A^{n-j} B^j. \qquad (4)$$

Proof. To prove this relation we write

$$\frac{\partial^n (1 + Aq + Bk)^{-2}}{\partial q^{n-j}\, \partial k^j} = \frac{\partial^j}{\partial k^j} F_{n-j},$$

where $F_{n-j} = \partial^{n-j}(1 + Aq + Bk)^{-2}/\partial q^{n-j}$. Putting $M = 1 + Bk$, $N = A$, $x = q$, $s = 2$, $w = n - j$, one sees that F_{n-j} is of the form $\partial^w (M + Nx)^{-s}/\partial x^w$, so, by virtue of Proposition 1 :

$$\frac{\partial^n (1 + Aq + Bk)^{-2}}{\partial q^{n-j}\, \partial k^j} = \frac{\partial^j}{\partial k^j} [(-1)^{n-j}(n - j + 1)!(1 + Aq + Bk)^{-n+j-2} A^{n-j}] =$$

$$= (-1)^{n-j}(n - j + 1)!\, A^{n-j} G_j,$$

where $G_j = \partial^j (1 + Aq + Bk)^{-n+j-2}/\partial k^j$. Putting now $M = 1 + Aq$, $N = B$, $x = k$, $s = n - j + 2$, $w = j$, one remarks that G_j acquires the same form $\partial^w (M + Nx)^{-s}/\partial x^w$. Using once again Proposition 1, we get

$$\frac{\partial^n (1 + Aq + Bk)^{-2}}{\partial q^{n-j}\, \partial k^j} =$$

$$= (-1)^{n-j}(n - j + 1)!A^{n-j}(-1)^j \frac{(n+1)!}{(n - j + 1)!} \times$$

$$\times (1 + Aq + Bk)^{-n-2} B^j = (-1)^n (n+1)!(1 + Aq + Bk)^{-n-2} A^{n-j} B^j,$$

which is just the relation (4). So, Proposition 2 is proved.

3. CASE OF RADIAL PERTURBING FORCE

3.1. Basic Equations

Considering that the perturbing force is radial, we have $T = 0$, $W = 0$, and, as a direct sequel of the second equation (1), $Z = 1$. Also, using the orbit equation in polar coordinates $r = p/(1 + e \cos v)$, where $v = u - \omega$ is the true anomaly, we have

$$r = p(1 + Aq + Bk)^{-1}. \qquad (5)$$

So, equations (1) reduce to

$$\mathrm{d}p/\mathrm{d}u = 0,\ \mathrm{d}\Omega/\mathrm{d}u = 0,\quad \mathrm{d}i\,/\mathrm{d}u = 0,$$

$$\begin{aligned} \mathrm{d}q/\mathrm{d}u &= p^2\mu^{-1}B(1 + Aq + Bk)^{-2}S,\\ \mathrm{d}k/\mathrm{d}u &= -\,p^2\mu^{-1}A(1 + Aq + Bk)^{-2}S,\\ \mathrm{d}t/\mathrm{d}u &= p^{3/2}\mu^{-1/2}(1 + Aq + Bk)^{-2}, \end{aligned} \tag{6}$$

where the expression of S remains unspecified.

By (6) follows immediately $p = p_0$, $\Omega = \Omega_0$, $i = i_0$ (the perturbed orbit is planar and of constant semilatus rectum), where subscripts refer to the initial position $u = u_0$. Also, supposing that $y \in Y = \{q, k\}$ undergoes small changes $\Delta y = y - y_0$ over time intervals short enough, and integrating the fourth and fifth equations (6) by successive approximations, we get the changes of q, k in the interval $[u_0, u]$ to first order in σ (hidden into S):

$$\begin{aligned} \Delta q &= p_0^2\mu^{-1}\int_{u_0}^{u} B(1 + Aq_0 + Bk_0)^{-2}S\,\mathrm{d}u,\\ \Delta k &= -\,p_0^2\mu^{-1}\int_{u_0}^{u} A(1 + Aq_0 + Bk_0)^{-2}S\,\mathrm{d}u. \end{aligned} \tag{7}$$

As to the nodal period, let us denote

$$f(y\,;u) = (1 + Aq + Bk)^{-2},\quad y \in Y. \tag{8}$$

So, by (8) and the last equation (6), (2) becomes

$$T_\Omega = p_0^{3/2}\mu^{-1/2}\int_0^{2\pi} f(y\,;u)\,\mathrm{d}u. \tag{9}$$

To find T_Ω we still have to express the integrand of (9) in terms of u only.

3.2. Nodal Period

We shall express the main result of this Section under the form of

THEOREM 1. *If the perturbed motion of a point mass in an attractive field is described by equations* (6), *then the nodal period corresponding to this motion is given by*

$$T_\Omega = p_0^{3/2}\mu^{-1/2}\sum_{n=0}^{\infty}(-1)^n(n+1)I_n, \tag{10}$$

where

$$I_n = \int_0^{2\pi} (A\,\Delta q + B\Delta k)^n (1 + Aq_0 + Bk_0)^{-n-2}\,\mathrm{d}u,$$

with Δq, Δk *provided by* (7).

Proof. Let us Taylor-expand the function f given by (8) on the hypersurface $H = H(y_0\,;\,u)$, $y \in Y$, with respect to the small quantities Δy; we have

$$f(y\,;\,u) = \sum_{n=0}^{\infty} \frac{1}{n!}\left(\Delta q \frac{\partial}{\partial q} + \Delta k \frac{\partial}{\partial k}\right)^n f(y_0\,;\,u) =$$

$$= \sum_{n=0}^{\infty} \frac{1}{n!} \sum_{j=0}^{n} \binom{n}{j} (\Delta q)^{n-j} (\Delta k)^j \frac{\partial^n}{\partial q^{n-j}\,\partial k^j} f(y_0\,;\,u),$$

where it is meant that the zeroth order derivative is the function itself, and $\binom{0}{0} = 1$. Taking into account (8), and using Proposition 2, we obtain successively

$$f(y\,;\,u) = \sum_{n=0}^{\infty} \frac{1}{n!} \sum_{j=0}^{n} \binom{n}{j} (\Delta q)^{n-j} (\Delta k)^j \left[\frac{\partial^n (1 + Aq + Bk)^{-2}}{\partial q^{n-j}\,\partial k^j}\right]_{y=y_0} =$$

$$= \sum_{n=0}^{\infty} (-1)^n (n+1)(1 + Aq_0 + Bk_0)^{-n-2} \sum_{j=0}^{n} \binom{n}{j} (A\Delta q)^{n-j} (B\Delta k)^j =$$

$$= \sum_{n=0}^{\infty} (-1)^n (n+1)(1 + Aq_0 + Bk_0)^{-n-2} (A\Delta q + B\Delta k)^n.$$

Replacing now $f(y : u)$ in (9), we get the expression (10), and the theorem is proved.

4. CASE OF NONRADIAL PERTURBING FORCE ACTING IN ORBIT PLANE

4.1. Basic Equations

We shall now consider that the perturbing force, lying in the orbit plane, is nonradial. In this case $S \neq 0$, $T \neq 0$, $W = 0$, $Z = 1$. With r given by (5), equations (1) reduce to

$$\mathrm{d}p/\mathrm{d}u = 2p^3\,\mu^{-1}(1 + Aq + Bk)^{-3}\,T,$$

$$\mathrm{d}\Omega/\mathrm{d}u = 0,$$

$$\mathrm{d}i/\mathrm{d}u = 0, \qquad (11)$$

$$\mathrm{d}q/\mathrm{d}u = p^2\mu^{-1}(1 + Aq + Bk)^{-2}[((1 + Aq + Bk)^{-1}(q + A) + \\ + A)T + BS], \tag{11}$$

$$\mathrm{d}k/\mathrm{d}u = p^2\mu^{-1}(1 + Aq + Bk)^{-2}[((1 + Aq + Bk)^{-1}(k + B) + \\ + B)T - AS)],$$

$$\mathrm{d}t/\mathrm{d}u = p^{3/2}\mu^{-1/2}(1 + Aq + Bk)^{-2},$$

the expressions of S and T remaining unspecified.

The perturbed orbit lies in a fixed plane, too ($\Omega = \Omega_0, i = i_0$), but the semilatus rectum is no more constant. Using also successive approximations, the changes of $y \in Y = \{p, q, k\}$ in the interval $[u_0, u]$ are (to first order in σ hidden into S and T):

$$\Delta p = 2p_0^3\mu^{-1}\int_{u_0}^{u}(1 + Aq_0 + Bk_0)^{-3}T\,\mathrm{d}u,$$

$$\Delta q = p_0^2\mu^{-1}\int_{n_0}^{n}(1 + Aq_0 + Bk_0)^{-2}[((1 + Aq_0 + Bk_0)^{-1}\times \\ \times (q + A) + A)T + BS]\,\mathrm{d}u, \tag{12}$$

$$\Delta k = p_0^2\mu^{-1}\int_{u_0}^{u}(1 + Aq_0 + Bk_0)^{-2}[((1 + Aq_0 + Bk_0)^{-1}\times \\ \times (k + B) + B)T - AS]\,\mathrm{d}u.$$

Denoting now

$$f(y\,;u) = p^{3/2}(1 + Aq + Bk)^{-2}, \quad y \in Y, \tag{13}$$

and taking into account the last equation (11), the nodal period (2) will be given by

$$T_\Omega = \mu^{-1/2}\int_0^{2\pi} f(y\,;u)\,\mathrm{d}u. \tag{14}$$

It is now the integrand of (14) to be expressed in terms of u only.

4.2. Nodal Period

The main result of this Section will be expressed as

THEOREM 2. *If the perturbed motion of a point mass in an attractive field is described by equations* (11), *then the nodal period corresponding to this motion is given by*

$$T_\Omega = P_0^{-1}\mu^{-1} \sum_{n=0}^{\infty} \sum_{j=0}^{n} (-1)^n (j+1) I_{nj}, \tag{15}$$

where

$$I_{nj} = \int_0^{2\pi} (\Delta P/P_0)^{n-j}(A\Delta q + B\Delta k)^j (1 + Aq_0 + Bk_0)^{-j-2}\, du,$$

with $P = p^{-3/2}$ *and* ΔP, Δq, Δk *provided by* (12) *in which this transformation was performed.*

Proof. Let us Taylor-expand the function

$$f(y\,;u) = P^{-1}(1 + Aq + Bk)^{-2}, \quad y \in Y' = \{P, q, k\},$$

given by (13), in which we replaced $p^{3/2}$ by P^{-1}, on the hypersurface $H = H(y_0\,;u)$, $y \in Y'$, with respect to the small quantities Δy ; we have

$$f(y\,;u) = \sum_{n=0}^{\infty} \frac{1}{n!}\left(\Delta P\frac{\partial}{\partial P} + \Delta q\frac{\partial}{\partial q} + \Delta k\frac{\partial}{\partial k}\right)^n f(y_0\,;u),$$

from which, taking into account the expression of $f(y\,;u)$, we get

$$\begin{aligned} f(y\,;u) = \sum_{n=0}^{\infty}\frac{1}{n!}\sum_{j=0}^{n}\binom{n}{j}(\Delta P)^{n-j}\left[\frac{\partial^{n-j}P^{-1}}{\partial P^{n-j}}\right]_{y=y_0} \times \\ \times \sum_{i=0}^{j}\binom{j}{i}(\Delta q)^{j-i}(\Delta k)^i\left[\frac{\partial^j(1+Aq+Bk)^{-2}}{\partial q^{j-i}\,\partial k^i}\right]_{y=y_0}. \end{aligned} \tag{16}$$

By Proposition 1 follows immediately

$$\frac{\partial^{n-j}P^{-1}}{\partial P^{n-j}} = (-1)^{n-j}(n-j)!\,P^{-n+j-1},$$

and by Proposition 2

$$\frac{\partial^j(1+Aq+Bk)^{-2}}{\partial q^{j-i}\,\partial k^i} = (-1)^j(j+1)!\,(1 + Aq + Bk)^{-j-2}A^{j-i}B^i.$$

Replacing these expressions in (16), after simple calculations similar to those from the proof of Theorem 1, we obtain

$$f(y\,;u) = \sum_{n=0}^{\infty} \sum_{j=0}^{n} (-1)^n (j+1)(\Delta P)^{n-j} P_0^{-n+j-1} (A\Delta q + B\Delta k)^j \times$$

$$\times (1 + Aq_0 + Bk_0)^{-j-2}.$$

Introducing this expression of $f(y\,;u)$ in (14), we get (15), and the theorem is proved.

5. PARTICULAR CASES

Suppose that the perturbing force acts in the orbit plane normally to radius vector ($S = 0$, $T \neq 0$, $W = 0$). In this case the expression (15) of Theorem 2 is preserved, but Δq, Δk are respectively given by

$$\Delta q = p_0^2 \mu^{-1} \int_{u_0}^{u} (1 + Aq_0 + Bk_0)^{-2}((1 + Aq_0 + Bk_0)^{-1}(q + A) + A)T\,\mathrm{d}u,$$

$$\Delta k = p_0^2 \mu^{-1} \int_{u_0}^{u} (1 + Aq_0 + Bk_0)^{-2}((1 + Aq_0 + Bk_0)^{-1}(k + B) + B)T\,\mathrm{d}u. \tag{17}$$

Suppose now that the conditions of Theorem 2 are fulfilled and, in addition, the initial orbit is circular ($q_0 = 0$, $k_0 = 0$) of radius p_0. Formula (15) still holds, but I_{nj} is given by

$$I_{nj} = \int_{0}^{2\pi} (\Delta P/P_0)^{n-j} (A\Delta q + B\Delta k)^j\,\mathrm{d}u,$$

while (12) become

$$\Delta p = 2p_0^3 \mu^{-1} \int_{u_0}^{u} T\,\mathrm{d}u,$$

$$\Delta q = p_0^2 \mu^{-1} \int_{u_0}^{u} ((q + 2A)T + BS)\,\mathrm{d}u, \tag{18}$$

$$\Delta k = p_0^2 \mu^{-1} \int_{u_0}^{u} ((k + 2B)T - AS)\,\mathrm{d}u.$$

6. COMMENTS

REMARK 1. Theorem 1 results from Theorem 2 as a corollary. However we separated the two cases since there exist many astronomical situations in which the perturbing force acts radially.

REMARK 2. Formulae (10) and (15) provide the nodal period to any order in σ (hidden into Δy given by (7) and respectively (12), which are of first order in σ). Of course, Δy can be determined with a higher order accuracy in σ, but this entails great complications in the effective calculations, as well as reordering in power series of σ.

REMARK 3. To use effectively formulae (10) and (15), the expression $(1 + Aq_0 + Bk_0)^{-s}$, which appears under integrals, and can also appear from S, T when these ones are analytically specified for a concrete perturbing factor, must be expanded in power series of q_0, k_0. So, truncating the series, the result is obtained with the corresponding accuracy in eccentricity (determined by q_0, k_0), besides the accuracy of any order in σ.

REMARK 4. To obtain separately the perturbation of a certain order, it is sufficient to assign the corresponding value to n in formulae (10) and (15).

REMARK. 5 The conditions of Theorems 1 and 2 are fulfilled in many concrete astronomical situations. Among such situations we mention: motion around sources whose luminosity changes (Saslaw, 1978), orbits in anisotropic radiation fields (Mioc and Radu, 1993), motions in certain post-Newtonian and relativistic gravitational fields (Mioc and Blaga, 1991; Blaga and Mioc, 1992), theory of gravitational constant anisotropy (Mioc and Blaga 1993), motions with changing equivalent gravitational parameter (Mioc et al., 1988; Şelaru et al., 1992), artificial satellite motion under the influence of certain perturbing factors, etc.

REFERENCES

Blaga, P., Mioc, V.: 1992, *Europhys. Lett.*, **17**, 275.
Mioc. V.: 1992, *Romanian Astron. J.*, **2**, 53.
Mioc, V.: Blaga, C.: 1993, *Romanian Astron. J.*, **3**, 65.
Mioc, V., Blaga, P.: 1991, *Romanian Astron. J.*, **1**, 103.
Mioc, V., Radu, E.: 1991, *Astron. Nachr.*, **312**, 327.
Mioc, V., Radu, E.: 1992, *Astron. Nachr.*, **313**, 353.
Mioc, V., Pál, A., Giurgiu, I.: 1988, *Babeş-Bolyai Univ. Fac. Math. Phys. Res. Sem.*, **10**, No. 1, 79.
Mioc, V., Radu, E., Blaga, C.: 1992, *Rev. Mexicana Astron. Astrofis.*, **24**, 15.
Saslaw, W. C.: 1978, *Astrophys. J.*, **226**, 240.
Şelaru, D., Cucu-Dumitrescu, C., Mioc, V.: 1992, *Astron. Nachr.*, **313**, 257.
Zhongolovich, I. D.: 1960, *Byull. Inst. Teor. Astron.*, **7**, 521.

PROFESSOR GHEORGHE CHIŞ (1913–1981) – AN INITIATOR OF VARIABLE STAR RESEARCH IN ROMANIA AND OF ARTIFICIAL SATELLITE OBSERVATIONS IN CLUJ

Now, at 80 years from the birth of Gheorghe Chiş, a man who served the astronomical science for more than 46 years as an astronomer, professor and director of the Astronomical Observatory of the University in Cluj-Napoca, it is properly to reveal his special merits and the main trends opened by him in this field.

Professor Gheorghe Chiş was born on the 8th of August 1913 in a village called Santău, in the Satu Mare country, in a modest family. His father passed away untimely, dying on the battle fields of the first World War, so he became an orphan very soon. He finished the primary studies in his native village, the secondary studies in Carei, in 1931, with the highest qualification. In 1935 he graduated from the Faculty of Sciences of the Dacia Superior University in Cluj, as a bachelor of physical-mathematical sciences, with the same highest qualification. While he was studying as a student, the astronomer Gheorghe Bratu, one of his professors, remarked Gh. Chiş's passion for astronomy and employed him at the Astronomical Observatory as a secretary. After graduation, on the 1st of February 1936, Gheorghe Chiş was appointed a préparateur at the Astronomical Observatory of the Cluj University, function which he kept until the 1st of February 1943. Meanwhile he was called up and sent on the Eastern front, where he participated in several battles. Hurt, demobilized, he was then appointed assistant for some months and on the 1st of December 1943 Gheorghe Chiş became a lecturer at the Faculty of Sciences (he was a refugee in Timişoara at that time). Beginning with the 1st of October 1950 he was a lecturer, giving courses of lectures on geodesy-topography, general mathematics, astronomy. In 1960 he became a professor of astronomy and astrophysics, and head of the Chair of Theoretical Physics and Astronomy at the Faculty of Mathematics – Physics of the Cluj University. Between 20th of July 1962 and the 15th of October 1968 he was a dean of the Faculty of Mathematics – Mechanics at the same university.

Due to his special didactic qualities, Gheorghe Chiş was also asked to teach mathematics classes at the Normal School in Cluj (1937–1940), at the Constantin Diaconovici-Loga Secondary School in Timişoara (1941–1945) and at the Secondary School No. 2 in Cluj (1945–1946).

In 1949 he obtained his doctoral degree (in mathematics), with a thesis entitled *The Definitive Orbit of the Comet 1937 b (Whipple)*, presented at the Faculty of Mathematics–Physics of the Victor Babeş University in Cluj, which was published in the journal *Studii şi Cercetări Ştiinţifice 1* (1950).

The scientific activity of Professor Gheorghe Chiş covered several fields of astronomy: astrometry, astrophysics, celestial mechanics, space research and archaeoastronomy.

The Cluj Astronomical Observatory had the necessary instruments for starting its own scientific research only beginning with 1938; two years after that it was moved to Timişoara. That is why the first researches of Professor Chiş were connected with the observational data processing for the *Catalogue de 11755 étoiles de la zone 17° à 25° et de magnitudes 9.5 à 10.5* (elaborated by the Paris Observatory) and with the determination of the geographic coordinates imposed by the return of the observatory in Cluj, at the end of the second World War.

We do not intend to present the whole activity of Professor Gheorghe Chiş (see N. N. Teodorescu, *Gazeta Matematică 89* (1981), 369), but only to emphasize the open character of his scientific research. So, the knowledge about the stellar photometry handed down by Professor Ioan Armeanca (an initiator of the astrophysical research in Romania) to his younger collaborator Gheorghe Chiş was used by the latter one to initiate a program of visual observations on photometric binaries. On the basis of the observations performed between 1948–1951 he deduced moments of minima for the following three systems: TZ Lyr, SZ Her, KR Cyg (G. Chiş, *St. Cerc. Ştiinţifice* 3 (1952), Nos 3–4, 28). These ones constitute, as far as we know, the first observations of this kind published by a Romanian astronomer. However, Ioan Armeanca also performed photovisual observations on photometric binaries; those were mentioned by Professor Gheorghe Chiş in his paper on RW Com (G. Chiş, *Bul. St. Secţ Mat. Fiz. Acad. R.P.R.* 8 (1956), 773), where he showed that 25% of the respective observations were performed by Ioan Armeanca.

Increasing the observational accuracy by securing a photometer able to measure photoelectrically the stellar brightness (by measuring the blackening produced on photographic plates), Professor Gheorghe Chiş continued and went thoroughly into the research in this direction, with determinations of photometric elements of binary systems, studies of orbital period variations connected with the instabilities on the respective systems, as well as with determinations of the absolute elements of the system Y Leo and of the evolution of the latter one during the mass loss phase. He had significant contributions to the study of 16 photometric binaries: TZ Lyr, SZ Her, KR Cyg, BR Cyg, WW Cyg, VY Lac, RW Com, UZ Lyr. CH Lac, ZZ Cyg, RZ Dra, TU Her, RV Lyr, RV Per, Y Leo, V Tri.

As an acknowlegement of his merits in this domain, Professor Gheorghe Chiş coordinated between 1974—1981 the activity of the Subcommission No. 5 Binary Stars, in the framework of the international cooperation "Physics and Evolution of Stars" between the Academies of Sciences of the East-European countries.

As a result of the request for cooperation of the Odessa Astronomical Observatory, Professor Gheorghe Chiş introduced (for the first time in our country) the systematic study of the RR Lyrae pulsating stars. Before that, during 1953, he performed the first observations of this kind on the Cepheid S Com (G. Chiş, S. Radu, *St. Cerc. Astron. Seism* 4 (1959), 393) and studied the light curves and the Blazhko effect at six RR Lyrae pulsating stars: WZ Boo, RU Boo, SV Boo, WY Dra, XX Boo, WW Boo. The Cluj research school on RR Lyrae pulsating stars was born under his direction; this activity was appreciated by a renowned astronomer V.P. Tssessevich in his book *RR Lyrae-Type Stars* (Kiev, 1966; in Russian), where it is mentioned that "The Romanian astronomers, under the direction of G. Chiş, also worked actively in this field".

Taking care of the improvement of the accuracy of the astronomical observations, Professor Gheorghe Chiş had a significant contribution to the introduction of photoelectric photometry and of the displacement of the observation instruments in a new station built near the village Feleacu, south of Cluj-Napoca. In this way the perturbing effects of the city lights and smog on the photometric observations were removed.

Professor Gheorghe Chiş can be considered to be the initiator of the archaeastronomical research in Romania. He determined the astronomical orientations of the Dacian sanctuaries from Sarmizegetusa Regia, Orăştie Mountains (see N. Teodorescu, G. Chiş, *Cerul o taină descifrată*, Ed. Albatros, Bucureşti, 1982).

When the first artificial Earth satellite was launched (USSR, 1957), Professor Gheorghe Chiş mobilized the whole staff of the Astronomical Observatory, his family, students, pupils, amateur astronomers to observe it (and other satellites, later). The tracking station he created received the COSPAR code 1132 and is included into an international network (together with the other two Romanian tracking stations 1131 Bucharest and 1133 Timişoara). The research activity of this station joined the international programmes *INTEROBS, EUROBS, ATMOSPHERE, SPIN, INTERCOSMOS* etc., being often appreciated by the coordination centres of these programmes. The space research staff directed by Professor Chiş was distinguished in 1970 with the 2nd prize of the Ministry of Education for the results obtained in this domain.

The writing of astronomical textbooks, courses of lectures and books constitutes another important aspect of Professor Chiş's activity. Among the eight books whose author or co-author he is, we mention the textbook of astronomy for secondary schools, which is the first and the only such textbook written by a Romanian author after the second World War. Made topical, this textbook is used even today.

We cannot end without mentioning the special contribution of Professor Gheorghe Chiş to the popularization of astronomy (and other sciences) through the lectures and conferences held all over the country.

He was a fellow and Vice-President of the Romanian National Astronomical Committee, and was distinguished with four orders and medals.

The scientific activity of Professor Ghorghe Chiş was also acknowledged by international organizations; thus he was elected fellow of the IAU and COSPAR.

His disciples and collaborators keep his memory and will always think of him with gratitude.

VASILE POP, TIBERIU OPROIU

FLORIN N. DIACU, *Singularities of the N-Body Problem. An Introduction to Celestial Mechanics*, Les Publications CRM, Montréal, 1992, ix + 175 p. ISBN 2-921120-20-8.

To emphasize again the importance of the N-body problem for celestial mechanics mainly, but also for other fields of astronomy, to show how many new ideas and techniques in various domains of mathematics it has generated, is superfluous. F. N. Diacu's book approaches one of the most fascinating aspects of this problem : the singularities. The text is structured on 14 chapters.

Chapter 1, of introductory character, presents the N-body problem with inverse α-force law in a k-dimensional Euclidean space, and the very well-known ten first integrals for $k = 3$ It is shown that the problem remains unsolved as long as a global description of the phase space does not exist.

Chapter 2 defines the singularities of the solutions, dividing them into collision and pseudocollision (noncollision) singularities. The conjecture that for any N the set of initial data leading to solutions with singularities is of Lebesgue measure zero and of first Baire category is stated, too.

Von Zeipel's theorem, which proves that a pseudocollision may occur only if the motion becomes unbounded in finite time, as well as Saari's generalization, based on the concept of slowly varying function, are discussed in Chapter 3.

Chapter 4 is intended to the famous theorem of Pollard and Saari, which features any collision involving the asymptotic behaviour of the potential function, for any N; the possibility to extend it to any inverse α-force law is also pointed out.

The central topic of Chapters 5 and 6 is constituted by pseudocollisions. Chapter 5 describes some classes of solutions that do not encounter pseudocollisions : that of the three-body problem (Painlevé's result), rectilinear solutions for any N (Saari's result), trapezoidal, rectangular, rhomboidal solutions for $N = 4$. Starting from Painlevé's conjecture on pseudocollisions, Chapter 6 sketches some examples of attempts to prove this one by means of concrete solutions, among which both Xia's example (for $N = 5$, but extensible to higher N) and Gerver's second example (for $3N$ bodies) solve the problem.

Another section with introductory character is Chapter 7, which, by means of definitions and theorems, provides some insight into the theory of central configurations, whose importance for the N-body problem is emphasized in the next chapters.

Chapter 8 deals with the regularization of colliding solutions. Suggestive examples point out the fact that Sundman's and Easton's regularization methods are not related. The ideas which led to Easton's block-regularization (by passing together two orbits which begin and end respectively in a singularity, such that the obtained solution is continuous relative to nearby orbits) are described in detail and the method is applied to the two-body problem. The regularization not only of solutions, but also of motion equations is used in Chapter 9 to the triple collision in the classical rectilinear three-body problem.

Chapter 10 provides a brief geometric description of the triple collision manifold, and of the flow behaviour on it. Definitions and results, among which the important theorems concerning the triple collision solutions approaching asymptotically a central configuration (Sundman), or the existence of masses such that triple collision solutions are not block-regularizable for all values of the energy (McGehee), are presented.

Chapter 11 refers to rectilinear homothetic solutions, and defines the structural stability, on the basis of the transverse intersection of the manifolds of distinct equilibria. Devaney's results, stating that in the N-body case this kind of solution starts and ends in total collapse is structurally stable, is discussed.

Closely related to the results given in Chapters 8—10 is the topic of Chapter 12, where one proves that in the rectilinear case simultaneous binary collisions can be block-regularized (result due to El Bialy). Still open problem to be mentioned are : can the smoothness of this regularization be improved? can the result be extended to planar or spatial cases?

Chapter 13 defines the partial collisions and deals with time regularization of them. The problem is presented in detail, and the troubles one can encounter if a block-regularization cannot be pursued are emphasized. Some important author's results are used.

Chapter 14 is intended to the solution of the N-body problem given by Wang in 1991 who brought a viewpoint differing from Sundman's one, and found the desired series expansion for any N. Stressing the avoidance of singularities and the very slow convergence of series expansions, which prevent this approach to constitute an acceptable solution, one asserts that Wang's result closes (probably forever) the chain of attempts to solve the N-body problem with series solution methods.

Although the book seems to deal with only one (but very important) aspect of only one (but fundamental) problem of celestial mechanics, the sub-title is not turgid. We think, together with the author, that "this text will provide an introduction and a background for students, professors, researchers and for anyone enjoying the beauty of mathematics, who wishes to understand this very old but always young field, whose name sounds like a happy combination between (heavenly) dreams and (pure) science : *celestial mechanics*".

VASILE MIOC

PRINTED IN ROMANIA

NOTICE TO AUTHORS

ROMANIAN ASTRONOMICAL JOURNAL is a journal which appears twice a year and is open to original contributions in Astronomy and related disciplines. The contributions — in English or French — can be accepted only if they were neither published before nor destined to any other publication.

Manuscripts should be submitted in duplicate; they must be typewritten on white A4-sized paper, onesided and doublespaced (enclosing abstract, references, footnotes and figure captions). The first page should contain: the article's title (brief and informative), author's name and affiliation, followed by an Abstract in English and Key words. The text should be clear and concise (it is recommended not to exceed 10 pages). *The Abstract* will present clearly the principal conclusions of the work, in no more than 10 —15 lines.

Chapters and Paragraphs. Papers, except, short notes, should be divided into Chapters, numbered by Arabic numerals. Chapters may be divided into Paragraphs denoted by the number of the Chapter and the number of the Paragraph; each Chapter and each Paragraph should have a short descriptive title (e.g. "3.2. Results").

Formulae have to be numbered consecutively in Arabic numerals, too, but included in parenthesis on the right side of the manuscript; all formulae should be written in legible form.

Tables should be numbered consecutively in Arabic numerals; each should be typed on a separate sheet.

Figures and Illustrations should be submitted separately in such a form as to permit reroduction without retouching. Any lettering should be large enough to be legible after the figure has been reduced in size for printing. Captions should be given on a separate sheet and labeled to show which illustration each is accompanying. All the figures should be numbered consecutively in Arabic numerals and referred to in the text as e.g. Fig. 2 or Figs. 2 —5. *Photographs* should be given only if essential and should be enlarged enough to permit clear reproduction.

The Places of tables and figures within the text have to be marked with lead pencil on the left margin of the manuscript.

References are indicated in the text by the author's name and year of publication. They should be listed in alphabetic and chronologic order at the end of the paper, as follows: name and the initials of the author(s), the year of publication, suitable abbreviation of the journal (or title of the book and editing house), its volume and page.

Please pay attention to these recommendations; it will contribute to a faster publishing of the manuscript.

ROMANIAN ASTRONOMICAL JOURNAL

Vol. 3, No. 1, 1993

CONTENTS

ISSN 1210–5168

Rom. Astr. J., Vol. 3, No. 1, p. 1–86, Bucharest, 1993

S.C. „Universul" S.A. – c. 3804

Lei 300 pentru persoane fizice
Lei 500 pentru persoane juridice